Faculté des Sciences Exactes

Département de physique

Laboratoire (LPQ3M), Université de Mascara, Algérie

Thèse L.M.D

Soumis en satisfaction partielle de l'exigence du doctorat

Dans : Physique

Option : Energie et Matériaux Photovoltaïques

Modélisation de systèmes photovoltaïques-thermiques (PVT) basés sur des nanofluides et des matériaux à changement de phase

Présenté par : M. Belazreg Abdeldjalil

Soutenu publiquement à Mascara devant le jury composé de :

Président	Bouadi Abed	Pr	Université de Mascara
Examinateur	Houcine Naim	MCA	Usto-Mb
Examinateur	Mouchaal Younes	MCA	Université de Mascara
Examinateur	Laidoudi Houssem	MCA	Usto-Mb
Superviseur	Mohammed Sahnoun	Pr	Université de Mascara
Co-superviseur	Aissa Abderrahmane	Pr	Université de Mascara

Année Universitaire : 2023 - 2024

PEOPLE'S DEMOCRATIC REPUBLIC OF ALGERIA

MINISTRY OF HIGHER EDUCATION AND RESEARCH SCIENTIFIC

MUSTAPHA STAMBOULI UNIVERSITY OF MASCARA

Faculty of Exact Science

Department of Physics

Laboratory (LPQ3M), University of Mascara, Algeria

Thesis L.M.D

Submitted in Partial Fulfilment of The Requirement of Doctorat

In: Physics

Option: Photovoltaic Energy and Materials

Modelling of Photovoltaic-Thermal (PVT) Systems Based on Nanofluids and Phase Change Materials

Presented By: Mr. Belazreg Abdeldjalil

Publicly Defended on At Mascara in Front of The Jury Composed Of:

Président	Bouadi Abed	Pr	University of Mascara
Examinateur	Houcine Naim	MCA	Usto-Mb
Examinateur	Mouchaal Younes	MCA	University of Mascara
Examinateur	Laidoudi Houssem	MCA	Usto-Mb
Superviseur	Mohammed Sahnoun	Pr	University of Mascara
Co-superviseur	Aissa Abderrahmane	Pr	University of Mascara

Année Universitaire : 2023 - 2024

Acknowledgments

In the name of Allah, the Most Gracious and the Most Merciful, Alhamdulillah, all praise goes to Allah for His strengths and His blessing in completing this thesis. Without His will, kindness, and mercy, the completion of this work would have never been possible.

It is my pleasure to thank those who made this research possible. I would like to express my sincere gratitude and heartfelt indebtedness to my supervisor, **Pr. Aissa Abderrahmane**, associate professor, Department of Mechanical Engineering at the University Mustapha Stambouli of Mascara, Algeria, for his valuable guidance and advice. He has been very supportive and patient throughout the progression of my thesis. His inspiring comments and suggestions motivated me to continue my research work. From his remarkable support and advice during my PhD studies, I gained a lot of experience and knowledge that will help me in the future. Without his support, I would have never been able to reach my goal.

I would like to express my appreciation to **Pr. Mohammed Sahnoun** for his time and advice and for his thorough help.

Many thanks to all my parent for their support and patient along my study.

Finally, I would like to take a moment to acknowledge the personal resilience and dedication that I brought to this project. The countless hours of research, the meticulous analysis, and the persistent drive to refine my arguments have not only contributed to the completion of this thesis but have also been instrumental in my personal and academic growth. This work stands as a testament to the hard work and commitment I have invested, and I am proud to present it as a reflection of my capabilities and the depth of my passion for Physics

ABSTRACT

The escalation in global growth has resulted in a heightened reliance on fossil fuels for energy generation. This significantly affects the amount of greenhouse gases released into the atmosphere. Researchers worldwide are exploring novel, cost-effective, and sustainable energy alternatives. An alternative strategy is to enhance the current energy storage systems, which are equally crucial to the development of new energy sources. Thermal energy is abundantly present in nature as a secondary result of many energy conversion facilities. Thermal energy may be stored utilising latent, sensible, and thermo-chemical storage techniques.

The usage of phase Transition materials in the latent heat thermal energy storage method is considered the most capable strategy for energy storage. The approach has a high energy storage density and is distinguished by minimal temperature fluctuations throughout the energy storage process. The limited thermal conductivity of phase change materials (PCMs) is a significant disadvantage that restricts their use as materials for storing thermal energy via latent heat. The poor thermal conductivity of Phase Change Materials (PCMs) prolongs their thermal energy storage and release durations. The current research examines several methods based on phase change materials (PCMs) to improve the overall thermal efficiency of storage systems.

The solutions presented in this thesis include a novel design of metallic fins and the incorporation of nanoparticles and varying HTF temperature into the heat exchanger. Computing simulations are performed to assess the suggested solutions by monitoring the melting process.

This publication is organised into two primary parts that provide the findings of the research aimed at enhancing the efficiency of latent thermal energy storage systems using phase change materials (PCMs):

In the first part of this study paper offers the findings of a study focusing on four various types of stepped fins, including two-downward step wings, two-upward step wings, an ascendent and descending stepped fin, and two-stepped wings opposite one another. The calculation of the force of buoyancy in the vertical thermal energy storage system, which is filled with rubitherm (RT27) phase change material and Cu nano-additives, was performed using the Boussinesq approach. The numerical simulation of the governing equation was performed using the enthalpy porosity approach, namely the Generalized Finite Element Method (GFEM). The distinctive nature of the thermal and functional entropies for two-ascendent stepped fins and

two-descending stepped fins may be attributed to the effect of acceleration caused by gravity, the mass of phase transition material, and the orientation of the intake fins. The container with two downward-sloped fins facilitated a melting time of no less than 71 minutes. There is a 6.58% variance in the charging time among instances 1 and 2. Nonetheless, a notable disparity of 26.76% is seen in the period required for charging.

The second phase of this work included the implementation of Y-shaped fins integrated with nano-improved phase transition material. The study included examining and contrasting three distinct setups of the TESS system: case 1, which served as the reference without any fins, case 2, which had two Y- formed fins linked to the tubes, and case 3, which featured four Y-formed fins attached to the tubes. The system's governing equations are discretized using the finite element approach. In addition to examining the impact of the TESS arrangement, we also investigated the effects of the HTF temperature (338 and 348 K) and the volume percentage of the nanoparticles (ranging from 0 to 0.08). The analysis focuses on the changes in temperature contours and liquid fractions of three distinct designs when subjected to two different HTF temperatures. The results indicated that the use of nanoparticles with a volume fraction of 8% increased the thermal conductivity by 19% during the process of melting. Raising the HTF temperature to 348 K resulted in an 87% acceleration of the melting process. Ultimately, it was determined that TESS, equipped with four Y-shaped fins, proved to be the most efficient. It managed to decrease the changing time by 48% when related to the base case, also known as case 1.

RÉSUMÉ

La montée en puissance de la croissance globale a entraîné une dépendance accrue aux combustibles fossiles pour la production d'énergie. Cela a un impact significatif sur la quantité de gaz à effet de serre émis dans l'atmosphère. Des chercheurs du monde entier explorent de nouvelles alternatives énergétiques abordables et durables. Une stratégie alternative consiste à améliorer les systèmes de stockage d'énergie actuels, qui sont tout aussi cruciaux pour le développement de nouvelles sources d'énergie. L'énergie thermique est abondamment présente dans la nature en tant que résultat secondaire de nombreuses installations de conversion d'énergie. L'énergie thermique peut être stockée en utilisant des techniques de stockage par chaleur latente, sensible et thermochimique.

L'utilisation de matériaux à changement de phase dans la méthode de stockage thermique par chaleur latente est considérée comme la stratégie la plus efficace pour le stockage d'énergie. Cette approche offre une densité de stockage d'énergie élevée et se distingue par des fluctuations de température minimales pendant le processus de stockage d'énergie. La faible conductivité thermique des matériaux à changement de phase (PCM) est un inconvénient majeur qui limite leur utilisation comme matériaux de stockage d'énergie thermique par chaleur latente. La mauvaise conductivité thermique des matériaux à changement de phase (PCM) prolonge leurs durées de stockage et de libération d'énergie thermique. Les recherches actuelles examinent plusieurs méthodes basées sur les matériaux à changement de phase (PCM) pour améliorer l'efficacité thermique globale des systèmes de stockage.

Les solutions présentées dans cette thèse incluent une conception innovante de ailettes métalliques et l'incorporation de nanoparticules et de variatîons de température du fluide caloporteur dans l'échangeur de chaleur. Des simulations informatiques sont réalisées pour évaluer les solutions proposées en surveillant le processus de fusion.

Cette publication est organisée en deux parties principales qui présentent les résultats de la recherche visant à améliorer l'efficacité des systèmes de stockage thermique latent utilisant des matériaux à changement de phase (PCM) :

La première partie de cet article de recherche présente les résultats d'une étude axée sur quatre types différents d'ailettes en gradins, y compris deux ailettes en gradins vers le bas, deux ailettes en gradins vers le haut, une ailette en gradins ascendante et descendante, et deux ailettes en

gradins opposées. Le calcul de la force de flottabilité dans le système de stockage d'énergie thermique vertical, rempli de rubitherm (RT27) et d'additifs nano-Cu, a été effectué en utilisant l'approche de Boussinesq. La simulation numérique de l'équation gouvernante a été réalisée en utilisant l'approche enthalpie porosité, à savoir la Méthode des Éléments Finis Généralisés (GFEM). La nature distinctive des entropies thermiques et fonctionnelles pour deux ailettes en gradins ascendantes et deux ailettes en gradins descendantes peut être attribuée à l'effet de l'accélération due à la gravité, la masse du matériau à changement de phase et l'orientation des ailettes d'entrée. Le conteneur avec deux ailettes en pente vers le bas a facilité un temps de fusion d'au moins 71 minutes. Il y a une variation de 6,58% dans le temps de charge entre les cas 1 et 2. Néanmoins, une différence notable de 26,76% est observée dans la période requise pour la charge.

La deuxième phase de ce travail incluait la mise en œuvre d'ailettes en forme de Y intégrées avec un matériau à changement de phase nano-amélioré. L'étude incluait l'examen et la comparaison de trois configurations distinctes du système TESS : le cas 1, qui servait de référence sans ailettes, le cas 2, qui avait deux ailettes en forme de Y reliées aux tubes, et le cas 3, qui comportait quatre ailettes en forme de Y attachées aux tubes. Les équations gouvernantes du système sont discrétisées en utilisant l'approche des éléments finis. En plus d'examiner l'impact de la configuration TESS, nous avons également étudié les effets de la température du fluide caloporteur (338 et 348 K) et du pourcentage en volume des nanoparticules (allant de 0 à 0,08). L'analyse se concentre sur les changements dans les contours de température et les fractions liquides de trois conceptions distinctes soumises à deux températures de fluide caloporteur différentes. Les résultats ont indiqué que l'utilisation de nanoparticules avec une fraction volumique de 8% a augmenté la conductivité thermique de 19% pendant le processus de fusion. L'augmentation de la température du fluide caloporteur à 348 K a entraîné une accélération de 87% du processus de fusion. En fin de compte, il a été déterminé que le TESS, équipé de quatre ailettes en forme de Y, s'est avéré le plus efficace. Il a réussi à réduire le temps de changement de 48% par rapport au cas de base, également connu sous le nom de cas 1.

ملخص

زيادة النمو العالمي أدت إلى تبعية أكبر للوقود الأحفوري في إنتاج الطاقة. هذا له تأثير كبير على كمية الغازات الدفيئة المنبعثة إلى الغلاف الجوي. يتم استكشاف بدائل طاقة جديدة وفعالة من حيث التكلفة ومستدامة من قبل الباحثين في جميع أنحاء العالم. تتمثل استراتيجية بديلة في تحسين أنظمة تخزين الطاقة الحالية، والتي تعتبر مهمة أيضًا لتطوير مصادر الطاقة الجديدة. الطاقة الحرارية وفيرة في الطبيعة كنتيجة ثانوية للعديد من منشآت تحويل الطاقة. يمكن تخزين الطاقة الحرارية باستخدام تقنيات تخزين الحرارة الكامنة والحسية والكيميائية الحرارية.

يعتبر استخدام مواد التحول الطوري في طريقة تخزين الحرارة الكامنة الأكثر كفاءة لتخزين الطاقة. تتميز هذه الطريقة بكثافة تخزين طاقة عالية وتتميز بتقلبات درجة حرارة منخفضة خلال عملية تخزين الطاقة. الموصلية الحرارية المحدودة لمواد التغيير الطوري (PCMs) هي عيب كبير يحد من استخدامها كمواد لتخزين الطاقة الحرارية عن طريق الحرارة الكامنة. الموصلية الحرارية الضعيفة لمواد التغيير الطوري (PCMs) تطال أوقات تخزين وإطلاق الطاقة الحرارية. تدرس الأبحاث الحالية عدة طرق تستند إلى مواد التغيير الطوري (PCMs) لتحسين الكفاءة الحرارية الإجمالية لأنظمة التخزين.

تشمل الحلول المقدمة في هذه الرسالة تصميمًا جديدًا للزعانف المعدنية ودمج النانو-جسيمات وتغيير درجة حرارة HTF في مبادل الحرارة. يتم إجراء محاكاة الكمبيوتر لتقييم الحلول المقترحة عن طريق مراقبة عملية الذوبان.

تنظم هذه المنشور إلى جزأين رئيسيين تقدمان نتائج البحث المستهدفة على تحسين كفاءة أنظمة تخزين الطاقة الحرارية الكامنة باستخدام مواد التغيير الطوري (PCMs):

في الجزء الأول من ورقة البحث هذه تقدم النتائج من دراسة تركز على أربعة أنواع مختلفة من الزعانف المتدرجة، بما في ذلك زعانف متدرجة نحو الأسفل، وزعانف متدرجة نحو الأعلى، وزعنفة متدرجة متصاعدة ومتنازلة، وزعانف متدرجة متقابلة. تم حساب قوة الطفو في نظام تخزين الطاقة الحرارية العمودي، المملوء بمادة تغيير الطور (RT27) rubitherm والمضافات النانوية النحاسية، باستخدام نهج بواسينك. تم إجراء المحاكاة العددية للمعادلة الحاكمة باستخدام نهج المحتوى الحراري المسامي، أي طريقة العناصر المحدودة المعممة (GFEM). يمكن أن تُعزى الطبيعة المميزة للأنتروبيات الحرارية والوظيفية لزعانف متدرجة متصاعدة ومتنازلة إلى تأثير التسارع بسبب الجاذبية، وكتلة مادة التحول الطوري، واتجاه زعانف الإدخال. سهل الحاوية ذو الزعانف المائلة نحو الأسفل وقت ذوبان لا يقل عن 71 دقيقة. هناك تباين بنسبة 6.58٪ في وقت الشحن بين الحالات 1 و2. ومع ذلك، يُلاحظ اختلاف ملحوظ بنسبة 26.76٪ في الفترة المطلوبة للشحن.

تضمنت المرحلة الثانية من هذا العمل تنفيذ زعانف على شكل حرف Y مدمجة مع مادة تحول الطور المحسنة بالنانو. شملت الدراسة فحص ومقارنة ثلاث ترتيبات مختلفة لنظام TESS: الحالة 1، التي خدمت كمرجع بدون زعانف، والحالة 2، التي كانت زعانف على شكل حرف Y متصلة بالأنابيب، والحالة 3، التي تتضمن أربعة زعانف على شكل حرف Y مرفقة بالأنابيب. تم تفريغ المعادلات الحاكمة للنظام باستخدام نهج العناصر المحدودة. بالإضافة إلى فحص تأثير ترتيب TESS، قمنا أيضًا بدراسة تأثير درجة حرارة HTF (338 و348 كلفن) ونسبة الحجم المئوية للنانو-جسيمات (تتراوح من 0 إلى 0.08). تركز التحليل على التغيرات في مخططات درجة الحرارة والكسور السائلة لثلاث تصاميم مختلفة عندما تخضع لدرجتي حرارة HTF مختلفتين. أظهرت النتائج أن استخدام النانو-جسيمات بنسبة حجمية 8٪ زادت الموصلية الحرارية

بنسبة 19٪ خلال عملية الذوبان. زيادة درجة حرارة HTF إلى 348 كلفن أدت إلى تسريع بنسبة 87٪ في عملية الذوبان. في النهاية، تبين أن TESS ، مجهز بأربعة زعانف على شكل حرف Y ، كان الأكثر كفاءة. تمكن من تقليل وقت التغيير بنسبة 48٪ مقارنة بالحالة الأساسية، المعروفة أيضًا باسم الحالة 1.

في النهاية، تبين أن TESS ، مجهز بأربعة زعانف على شكل حرف Y ، كان الأكثر كفاءة. تمكن من تقليل وقت التغيير بنسبة

Table of Contents

List of Figures

List of Tables

c_p Specific heat (J/kgK)

C Mushy region morphology constant, $(kg/m^3.s)$

dp Nanoparticle diameter, (nm)

g Gravitational acceleration, (ms^{-2})

H Total enthalpy, (kJ/kg)

h Sensible enthalpy (kJ/kg)

h_{ref} Enthalpy reference, (kJ/kg)

k Thermal conductivity (W/m K)

P Pressure, (Pa)

S_a Source term of porosity function, $(kg \cdot s^2 \cdot m^{-2})$

S_b Boussinesq approximation of buoyancy force, $(kg \cdot s^2 \cdot m^{-2})$

T Temperature, (K)

T_m Melting Point, (K)

T_l Liquid temperature, (K)

T_s Solid temperature, (K)

T_{in} Initial temperature, (K)

t	Time, (s)
Q_0	Heat flux (W/m^2)
t_m	Melting time (s)
u	Velocity in the x-direction, (ms^{-1})
v	Velocity in the y-direction, (ms^{-1})
L	Latent Heat

Greek letters

g	Thermal expansion coefficient, (1/K)
β	Liquid fraction
ΔH	Latent heat, (kJ/kg)
ΔT	Transition temperature range, (K)
η	Porosity function
κ	Permeability, (m^2)
μ	Dynamic viscosity, (Pa.s)
ρ	Density (kg/m^3)
ϕ	Nanoparticle concentration

l   Liquid state

np   Nanoparticle

s   Solid state

Chapter: Background 1

CHAPTER.I : Background

I.1   Introduction :

The persistent need for energy has resulted in widespread concerns about climate change, owing to the increasing utilisation of energy resources such as fossil fuels. Reducing the reliance on fossil fuels and giving preference to renewable energy sources is crucial. Solar energy is a promising and accessible replacement power source that is both cost-free and readily accessible. Created on the forecasts from the Paris-based International Energy Agency of the Organisation for Economic Co-operation and Development (OECD), it is predictable that solar power will account for 27% of the world's electricity generation by 2050. A significant obstacle in harnessing solar energy is its reliance on variables such as time, weather conditions, and geographical location. Hence, it is imperative to implement energy storage technologies to efficiently store solar energy, either through electrochemical or thermal means [2], [3]. The intermittent nature of solar energy limits its broad application in powering cooling systems [4]. Therefore, it is crucial to include a thermal energy storage system, whether it be for cold or hot temperatures, Within the solar cooling system [5], [6]. Latent heat thermal energy storage (LHTES) is advantageous compared to sensible heat thermal energy storage (SHTES) due to its greater energy storage density. [7]. Phase change materials (PCMs) are the materials utilised in LHTES systems to store thermal energy. Phase Change Materials (PCMs) can efficiently store large quantities of thermal energy during their phase transition, even with a minor temperature variation in the material [8]. Phase change materials (PCMs) have found extensive use in various applications, such as air conditioning systems in buildings, solar cooling systems, greenhouses, electronic cooling, food refrigeration, solar water heating, solar power plants, medical applications like blood transportation, and fabrics designed to improve human comfort. [9],[10]

I.2   Energy Storage:

Energy storage devices have become a vital element of green energy technologies. Storage systems are essential for managing the disparity among energy supply and demand, as well as for absorbing and utilising excess or otherwise unused energy. Multiple energy storage systems

are accessible, encompassing mechanical, electric, and thermal options. [11]. **Figure I.1** provides a summary of different energy storage methods.
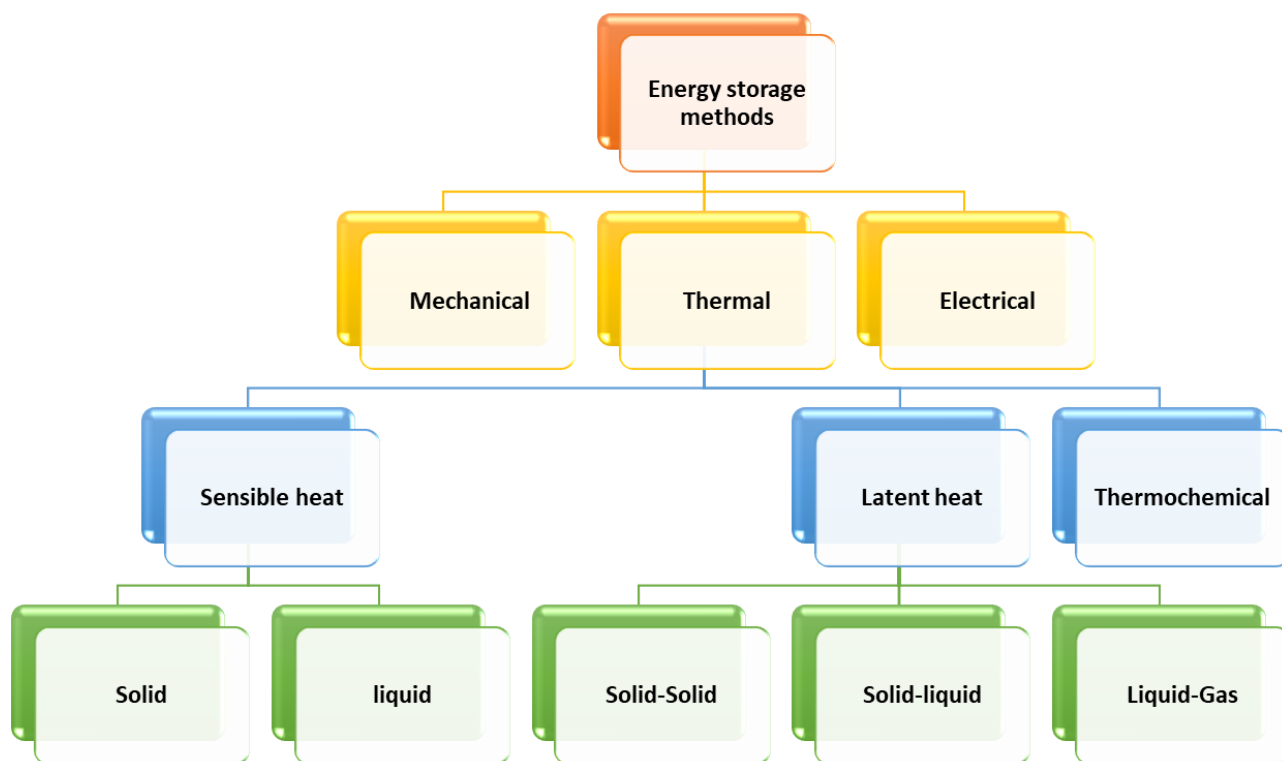
Figure I-1Energy storage methods

I.2.1   Thermal Energy Storage:

Thermal energy storage (TES) systems store thermal energy by altering the temperature of the storage medium through cooling/heating, melting/solidifying, or condensing/evaporating, as well as through the utilisation of thermo-chemical processes. Additionally, the stored energy can be utilised for cooling, heating, and generating electricity. [12]. TES is an advantageous option for solar power systems because of its significant storage capacity and highly reasonable price. Thermal energy storage (TES) often has a heat storage capacity that is 1000 times greater than hydraulic energy storage and twice as high as electric energy storage capacity. [13]. There are three main types of thermal energy storage: latent heat thermal energy storage (LHTES), sensible heat thermal energy storage (SHTES), and thermochemical energy storage. **Figure I.2** illustrates several methods for storing thermal energy. Sensible heat thermal energy storage (SHTES) refers to the process of storing or releasing energy by changing the temperature of the storage medium, which may be materials like rock, water, brine, soil, or oil. The quantity of thermal energy stored in a sensible heat thermal energy storage (SHTES) system is dictated by

the mass of the storage material, its heat capacity, and the temperature variance before and after the storage process.

The sensible heat storage ($Q_{sensible}$) may be defined as:

$$Q_{\text{sensible}} = m \times C_p \times \Delta T \qquad \text{I-1}$$

Energy is stored throughout a phase shift in LHTES [14]. Phase change materials (PCMs) are the materials utilised in LHTES. Typical instances of phase change materials include water/ice, paraffin, and eutectic salts. The representation of latent heat storage (Q_{latent}) is as follows:

$$Q_{latent} = m \times L \qquad \text{I-2}$$

The variables in the equation are as follows: C_p represents the specific heat, m represents the mass of the storage material, ΔT represents the temperature change, and L represents the latent heat of charing. LHTES has superior energy storage capability in comparison to SHTES, resulting in reduced physical dimensions for LHTES units.

Thermochemical storage devices store energy by harnessing exothermic or endothermic chemical processes [15]. Thermal energy storage (TES) systems that rely on chemical processes are suitable for long-term storage applications since they do not experience any energy losses throughout the storage time. Thermochemical energy storage devices are designed to store thermal energy at typical room temperature. The fundamental concept of thermochemical thermal energy storage (TES) relies on the usage of a chemical process that is capable of being reversed. -

$$C + \text{ heat } \rightleftharpoons A + B \qquad \text{I-3}$$

By absorbing thermal energy, thermochemical material (C) is chemically transformed into two substances (A and B) in this thermochemical reaction. The reverse chemical reaction takes place upon the combination of components A and B, resulting in the formation of C. A release of thermal energy occurs throughout this reaction. The thermochemical TES system's storage capacity is determined by the heat of reaction during the formation of material C. As shown in Fig. I.2 (a), the thermochemical TES cycle consists of three primary processes: charging, storage, and discharging. Although thermochemical energy storage has a high capacity for storing energy, it is costly and in its infancy as a field of study. [16]
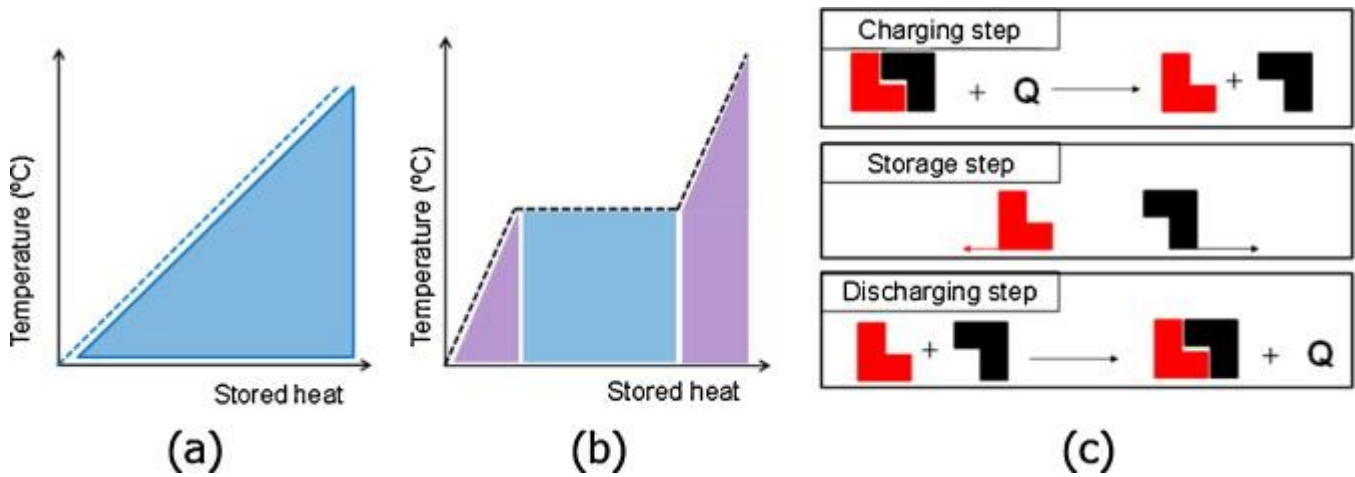
Figure I-2 Methods of thermal energy storage: (a) sensible heat storage; (b) latent heat and (c) thermochemical reactions

I.2.2   Latent Heat Thermal Energy Storage:

The large energy storage capacity of LHTES makes it a potential approach for energy storage. In addition, LHTES allows for the storage or discharge of energy at a relatively consistent temperature in comparison to SHTES. LHTES relies on the heat gained or lost during a phase transition, such as the conversion from a solid to a liquid, solid to a different solid, or liquid to a gas, and vice versa. The transition from liquid to gas phase necessitates a vessel with a substantial volume, while the transition from solid to solid phase has a relatively limited capacity for storing energy per unit volume of the material. Hence, the transition from a solid to a liquid state is favoured over other forms of phase changes due to its significant ability to store energy and little alteration in volume throughout the process [17]. Phase change materials (PCMs) are the materials used in LHTES for energy storage. PCMs' applicability in TES is hindered by their low thermal conductivity, resulting in longer energy storage and release times.

I.2.3   Description of the Problem

The low thermal conductivity of phase change materials (PCMs) hinders efficient heat transfer and limits the pace at which heat can be stored or released. This is the primary challenge that prevents the widespread use of PCMs in thermal energy storage (TES) systems that need fast energy storage and release. Therefore, the use of heat transmission improvement strategies is crucial for any Thermal Energy Storage (TES) systems that rely on Phase Change Materials (PCMs).

I.3 Aims and Objectives

The aim of this study endeavour is to conduct an empirical investigation on the thermal control

- To understand the complex physics governing the characteristics of PCM

- To study the influence of insertion of nanoparticles in PCM

- To study fins geometry and arrangement effect Heat transfer enhancement

I.4 Thesis Outline

The thesis is organised into five chapters. Chapter 2 presents a full review of the present literature and research discoveries on the usage of phase transition materials in thermal energy storage. The chapter primarily concentrates on methodologies that enhance heat conduction. Nanoparticles that conduct heat very well can be scattered into phase change materials (PCM), permeable materials can be used, multiple PCMs can be combined, and metal fins can be added. Research has shown that fins are the most common method for improving heat transmission in phase change materials (PCMs). The energy preservation and discharge timings of LHTES systems based on PCMs have been significantly impacted by the geometric shape of fins. Hence, it is crucial to investigate the potential inventive geometric configurations of the fins in order to improve the thermal efficiency of PCM-LHTES systems. The literature study also shows that modifying the heat exchanger shape has the potential to improve the thermal efficiency of PCM LHTES systems. Chapter 3 discusses the governing equations employed to address the issue of phase transition materials. In Chapter 4, an evaluation is made among upward and downward-stepped fins with four different step ratios. The purpose of this comparison is to improve heat transmission and promote the melting of PCM (RT-27) within a rectangular cavity. The cavity absorbs thermal heat from one side. The TES system uses a pair of wings. In Chapter 5, this subsection discusses a thermal energy storage (TES) unit shaped as a shell and tube. Four tubes, including and finless, are being cooled by a shell filled with PCM (RT27) in order to store thermal energy for a hot liquid flow. The heat transmission rates and PCM melting processes are examined between two Y-shaped fins with two and four fins respectively. To boost the melting ability of the PCM, we use nanoparticles (specifically copper) at various concentration ratios (0, 2, 4, 6, and 8 vol%). An investigation was conducted

to examine and report on the impact of temperature, liquid fraction, and the addition of nanoparticles on heat transmission and melting processes.

I.5   Conclusion

This chapter provides a thorough discussion on the definitions of energy storage, thermal energy, and latent heat energy storage. We also discussed the aims and objectives of the problem in detail. Thesis Outline

Chapter 2: Literature Review

CHAPTER.II : Literature Review

T hermal energy may be stored in two ways: as perceptible energy or as latent energy. The latent heat storage system has many benefits compared to the sensible heat storage system, such as a greater heat of fusion and increased energy density. In a latent heat storage system, the transition from liquid to solid phase offers more versatility compared to the transition from liquid to gas phase. Phase change material (PCM) refers to a substance that undergoes a transition from a liquid state to a solid state, which is often used for latent storage purposes.

II.1 Phase change materiel:

Phase transition materials are the elements which have high latent heat of fusion, charging is occurred at a fixed temperature, stores and releases large amount latent heat energy.

II.1.1 Categorization of PCMs

An extensive range of PCMs with varying working temperature and thermal properties are available. The classification of PCM (solid-liquid families) shown in Figure II-1. These PCMs broadly categorized as eutectic, inorganic and organic [34].
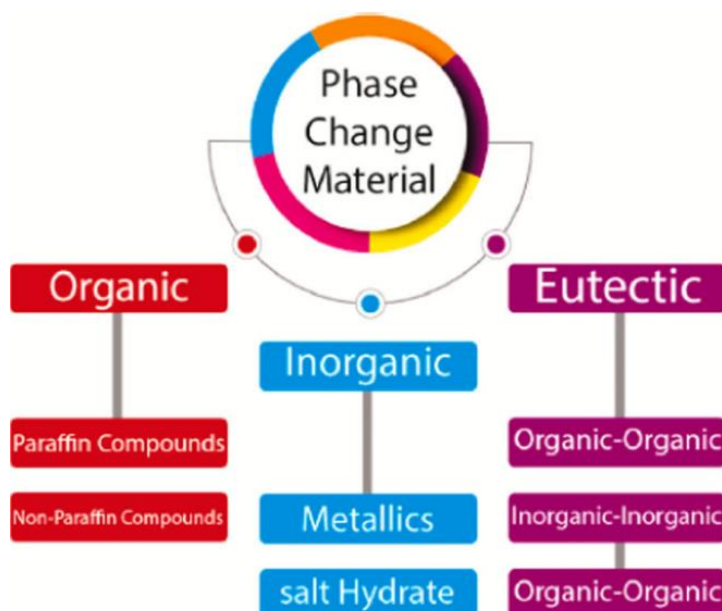
Figure II-1Classification of phase change materials

II.1.2   PCMs classification:

Phase-shifting substances are frequently classified according to their thermal characteristics, including but not limited to their phase transition temperature and latent heat. All of the aforementioned, however, is contingent upon the chemical constituents of the PCMs, as stated by Abhat [18]. The organic, inorganic, and eutectic states of PCMs [40] are illustrated in Fig.II-1

II.1.3   Organic PCMs

Due to their charging temperature range of 0–150 C, they have become widely used in thermal storage use [19]. In addition, they possess several qualities that make them a strong choice for TESA. The chemical properties of these substances exhibit excellent stability, with high energy storage capabilities during phase shifting. They are also non-corrosive and non-toxic, and do not experience supercooling during solidification. Additionally, they demonstrate a favourable nucleation rate [20]– [22]. They also have their drawbacks, as their density is low and they cannot withstand temperatures above 150 C [23]. Typically, they come in paraffin and non-paraffin forms.

II.1.4   Paraffin:

These are saturated hydrocarbons with the formula $C_n H_{2n+2}$. They offer melting temperatures ranging from 10 to 100 degrees Celsius [24]. They are widely used as organic PCM due to their availability, but they do have certain limitations such as their high cost. Additionally, they experience volume changes during phase change. Their thermal conductivity is only about 0.2 W/m.K [25]-[27].

II.1.5   Non-Paraffin:

The substances known as fatty acids (F.A.) have the chemical formula $CH_3(CH_2)_{2n}COOH$ [28]. They possess similar traits to paraffin, such as a melting temperature range of 40 to 150 degrees Celsius, but exhibit enhanced stability. 29- [32]

II.1.6   Inorganic PCMs

Inorganic phase change materials (PCMs) have melting points ranging from 100°C to 1000°C, which is about ten times higher than that of organic PCMs [30]. This makes them very suitable for use in solar applications. Moreover, they are both affordable and non-flammable [33]. However, they are unable to exist independently; they constantly need containers, which poses a significant barrier in their production due to the risk of corrosion. The range of numbers

is from 29 to 34. Typically, they consist of salt hydrates and metallic phase change materials (PCMs).

II.1.7 Salt hydrates

These materials may be regarded as the most significant substances for storing thermal energy due to their high latent heat of around 240 kJ/kg [29]. Their chemical formula is ABnH2O, indicating the presence of water [35]. The primary benefits of these materials are minimal volume fluctuations and a thermal conductivity of around 0.5 W/m. K, which is more than double that of organic PCMs [30], [36].

II.1.8 Metallic PCMs:

By using metallic compounds, they have achieved satisfactory thermal conductivity. The need also sets them apart for their large capacity for thermal storage due to their low storage-to-weight ratio.[37]

II.1.9 Eutectic PCMs:

These PCMs are created by combining two or more variations of the previous PCMs. They can come in various combinations, such as inorganic-inorganic mixtures, organic-inorganic, and organic-organic [38]. They are not commonly utilised in construction due to their robust door [39], but they are frequently employed in the field of solar energy storage [40]. Although there is limited data available, it is worth noting the advantages of these materials, such as their precise melting temperature, lack of segregation and consistent phase-change, and high volumetric thermal storage density [41].

II.1.10 Implementation of PCMs as Thermal Energy Storage

PCMs have extensive commercial applications in thermal energy storage (TES) systems. This section will focus on the application. PCMs may be used in many applications to decrease the cost and increase the capacity of thermal energy storage. It is a methodical and eco-friendly approach to energy use. Implementing Phase Change Materials (PCM) for Thermal Energy Storage (TES) may result in a significant reduction of greenhouse gas emissions, up to 40% as reported in reference [42]. Phase change materials (PCMs) are crucial for thermal energy storage (TES) applications. However, under some exceptional circumstances, the use of Phase Change Materials (PCMs) might result in a 50% reduction in energy consumption in Thermal Energy Storage (TES) systems. [43]

II.1.11 Application in photovoltaic

PCM's phase change heat absorption qualities are used by people to combine it with solar panels in various structural configurations. This integration serves the purpose of lowering the temperature of the panels and recovering waste heat. Due to the significant latent heat value and consistent phase change temperature of phase change materials, researchers and academics have extensively investigated several integrated systems combining phase change materials with different solar systems. The text will provide a detailed introduction to many components of the system, including phase change material, photovoltaic, non-concentrating photovoltaic, photovoltaic photothermal integrated system, photovoltaic-microencapsulated phase change material, and phase change material-nanofluid. These components are shown in Figure II 2.
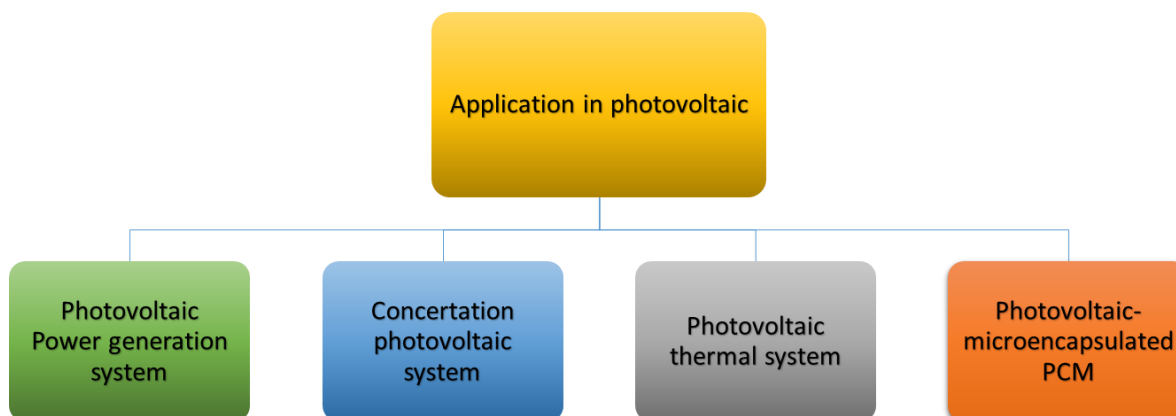
Figure II-2 Application framework in photovoltaics.

By using Phase Change Materials (PCM) to store cooling and heating energy, it is possible to decrease the consumption of cooling and heating energy by transferring the peak load to hours when demand is lower. Utilising Phase Change Material (PCM) to retain frigid temperatures throughout a cold night might save energy use for the cooling system employed to charge it, since it operates with greater efficiency during night time hours.

An innovation related to PCM was granted a patent in 2005 [44]. The patented device in the present innovation primarily utilises the discharging and charging procedure for PCM to soak up waste heat produced during the charging and discharging of battery modules. The main purpose of the system is to regulate temperature fluctuations in the system by using PCM to preserve it at the optimal temperature. This, in turn, enhances the general effectiveness of charging and discharging the battery module.

Huang et al. [45] developed a computational model to predict the thermal performance of PV-PCM. The system employs fluid mechanics to solve the Navier-Stokes equations and the energy equation. The system creates model configurations in three separate environments: (i) an aluminium plate that emulates a photovoltaic (PV) cell; (ii) an aluminium plate with a container containing phase change material (PCM); and (iii) an aluminium plate with a container containing PCM that has an integrated heat sink. The experimental results indicate that the phase change material (PCM) combined with a heat sink effectively regulates the temperature of the photovoltaic (PV) panel.

Huang et al. [65] conducted a research on the advancement of three-dimensional (3D) computational simulations, building upon a prior investigation. Figure II-3 displays the 3D model structure and simulation structure. This simulation was used to forecast the distribution of temperature, velocity, and vortex formation inside the PV-PCM system. The investigation revealed that the 2D model outperformed the 3D model in terms of prediction accuracy. Additionally, the 3D model provided a more complete and detailed prediction of the temperature distribution for the high thermal conductivity pin-fin reinforced PCM.
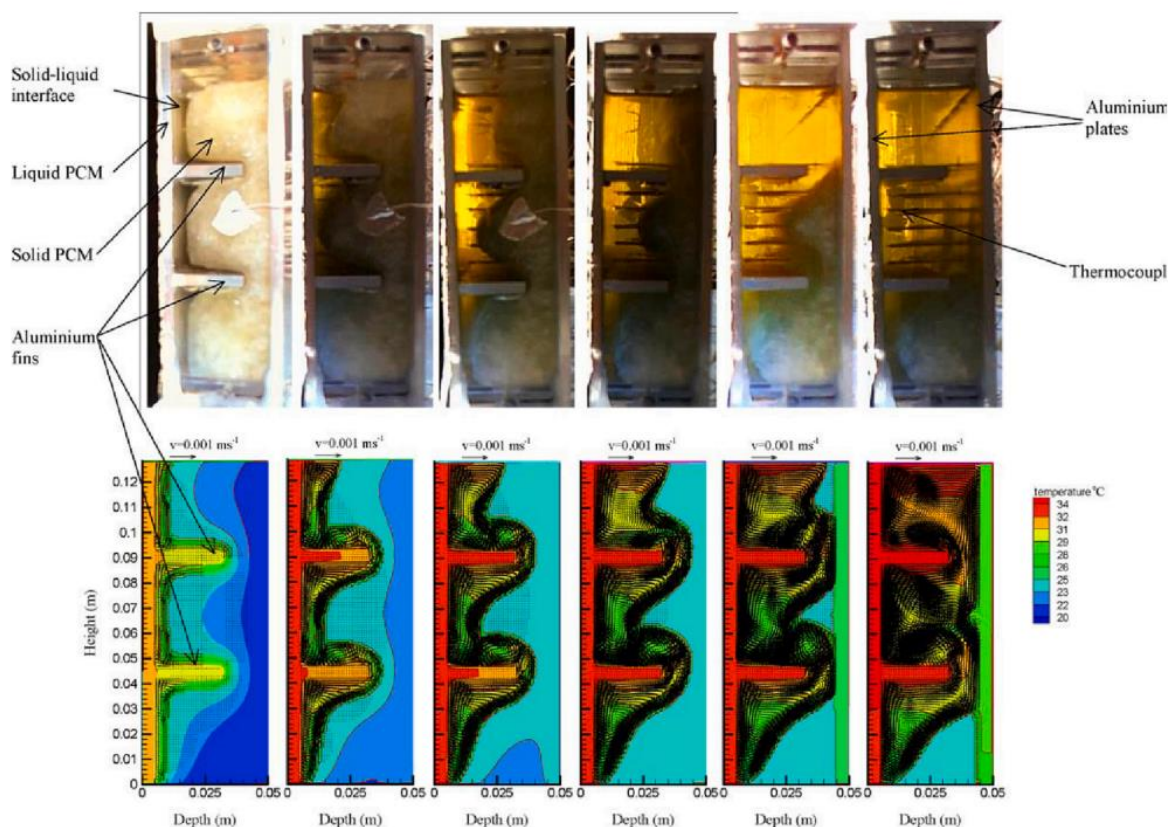
Figure II-3 A picture of the photovoltaic system, along with the anticipated temperatures and velocities, showcases the melt process of the PCM with fins.

Khanna et al. [46] included a thermal fin structure into the existing model by using PCM-PV panel thermal management, as seen in Figure II 4. Their findings indicate that in hotter climes, the addition of fins to the PCM may result in a 12.1% increase in electrical production. In colder climates, the increase is just 6.7% (b). In windy areas, the electrical output increases by 5.3% when using finned PCM. In less windy conditions, the increase is 10.5%.

In their study, Jawad Sarwar et al. [47] examined the temperature control and power generation of a concentrating photovoltaic (PV) system combined with a CPVPCM system, namely, a concentrating photovoltaic system with a single sun crystalline photovoltaic (PV) system. The concentration ratio of the concentrating photovoltaic system was 200. A simulation was conducted to analyse the temperature variation, thermal energy storage, and power production of a CPV-PCM system over a two-day period. The experimental findings demonstrate that the CPV-PCM system has a higher daily power generation capacity than the natural convection photovoltaic system. Additionally, the CPV-PCM system successfully maintains a maximum temperature below 85 ∘C. In July, the CPVPCM system's PV cell reaches a maximum temperature of 82.1 ∘C.

Emam et al. [48] examined the thermal efficiency of a slanted concentrated phase change material system. The current study includes a schematic design of the hybrid CPV-PCM system, which is shown in Figure II 5.
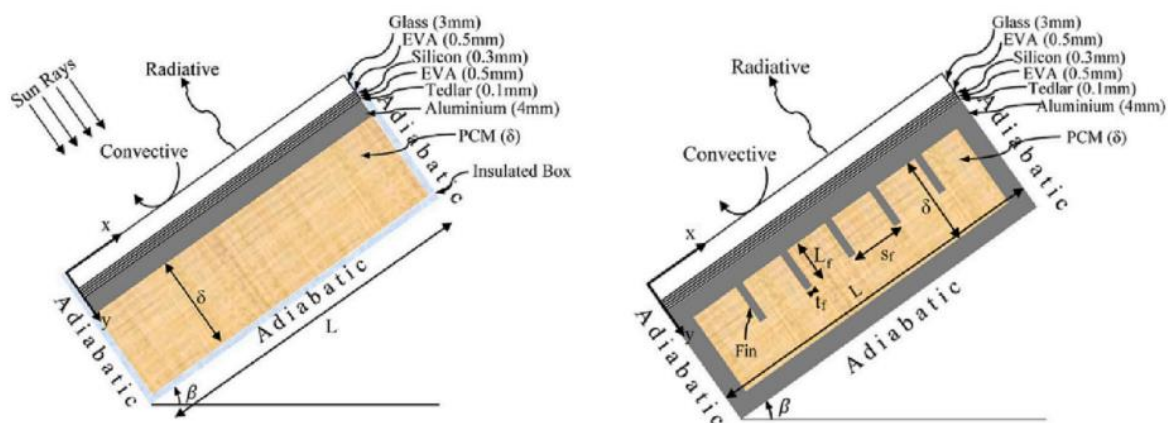
Figure II-4 (a)System chosen for the current study and (b)finned-PV-PCM setup.
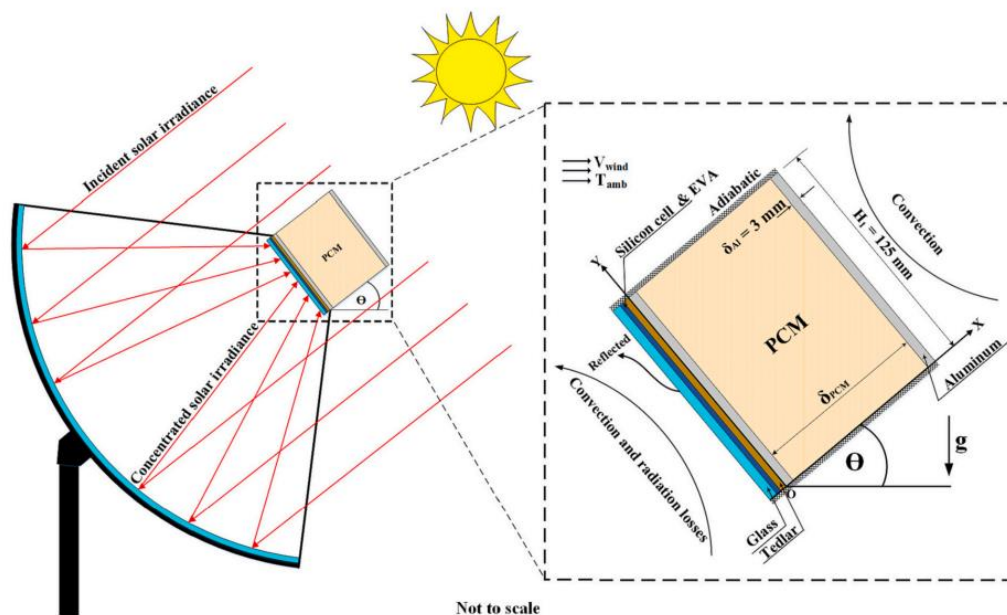
Figure II-5 Schematic diagram of CPV-PCM system.

In a study conducted by Ali et al. [49], they examined the experimental device, process flow, and practical application limitations of MPCM slurry in a PV-T system. The PV-T system utilises MPCMslurry to function effectively. It includes a PV module, an electrical control and storage unit, a flat plate heat exchanger for suspension, and a heat pump evaporator for cooling. Based on the experimental results, it is evident that with an MPCM concentration of 10%, the overall system efficiency is 83%, and the coefficient of performance (COP) reaches an impressive 5.9. The experimental results are satisfactory, however, the cooling medium (MPCMS) adds a level of complexity that the system is still grappling with.. Ghasemi et al. [50] conducted a study to analyse and enhance the movement of Microencapsulated Phase Change Material (MPCM) suspension in a porous double tube heat exchanger. The researchers constructed a heat exchanger using MPCMS as the base fluid, which served as the working fluid for the double-tube system.

Fu et al. [51] developed and implemented a novel photovoltaic-thermal (PV-T) module, shown in Figure II 6. The working fluid used in the module consists of either tap water or a slurry of Microencapsulated Phase Change Material (MPCM). The author used a serpentine form for the fluid channel, as seen in Figure II 7.
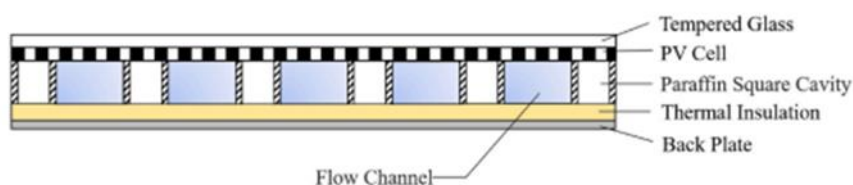
Figure II-6 Schematic diagram of the cross-section of PVT module
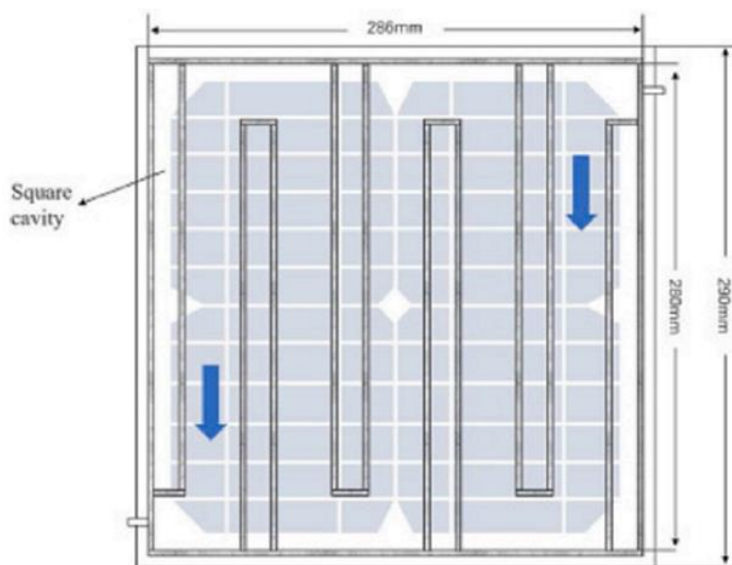
Figure II-7 Schematic diagram of solar PV module

Table II-1 Recent research conducted on the cooling process of solar systems employing pure phase change materials within 2020 and 2023, including study methodology, system configuration and setup, results obtained, and a concluding remarks.

Refs.	Year	PCM Used	Methods	Configuration	Results	Conclusion and notes
[52]	2023	Paraffin Wax (RT-42)	Experimental	Conducting experiments with various tilt degrees and thicknesses of phase change material (PCM) by affixing it to the rear surface of the panel.	With a thickness of 3 cm and a tilt angle of 30°, there is a 15.8% increase in electrical power and a 14.4% improvement in electrical efficiency.	The relationship between electrical power and efficiency is directly proportional to the thickness of the PCM (up to 3 cm) and the tilt angle (up to 30°).
[53]	2023	Hydrated salt (HS36) with latent heat 167 kJ/kg	Experimental	A trial configuration was devised and implemented at the institute's highest	The panel's operating temperature saw a reduction of 25.4%,	By incorporating phase change materials (PCMs) with various

				point, taking into account the latitude location and a tilt angle of 11.5°.	equivalent to a fall of 16.98 °C, while the electrical efficiency of the panel saw a rise of 17.5%.	encapsulating materials, the research may be expanded to include other kinds of PCMs suitable for diverse climatic conditions.
[54]	2022	PEG – Polyethylene glycol 1000 (melting temperature is 33–39 °C)	Experimental	Utilising phase change material (PCM) to capture excess heat emitted from the backside of solar panels, hence enhancing overall energy efficiency.	The system's electrical effectiveness has increased by 4.82%.	Phase change materials (PCMs) are valuable temperature regulators for photovoltaic (PV) solar cells.
[55]]	2022	Soybean wax	Software Simulation (Solar Simulator)	The solar cell panels were equipped with 50Wp polycrystalline solar cells. Some of the cells were blended with soybean wax, while others were not. A phase change material (PCM) container was used on the backplate of the panels to provide a passive cooling system.	The optimal temperature for Photovoltaic systems decreased from 60.7 °C to 54.7 °C when the intensity of sunlight was 1100 W/m2. Additionally, there was a 0.42% increase in the maximum efficiency of the system when the intensity was 900 W/m2.	The use of the soybean wax cooling technique has shown efficacy in reducing the temperature of PV.

[56]	2021	Polyethylene glycol 600 (PEG-600)	Experimental	PEG-600 has a melting temperature range of 23 to 26 °C. It is colourless, non-toxic, odourless, and non-acidic. And positioned on the rear surface of a 60 W photovoltaic panel.	The temperature decreases by 18.3 degrees and the efficiency increases by 2.45 percent.	Using materials with low melting points in areas with high ambient temperatures is not recommended.
[56]	2021	Paraffin	Experimental	The melting temperatures range from 56 to 58 °C. PCM is transparent, harmless, scentless, and non-acidic. positioned on the rear surface of a 60-watt photovoltaic panel	The temperature decreases by 40.2 °C, but the efficiency increases by 2.8%.	It is not advisable to use materials with low melting points in environments characterised by elevated ambient temperatures.
[57]	2020	RT-35HC (RUBITHERM) - Organic Paraffin PCM	Experimental	The experiments were conducted between 9 a.m. and 4 p.m. on days in July that had almost comparable environmental conditions. We used 30 monocrystalline PV panels with a power output of 30 watts each. The solar panel was positioned at an optimal tilt angle of around 34° (latitude angle: 33.7)	The temperature decreased by 11.9 degrees Celsius, but the electrical efficiency rose by 9.1 percent.	Using nanofluid in combination with PCM enhances system performance compared to using PCM alone. Moreover, a hybrid system consisting of PCM and nanofluid exhibits superior efficiency compared to the integrated PCM and water system.

				to maximise sun exposure and capture the most sunrays.		
[58]	2020	OM29	Experimental	In order to surmount the obstacle of conduction, a liquid phase change material (PCM) is positioned directly on the back surface of the photovoltaic (PV) module, allowing the PCM to directly absorb heat from the PV module. Moreover, the rear surface of the PCM is hermetically sealed using tin and aluminium to ensure that no leaks occur during the phase shift process.	The OM29 device effectively lowered the temperature of the PV module by an average of 1.2 °C till 08:30. Unfortunately, the OM29 PCM was unable to reduce it after 09:00.	The decreased melting point of the OM29 was associated with the inability of the supplied PCM to lower the operating temperature of the solar panel.
[59]	2020	Calcium Chloride Hexahydrate (CaCl2·6H2O)	Experimental with TRNSYS software simulation	The photovoltaic panels were placed in a "Sandwich model" for the PV-PCM panel. Two clear plexiglass sheets, each 8 mm thick, were fastened together using 5 mm screws.	There is a significant temperature decrease of 26.3 C (38% reduction) compared to the traditional PV module. With a significant increase in power output of	The maximum difference among the real and model results was 0.96% and 8.25%, suggesting a strong level of concurrence among both datasets.

				1.16 W (a 24.68% increase).	

II.1.12 Applications of PCMs in buildings

Hekimoglu et al. [60] successfully incorporated carbon-based nano additives into fly ash/octadecane shape-stabilized composite phase change materials (PCMs), demonstrating the potential of using fly ash, an industrial solid waste, to create eco-friendly composite PCMs.

Xu et al. [61] created a composite phase change material (PCM) for floor radiant heating. They used diatomite to minimise leakage and aluminium nitride (AlN) to improve thermal conductivity. The sodium acetate trihydrate-acetamide-AlN/diatomite SSPCM demonstrated exceptional thermal stability, with negligible effects on the phase change temperature and supercooling degree.

. Zhang et al. [62] used mica as a support material to create a composite phase change material (PCM) by decorating it with KH-550. The addition of EG improved the thermal conductivity of the mica/EG/PEG composite PCM. Huang et al. [63] used artificial culture techniques to produce a composite phase change material (PCM) consisting of diatoms and PEG. This PCM had a high melting latent enthalpy of 121.54 J/g and a high freezing latent enthalpy of 127.20 J/g. Additionally, it demonstrated an amazing relative enthalpy efficiency of 98.1%.

In their study, Yasiri et al. [64] examined how different thicknesses of typical expanded polystyrene (EPS) thermal insulation might improve the thermal performance of building envelope integrated phase change material (PCM) during hot summer months. The PCM-EPS rooms exhibited a significant improvement of 143% in maximum reduction of indoor temperature, 177.2% in time delay, 35% in average reduction of temperature fluctuation, and 8.5% in average reduction of operating temperature.

In a separate study, Ong et al. [65] investigated a passive cooling technique that involved adding microencapsulated PCMs and glass bubbles to paint and coatings on mortar panels in tropical regions. The PCM-based mortar panel, which included 30% PCM and 20% glass bubbles, showed notable decreases in surface temperature (3.2 °C) and ambient temperature (7.0 °C) in both laboratory and outdoor parametric studies. In a similar vein, Wi et al. [66] conducted research on optimising the external insulation plastering method by incorporating PCM to improve the efficiency of thermal energy utilisation.

II.1.13 Phase Change Materials (PCMs) used in sophisticated electronics for cooling and managing thermal conditions.

PCMs, in the field of electronics, are very important due to their capacity to control temperatures and handle the dispersion of heat. This is essential for ensuring the effective functioning and durability of electronic systems.

Liao et al. [67] presented a new kind of phase change material (PCM) film that has remarkable form stability and super elasticity. This film is well-suited for applications in the next generation of flexible heat management in electronics and wearable devices. The flexible film exhibited excellent long-term cycling stability after undergoing 700 heat cycles. Additionally, it had remarkable form foldability and stretchability, coupled with a high enthalpy value of 61.48 J/g. Conducted in a distinct research project

Zhang et al. [68] created flexible phase change films that had improved thermal and electrical conductivity. These films were particularly designed to effectively regulate heat.

Yang et al. [69] created a new CPCM that has outstanding characteristics and is especially tailored for efficient battery temperature control. The researchers developed a Composite Phase Change Material (CPCM) by using natural rubber as a flexible insulating layer between EG and OP44E PCM. This CPCM exhibited a high energy storage density of 156.5 J/g, enhanced resistivity of 2700 U/cm, and outstanding thermal conductivity of 3.4 W/m:K.

In their study, We et al. [70] introduced a novel approach for fabricating phase change composites that are leakage-proof, flexible, and highly thermally conductive. These composites find wide-ranging application in heat management, encompassing renewable energy thermal harvesting, building energy control, and electronic thermal management. At high discharge rates, the resulting flexible composite film effectively and dependably reduced the operational temperature of a commercial lithium-ion battery by more than 12 degrees Celsius.

Flexible PCM composite sheets were suggested by Ge et al. [71]. These sheets were composed of PCM PEG embedded in a polydimethylsiloxane matrix and single-walled carbon nanotubes. The PCM composite exhibited remarkable flexibility and resistance to bending and distortion at room temperature owing to the substantial bond angles and bond lengths of the SieOeSi backbones. Furthermore, it demonstrated exceptional microwave attenuation of over 20 dB and excellent frequency tunability spanning the entire 2e18 GHz range, all attained with a fixed CNT filling ratio of 0.2 vol%. In the interim, the composite material incorporated PEG at a

volumetric rate of 70% without compromising its mechanical strength or ability to prevent leakage. As a consequence, the latent heat storage density surpassed 110 J/g.

II.1.14 Application of PCMs in biomedical fields

Phase change materials (PCMs) have attracted considerable interest in biomedical applications owing to their exceptional thermal characteristics and capacity to store and discharge considerable energy during phase transitions. Thermoregulatory capabilities of these devices have demonstrated their worth in augmenting medical procedures, optimising drug delivery, and improving patient comfort. PCMs are utilised in a multitude of biomedical applications, such as medical transport, thermotherapy, cold compress therapy, drug delivery systems, anticancer therapies, wound healing, and bone cement.

Baniasadi et al. [72] created thermoregulating biomedical dressings using a combination of PEG and polycaprolactone. They also added gelatine and curcumin to improve the performance of the textiles in medical applications. The textiles containing curcumin displayed a latent heat of 61.7 J/g and showed consistent capacity to absorb and release energy throughout 100 cycles of heating and cooling. Initially, there was a rapid release of energy followed by a steady release over a period of one week.

Chen et al. [73] developed sophisticated carbon nanotube (CNT) bundles that were combined with flexible hierarchical framework-based phase change material (PCM) composites. This innovative design was aimed at achieving effective thermotherapy for allergic rhinitis, with enhanced performance. The structure was built by using table salt as a sacrificial template, leading to the formation of a hierarchical carbon nanotube (CNT) sponge. This sponge acted as a highly compatible and suitable host for polyethylene glycol (PEG). The pristine carbon nanotube (CNT) sponge shown exceptional efficacy in capturing particulate matter, but the CNT sponge infiltrated with polyethylene glycol (PEG) exhibited improved performance as a temperature regulator. This novel method has resulted in the development of a versatile PCM platform with intriguing characteristics, providing a fresh and exciting opportunity for cutting-edge biological applications. Zhou et al. [74] developed a technique to produce flexible phase change composites with two functional layers by combining a layer that undergoes phase change when exposed to light with a layer that conducts electricity when heated. This innovative method led to the development of a composite material that can undergo a phase transition and conduct electricity. As a consequence, it is well-suited for use in flexural heaters, medical electrothermal devices, and defrosting systems. Yu et al. [75] conducted a research where they created a textile that combines phase change and electrothermal functionalities. This

textile has shown promise for a wide range of practical applications. In addition, Ong et al. [76] sought to create a feasible method for preserving temperatures below freezing while transporting frozen blood samples. A heat-insulated system was developed using a phase change material (PCM) composed of 23.3% w/w seawater. This PCM was used to encapsulate a 1.5-mL vial containing frozen blood samples. Based on their model, they made a prediction that the phase change material (PCM), which was pre-cooled using dry ice, together with the vial sample originally held at 20 °C before a flight, would be able to maintain a consistent transport temperature of 20 °C for a minimum of 70 minutes.

II.2   Heat transmission improvement technique:

The low thermal conductivity of PCMs hampers their thermal response and prolongs the time required to store or release thermal energy, which restricts their widespread use. Thus, it is crucial to utilise heat transfer enhancement techniques in order to enhance the thermal response of PCMs, making them more suitable for utilisation in LHTES systems. Several techniques have been employed to improve the transmission of heat and address the subpar thermal efficiency of PCMs.

The strategies used in this study included the utilisation of extended metal surfaces (fins), the implementation of several phase change materials (cascaded storage), the dispersion of nanoparticles with high thermal conductivity into the phase change material, and the incorporation of permeable materials.
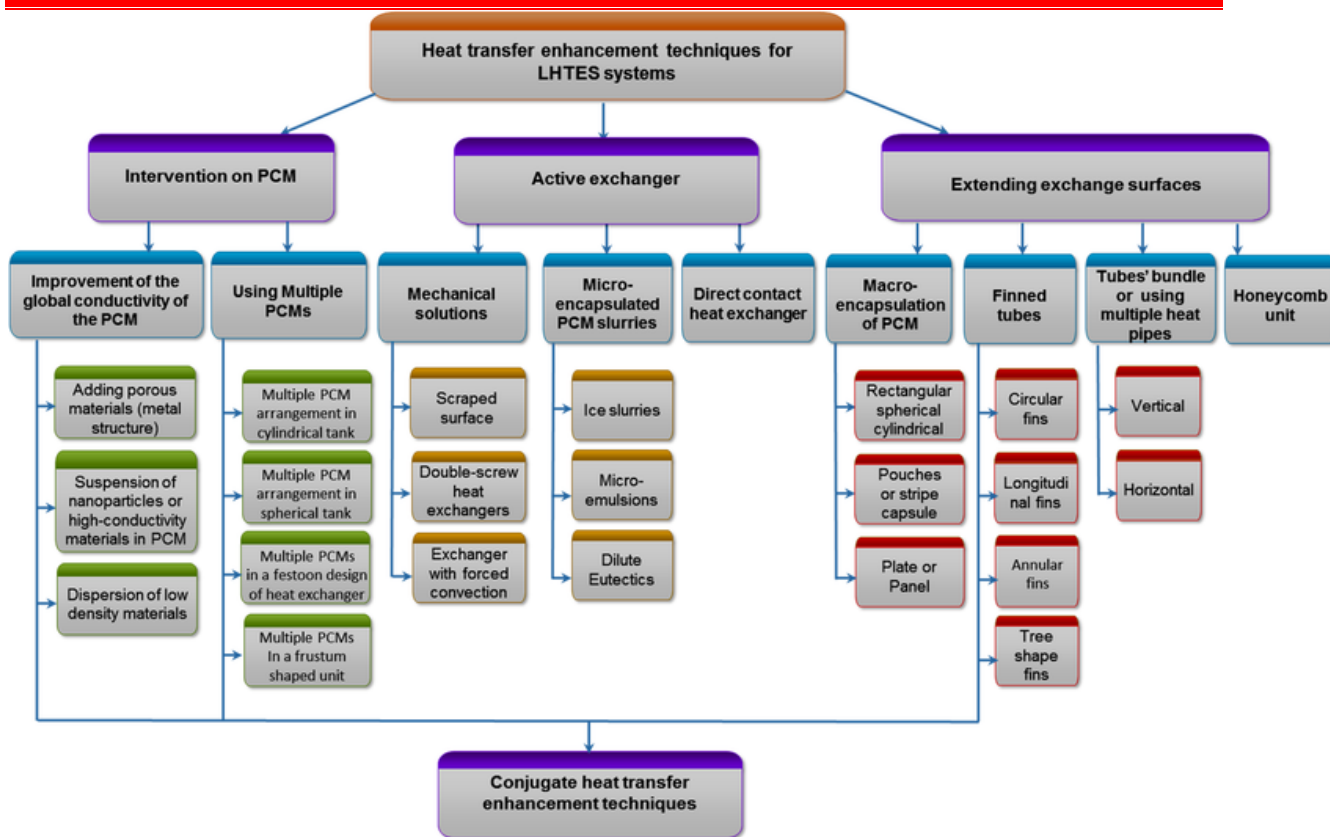
Figure II-8 Flow chart of different heat transfer enhancement techniques for LHTES systems

II.2.1 Fins:

The use of fins to improve the thermal efficiency of phase change materials (PCMs) is very advantageous due to its efficacy, cheap cost of construction, and simple manufacturing process [18]. Additionally, the design of the fins may be efficiently optimised by the use of computer simulation programmes, resulting in a reduction in research expenses. Fins enhance heat transfer between Phase Change Material (PCM) and Heat Transfer Fluid (HTF) by increasing the surface area available for heat transfer. Different kinds of fins, including as longitudinal fins and circular fins, have been used to improve the thermal efficiency of LHTES systems. Numerous researches have been published on the use of fins to improve the thermal efficiency of phase change materials (PCMs).

Qin et al. [77] performed a comparable experimental and numerical investigation, where they examined a rectangular container filled with RT43 as phase change material (PCM) and connected a single fin to one of the vertical sides that was being heated. The remaining walls of the container were thermally insulated. The rectangular fin was affixed to the vertical wall in five distinct orientations: 0◦, ±15◦, ±30◦. In each orientation, the edge of the fin that was

connected to the wall remained parallel to the ground. The digital camera captured the melting outlines, which are seen in Figure II 9.

The visual observation indicates that the presence of the fin speeds up the charging process at all degrees of inclination. This may also be quantitatively evaluated by referring to Figure II 9 - right. The melting process was expedited in the finned container with negative angles as compared to the container with positive angles.
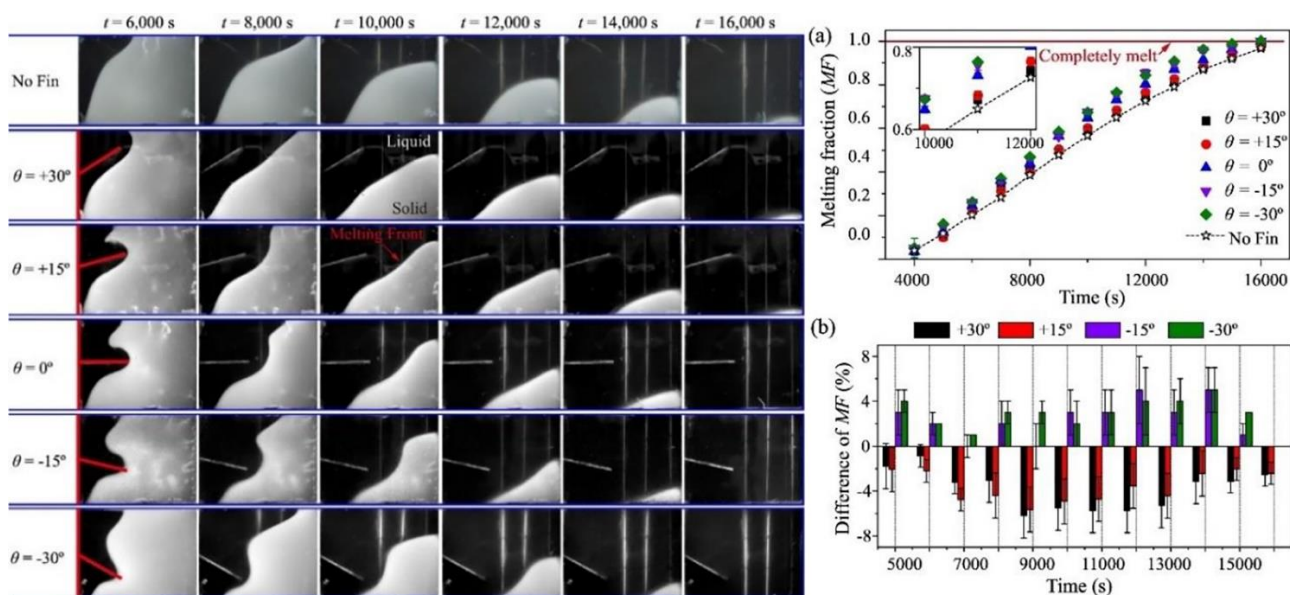
Figure II-9 The liquid/solid interface's progression [5] - left. LF and LF are the differences within the horizontal (baseline) and the angled wing.

The impact of the fin-type inserts on the dynamics of heat transmission gets more intricate as the LF (flow rate) rises. The inclusion of fins in the PCM mass significantly affects the development of natural convection flow. From this perspective, some fin configurations might impede the development of natural convection, resulting in the fins reducing heat transmission.

Al-Omari et al. [78] conducted a computational study on a heat sink that included vertical fins and a phase change material (PCM) enclosed between the fins. The fins were partly submerged in the PCM, namely Gallium. The metal base of the system was subjected to a heat flux, which was then dispersed via the fins to the surrounding air and the phase change material (PCM). The fins not only facilitated the transport of heat through the phase change material (PCM), but also generated a temperature differential inside the partly melted PCM, so enhancing natural convection. It has been discovered that the fins play a crucial function in restricting the temperature at high levels of heat flow.

Saeed et al. [79] conducted a computational study on a unique shape. This geometry consists of a pear-shaped confinement, which is made up of a hemisphere and a cone with a shared base. The vertex of the cone is positioned on the opposite side of the base compared to the hemisphere, and it points in the direction of $\vec{g}$. Additionally, there is an internal fin that is connected to the highest point of the spherical part. Please refer to Figure II 10 for a visual representation. The enclosure was filled with n-octadecane, a liquid compound, in which Al2O3 nanoparticles were evenly distributed at three distinct concentration levels: 0%, 3%, and 6%. The primary discoveries that have been reported are as follows: (1) The heat transmission rate exhibited a positive correlation with the concentration of Al_2O_3. (2) Among the several types of fins, the Y-shaped fins had the highest heat transmission rate. By studying the Y-shaped design variations, it is evident that they have the least impact on the creation of natural convection flows. This finding describes the superior heat transmission performance stated by the authors.

.

Two transverse fins   Y-shaped   T-shaped
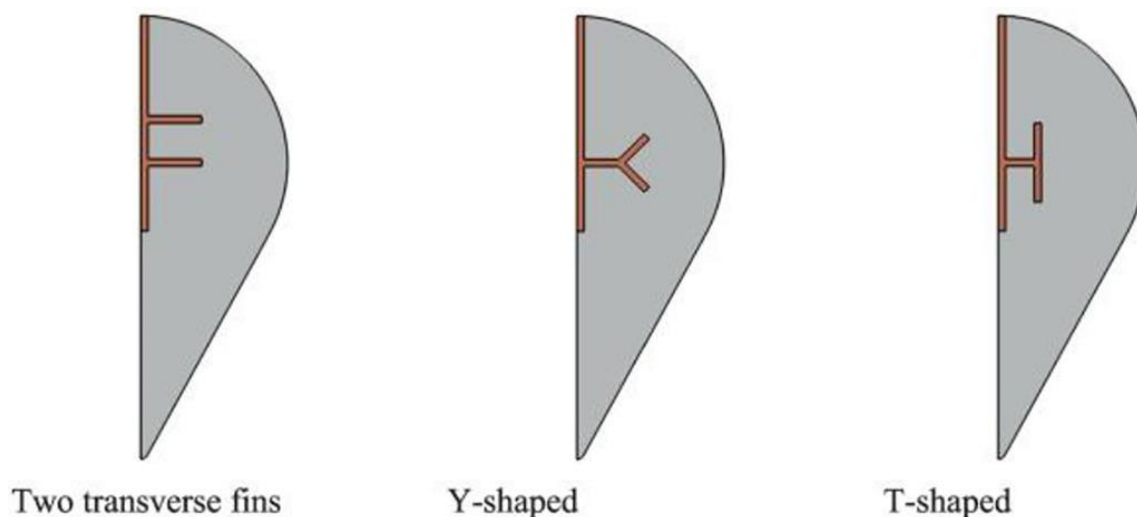
Figure II-10 . Container in the form of a pear with a variety of copper fin configurations

Laouer et al. [80] performed computational research to investigate the impact of three fins affixed to the heated bottom wall of a PCM-loaded cavity (Figure II 10) on the heat transfer rate. The values of the dimensionless fin length, a/H, and the dimensionless fin location, b/L, were altered. Figure II 12 displays the isothermal contour and the border between the liquid and solid phases.
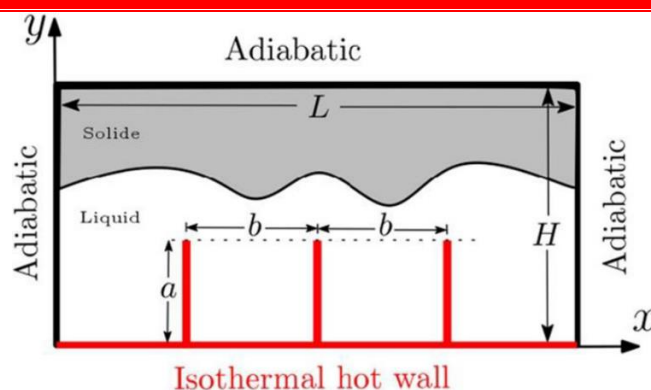
Figure II-11 PCM-filled enclosure with heat transfer enhancement fins
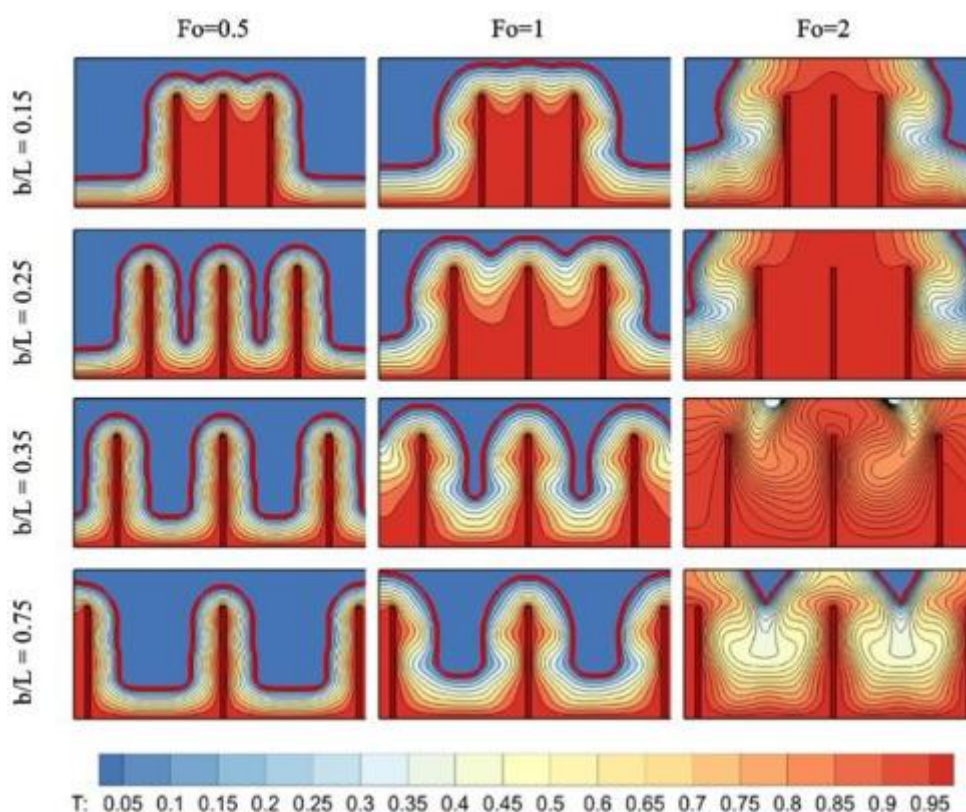
Figure II-12 Effect of the wing dimensions and layout on the charging procedure: temperature contour and solid/liquid boundary (a/H = 0.75, Ra = 105)

Izgi [81] performed a computational analysis on the motion of a phase shift in a phase transition material (PCM) inside an enclosed vertical cylinder. The cylinder had a diameter of 30 mm and a height of 170 mm. The study focused on the impact of introducing four longitudinal fins along the cylinder wall, extending from the base to the top. The fins had a width ranging from 6 to 12 mm, a length of 170 mm, and a thickness of 1 mm. The analysis was conducted under microgravity conditions. The PCM unit's total mass experienced a rise of 13.5%, 10.5%, and 7.2% respectively when fins with non-dimensional widths (width/radius) of 0.8, 0.6, and 0.4 were utilized. The investigation yielded the subsequent findings.:

The melting process is significantly prolonged by 39% in microgravity circumstances compared to normal gravity.

The inclusion of fins resulted in a reduction in charging time by 79%, 58%, and 30% for non-dimensional width values of 0.8, 0.6, and 0.4, respectively.

The addition of fins results in a substantial reduction in the stored energy per unit mass. The biggest decrease, amounting to 17.6%, is seen for non-dimensional fin widths of 0.8. This is followed by reductions of 13.7% and 9.4% for fin widths of 0.6 and 0.4, respectively. The section's analysis of many researches yields some incomplete conclusions:

The fins have distinct effects on the processes of melting and solidification. The vertical fins do not impede the upward flow of buoyant fluid that occurs throughout the charging process, whereas the straight fins impede the formation of convective flows. The impact of the tilted fins relies on the angle at which they are positioned. The vertical fins have a major role in reducing the stored energy per unit of system mass.

Tiari et al. [82] introduced a design for a horizontal annular fin with a diameter that may vary. The system included a vertical axis shell-and-tube heat exchanger, seen in Figure II 13, which had a central finned pipe for circulating a high-temperature fluid (water at 70 ∘C). The finned tube was submerged in RT55. The shell was constructed using a transparent acrylic tube with a height of 30 cm and an interior diameter of 19 cm. For comparative purposes, a baseline example was examined, which had a tube without any fins.
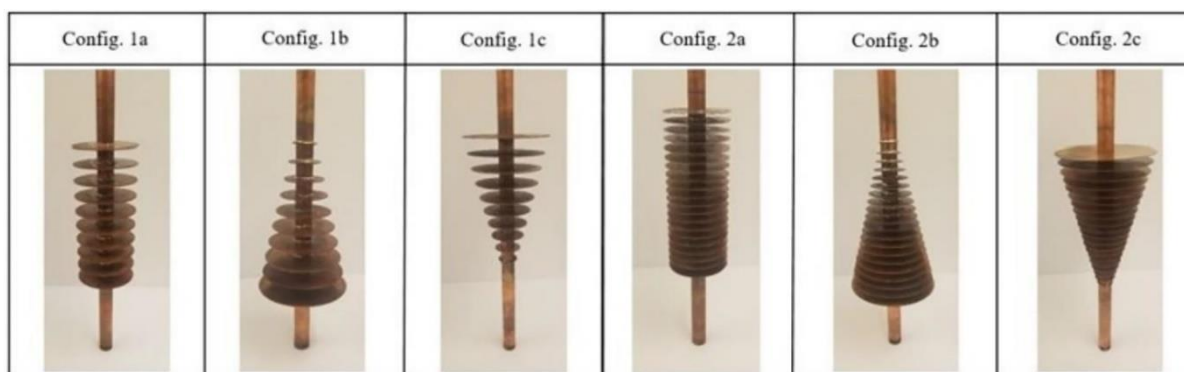
Figure II-13 Finned cylinder shape

In their study, He et al. [83] introduced a new fin design specifically aimed at mitigating the drawbacks of circular horizontal fins, which impede the creation and progression of natural convection flows. The LHS system included a vertical axis shell-and-tube exchanger including a central tube for the circulation of a high-temperature fluid (HTF). Two distinct kinds of fins were examined, as seen in Figure II 14: (1) The annular fins HSU has 12 fins evenly spaced at

a distance of 34 mm on the central tube. The fins have a thickness of 3 mm and a diameter of 100 mm. (2) The spiral finned HS unit is made up of spiral fins that are welded onto the HTF tube. The fins are spaced at equal intervals of 34 mm, have a thickness of 3 mm, and a diameter of 100 mm. The results presented in [83] are as follows: - In comparison to the UF-LHSU and AF-LHSU, the SFLHSU saw a 300% increase in charging rate and a 5.7% rise in solidification rate. Additionally, the solidification rate of SFLHSU rose by 793.5% compared to UF-LHSU and by 14.6% compared to AF-LHSU. No information provided. Spiral fins had a reduced inhibitory impact on free convection motions. The average Nusselt values for SF-LHSU are 2.7% higher compared to UF-LHSU and 28.6% higher compared to AF-LHSU. Based on these data, it can be deduced that both annular and spiral fins have a substantial inhibitory impact on passive convection. However, the inhibitory impact of the spiral fin is diminished.
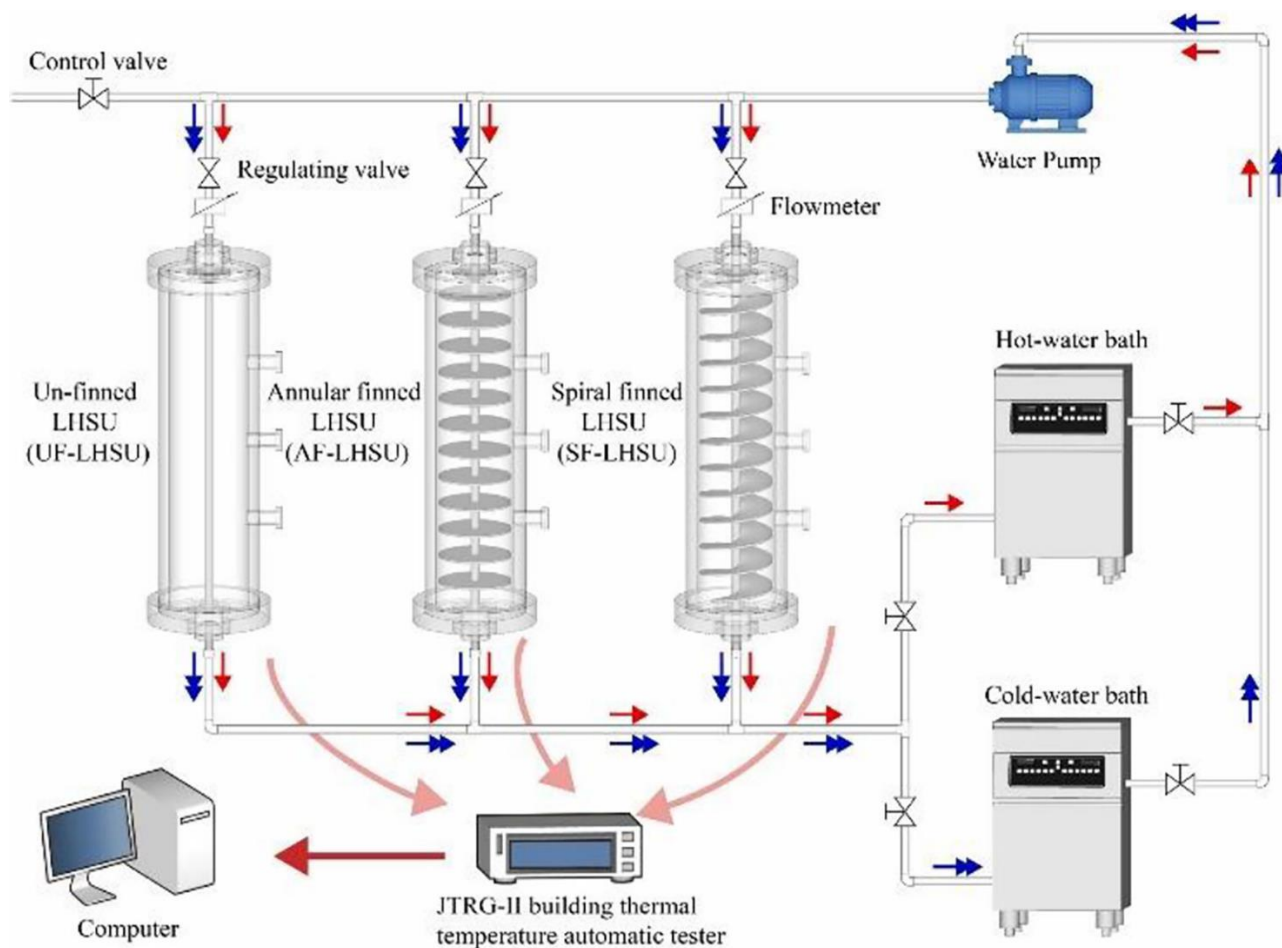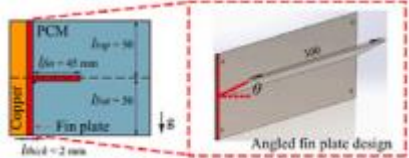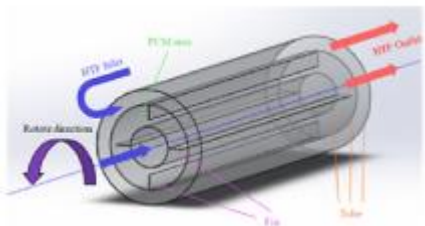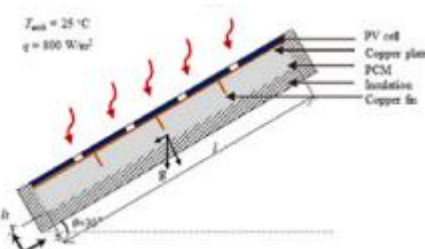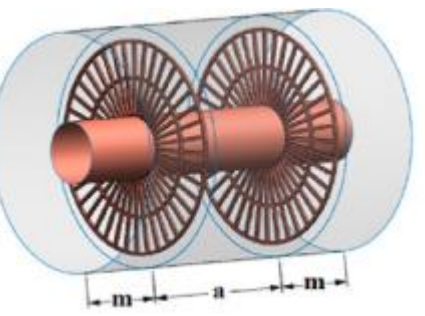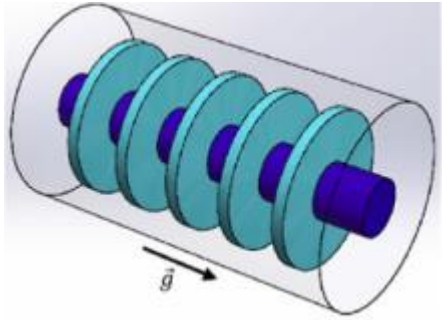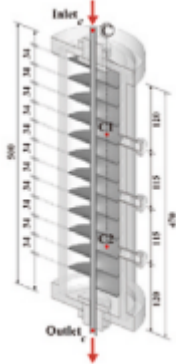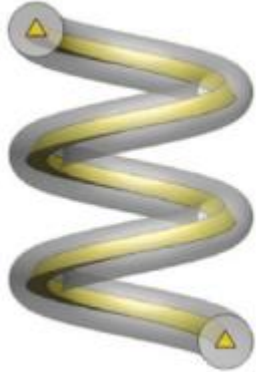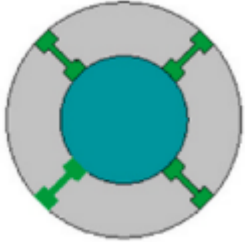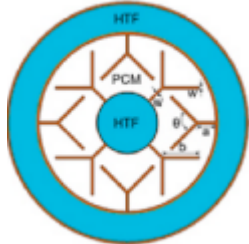
Figure II-14 Schematic of the system described in [16].

In a separate experimental examination, Li et al. [84] examined how the combination of fin shape and nano-additives loading affects the heat storage performance of a finned shell-and-tube thermal energy storage (TES) unit loaded with nano-improved phase change material (PCM). The study involved nine different experimental configurations, which included three
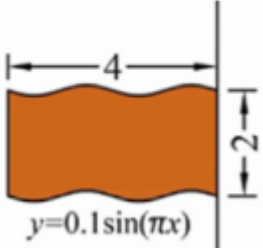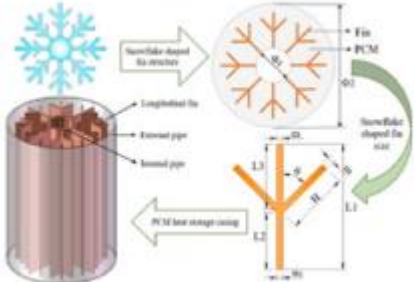
different loadings of graphene nanoplatelets nanoparticles and three different fin shapes (annular, helical, and longitudinal). It was discovered that the longitudinal fin, which has the greatest heat transmission area when the fin volume ratio is equal, had an advantage during the first phase of charging. A notable discovery from this research was that the efficiency of heat transmission is influenced by the combination of fin type and nanoparticle loading.

Table II-2 Studies on different fins by many scholars in recent years.

Fin shape	Fin material	Melting enhances the effect	Author	Fin shape Fin material Melting enhances the effect Author Structures of fin
Rectangular fin	Copper, Steel	5.2%	Qin et al. (2022) [85]	
Rectangular fin	Copper	45.99%	Huang et al. (2023) [86]	
Rectangular fin	Copper	4.62%	Zhang et al. (2023) [87]	
Annular fin	Copper	27%	Sanchouli et al. (2022) [88]	

Annular fin	Aluminium	41.4%	Shahsavar et al. (2020) [89]	
Helical fin	Aluminum	20.9%	He et al. (2023) [90]	
Helical fin	Aluminum	23%	Najafabadi et al. (2023) [91]	
I-shaped fin	Aluminum	9.28%	Choudhari et al. (2020) [92]	
Y-shaped fin	Copper	66%	Yan et al. (2022) [93]	

Wave shaped fin	Copper, Aluminum	65.74%	Khaboshan et al. (2023) [94]	
Snowflake shaped fin	Copper, Aluminum, Steel	45.59%	Ren et al. (2022) [95]	

II.2.2 Enhancement by utilizing multiple PC

One efficient method to enhance thermal control in a heat exchange unit with phase change materials (PCM) is to use several PCMs organised in layers, allowing the heat transfer fluid (HTF) to flow along either an axial or circular channel. Several phase change materials (PCMs) are arranged in a strategic, axial, or circular manner to enhance the flow of heat transfer fluid (HTF). PCMs, or phase change materials, have the ability to efficiently retain and release energy throughout phase transitions, enabling accurate temperature regulation. The thermal energy storage capacity of many phase change material (PCM) layers rise, making it ideal for effectively managing temperatures over long periods or for handling variable heat loads. Design flexibility may be achieved by choosing axial and circular paths for the flow of heat transfer fluid (HTF). This study demonstrates the collaboration between material science and engineering to enhance energy efficiency and sustainability in many fields, including solar power systems and industrial processes. Figure II-15 illustrates the generally used arrangement by most writers, regardless of variations in system orientation and the amount of PCMs.
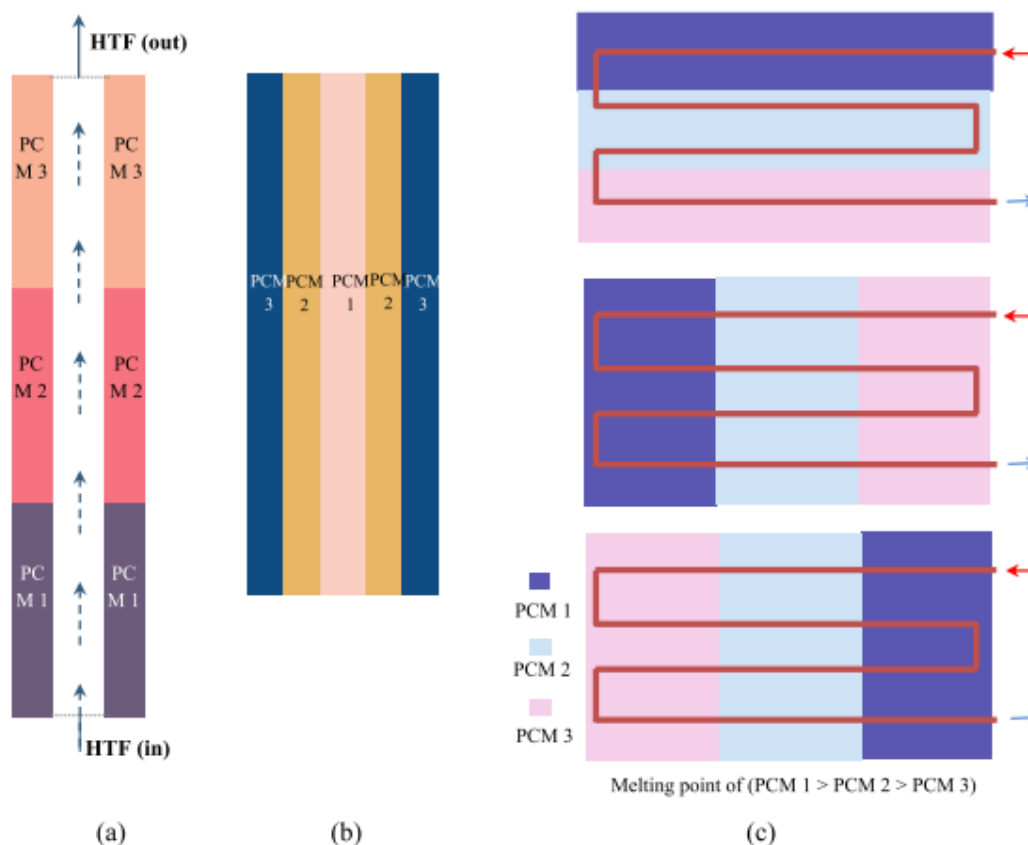
Figure II-15 Numerous forms of multiple-PCMs: a) Physical representation of various phase change material (PCM) configuration, b) cylindrical or capsule shape, and c) Festoon design H

Sun et al. [96] introduced a thermal conductivity model that showed a direct correlation between the input temperature of the heat transfer fluid (HTF) and the thermal and exergy storage of the CPCES system. The exergy efficiency was negatively affected by the quality of HTF.

Cheng et al. [97] created a one-dimensional dispersion-concentric model to optimise the structure of a CPCES configuration that contains several encapsulated PCMs. The findings from the experiment and simulation showed that the configuration of CPCES was advantageous in decreasing the time it takes to charge and raising the average rate of charging. In addition, it was advised to use 3-5 phases since they exhibited thermal characteristics that were most comparable to the 24 stages.

Zhang et al. [98] proposed the use of multiple phase change materials (PCMs) in combination with finned heat exchangers to enhance the rate at which thermal energy is stored in a configuration known as CPCES. The findings demonstrated that when numerous Phase Change Materials (PCMs) were present in the optimal proportion of 6:4, the duration required

for charging was shortened by 29% and the efficiency of heat storage was enhanced by 9% in comparison to using a single PCM.

Guo et al. [99] used CPCES technology in the packed bed thermal energy storage (PBTES) system. The cascade PBTES system exhibited a 6.96% enhancement in the average heat transfer rate when compared to the non-cascade PBTES system.

Elbahjaoui et al. [100] presented that the solar thermal energy storage device, when combined with the CPCES unit, had superior collecting efficiency. In addition, the limited temperature range of phase change materials (PCMs) significantly restricted the overall performance and energy storage capacity in building envelopes. Kishore et al. [101] used CPCES technology with adjustable PCMs to achieve energy conservation and load regulation throughout heating and cooling seasons. In comparison to traditional LHTES units, this particular unit has the capability to double the utilisation of PCMs. Additionally, it may result in a significant decrease of 99% in peak cooling load and 34% in peak heating loads. Based on the study provided, it is clear that the CPCES technology demonstrates a lucrative enhancement for traditional single PCM. Figure II-16 summarises the usual models of CPCES units, including simulation methodologies, enhancements, and application analysis. The purpose is to provide a reference for future study.
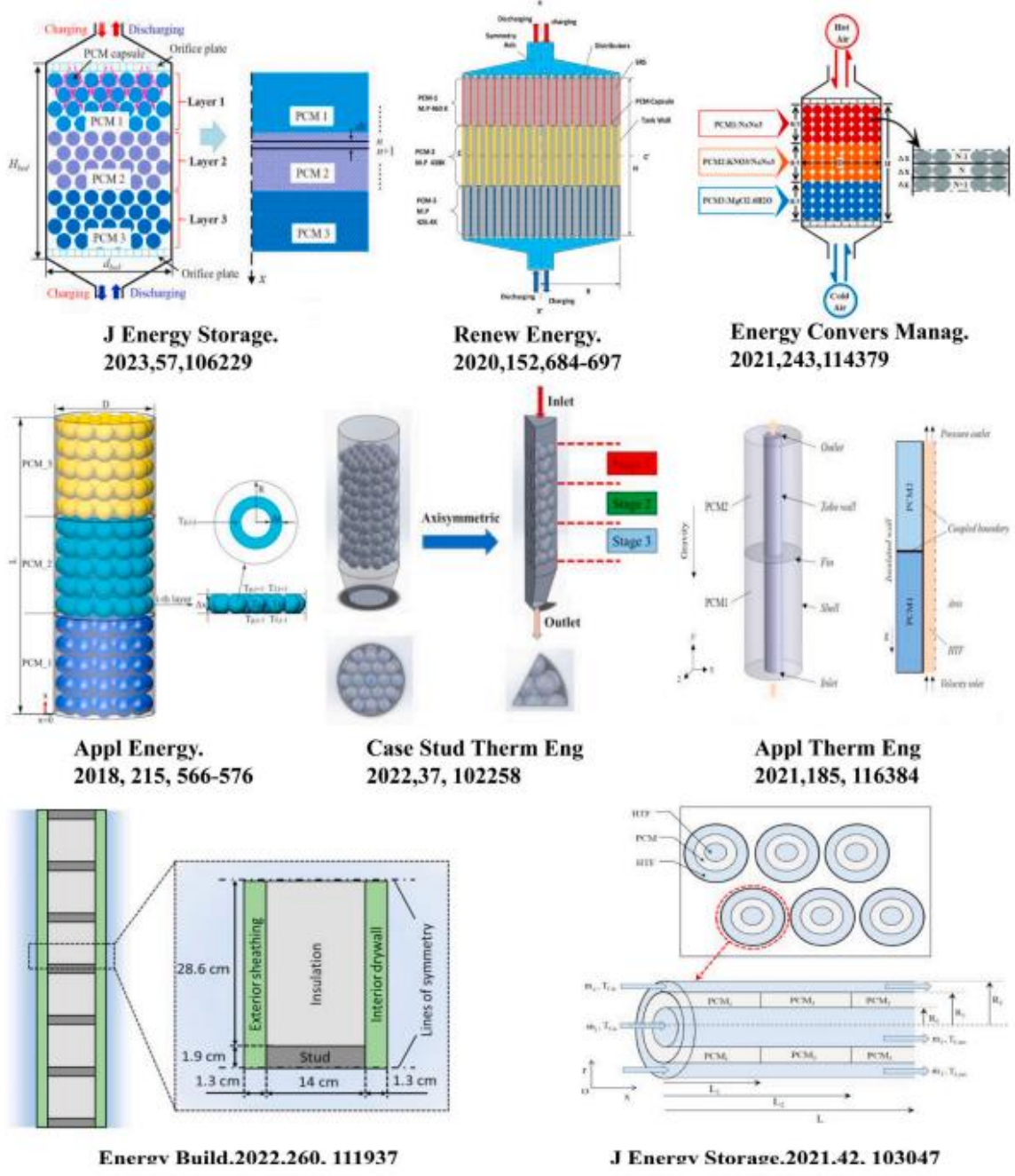
Figure II-16 The computational models stated in the overhead studies [97]–[106]

II.2.3 Enhancement by using nanoparticle:

Nanoparticles, also known as NPs, may effectively increase heat transfer in phase change materials (PCMs). Nanoparticles (NPs) may be used either as the primary method of enhancement or in conjunction with other enhancement strategies. These approaches include the usage of nano-enhanced phase change materials (PCMs) combined with highly conductive porous materials and multiple PCMs, as well as the incorporation of fins and heat pipes in nano-enhanced PCMs. Nanoparticles (NPs) enhance the overall thermal conductivity of a material without altering the volume of the phase change material (PCM).

Table II-3 Studies on nano-enhanced PCMs

Method	Temperature range (°C)	NePCMs	Experimental studies	Number of studies	Both	References
NePCMs as a sole enhancement	Low (14.8 to 85)	Cu, CuO, Al$_2$O$_3$, TiO2, MgO, ZnO, MWCNTs, Graphene, Si$_2$, multi-wall carbon nanotube, CeO$_2$, Ag, Fe$_2$O$_3$, Carbon, Al	16	11	3	[107]– [116] [117]– [127] [128]– [134]
	Middle (120– 250)	Graphene, COOH-functionalized graphene nanoplatelets (f-GNP), TiO2, CNTs, SiO2, Al2O3, MgO	6	1	1	([135]– [142]
	High (306– 399.7)	Al2O3, CuO, SiO2, and ZnO	3	0	0	[143]– [145]
NePCMs Combined with Fins	Low (0–85)	Cu, CuO, Al2O3, MOS2–TiO2, with fins, branched, and stair fins	0	7	0	[146]– [152]
NePCMs combined with Heat Pipes	h Heat Pipes Low (44–57)	Graphite nano-platelets, Cu, CuO, Al2O3, Ag, with horizontal, and finned heat pipes				[153]– [156]
	High (335– 485.85)	Cu, CuO, Al2O3, metal foam with finned heat pipes				[157]– [159]

	Low (41–62)	Nano-AlN, carbon nanotubes, graphene, Cu, Al, Fe, and Ni, CuO, Al2O3, with graphite, aluminum, and copper foam				[160], [161]
NePCMs combined with Highly conductive porous media	Middle (120)	Carbon nanotubes, Al, Ag, graphene NPs, with carbon foams				[160], [162]
	High (383.5)	Expanded graphite and SiO2, NPs	1	0	0	[163], [164]

II.2.4 Enhancement by using metal foam

Metal foams, such as aluminium and copper, possess a significant degree of porosity and exhibit excellent thermal conductivity. As a result, they are used to enhance the thermal efficiency of phase change materials (PCMs).

Sardari et al. [165] demonstrated an 85% reduction in melting time while using metal foam soaked with PCM. The influence of metallic foam is contingent upon its geometric parameters, which ascertain the volume percentage and properties of the pores. Zhu et al [166] conducted a study on the efficiency of a metal foam heat sink that was partly filled with RT40. The dimensions of the heat sink were 707025 mm3. The height of the metal foam filling δ has been varied from 0 to the entire height of the phase change material (PCM). The significance of heat conductivity is heightened by the cavity's tiny height. Comparing the heater temperature, it has been observed that the metal foam with a thickness of $\delta = 2/3$ and $\delta = 1$ exhibit similar performance at source powers of 40 W and 80 W. However, increasing the filling height ratio from 0 to 2/3 leads to a decrease in temperature to 40°C at a thermal load of 80 W.

Table II-4 Prior research has focused on the impact of nano-additives and metal foam on the melting behaviour of phase change materials (PCM).

Author, Ref	Study type	Heat transfer enhancers	Focus	Results

Mahdi et al. **[167]** (2020)	Num	Nanoparticles Al2O3, aluminum foam $0.92 \leq \varepsilon \leq 0.98$	A heat exchanger consisting of various segments of phase change material (PCM) and either metal foam or non-equilibrium phase change material (NePCM) is used.	Raising the concentration of nanoparticles to 5% may result in a 19% increase in the rate of solidification. Employing metal foam with progressively higher porosity towards the outer radius results in a reduction of solidification time exceeding 90%.
Heyhat et al. **[168]** (2020)	Num	Copper nanoparticles ($\varphi \leq$ 7%), copper foam ($\varepsilon \geq$ 0.85), copper concentric fins	Enhancing heat transmission in Li-ion battery thermal control via the use of various latent heat techniques.	The battery's heat dissipation powers of 4.6 W and 9.2 W have been taken into account, and the subsequent indications have been accomplished: At both power levels, nanoparticles do not have a substantial influence. However, the use of metal foam results in a reduction of the average temperature by 4°K and 6°K, respectively. Similarly, the implementation of copper fins leads to a temperature drop of 2°K and 4°K.
Nematpou rKeshteli**[169]**	Num	Nanoparticles metal oxides, metal foam $0.92 \leq \varepsilon \leq 0.95$	An investigation on the three-dimensional melting and freezing process of a NePCM (Nano-enhanced Phase Change Material) in a solar collector, considering the	The inclusion of metal foam results in a reduction of the charging time by 84.38%. When NePCM and metal foam are combined, the charging time may be lowered by 85.16%.

			inclusion of metal foam and a wavy-wall.	
Hashem Zadeh et al. **[170]** (2020)	Num	Cu/GO nano-additives ($0 \leq \varphi \leq 8\%$), metal foam ($0.8 \leq \varepsilon \leq 1$)	A a 2-D LHTES designs containing two inside heat pipelines clad in metal foam and loaded with NePCM	The system's effective heat capacity is reduced by the occurrence of particles and foam, which is caused by a drop in the volume fraction of the PCM. However, by intensifying conduction, it becomes possible to increase the charging power. When the enclosure is fully saturated with foam, the charging power, as measured by the storage capacity, experiences a rise of about 70-fold, but the heat capacity of the system reduces by 17%. Nanoparticles have a lesser impact compared to partial metal foam.
Farahani et al. **[171]** (2021)	Num	Al_2O_3, Fe_3O_4, CuO nanoaddtives ($\varphi \leq 3\%$), aluminum porous fin ($\varepsilon = 0.2$, $\varepsilon = 0.5$, $\varepsilon = 0.8$)	The cross section depicts a triple tube containing Helium Phase Change Material (HePCM) in the outer and middle layers, which is further improved by radial foam fins.	Aluminium oxide nanoparticles have the most favourable outcomes in terms of accelerating the solidification process. Research has shown that the inclusion of nanoparticles may decrease the duration of solidification by as much as 60%. By decreasing the amount of empty space inside a material and lowering the ratio of viscous forces to

				inertial forces, the duration required for melting may be lowered by 27%.
Li et al. [172] (2022)	Num	Nanoparticles Al2O3, copper foam $0.90 \leq \varepsilon \leq 0.96$ (pore size 5 mm)	Melting process of NePCM in a macroscale homogeneous porous region $10 \times 10 \times 30$ mm3	The inclusion of 1% nanoparticles may decrease the melting time by 7.77%. The permeable insert mitigates the impact of nanoparticles. At a value of $\varepsilon = 0.96$, the addition of nanoparticles at a mass fraction of 1% results in a reduction in the melting time by 2.55%.
Amudhala palli et al. [173] (2023)	Num	Graphene nanoplatelets ($\varphi \leq 1\%$), copper foam ($\varepsilon \geq 0.93$)	A shell and tube heat exchanger. The impact of permeability and the number of particles.	The phase transition rate exhibits the most notable alterations within the porosity range of 0.95 to 0.97. The most rapid melting is found when the value of ε is 0.93 and the value of φ is 1%.
Bondareva et al. 2024 [174]	Num	Al2O3 nanoparticles ($\varphi \leq 2\%$), copper foam ($\varepsilon \geq 0.9$)	The process of liquefaction of nano-improved lauric acid in a rectangular chamber that is only partly occupied by metal foam.	Nanoparticles expedite the process of melting, but, the temperature of the heater does not diminish. The foam filling capacity directly affects the duration it takes for the foam to melt and the distribution of temperature in the region. The most significant variations are noticed within the range of $0.5 \leq \delta \leq 1$.

II.2.5 Enhancement by using expanded graphite

The thermal conductivity of liquid PCMs may be enhanced and the heat transfer rates of LHTES systems can be increased by combining them with expanded graphite, which has a high absorbability and high thermal conductivity.

Lu et al. [175] examined PA/EG composites with varying mass percentages and investigated the impact of EG concentration on thermal conductivity. Jiang et al. [176] synthesised a composite material consisting of polyamide (PA) and ethylene glycol (EG) with a high thermal conductivity. They then used this material to improve the thermal management of lithium-ion batteries, resulting in a considerable reduction in the batteries' temperature increase. Karami et al. [177] implemented thermal control of the surface of a PV module by incorporating ethylene glycol (EG) into phase change material (PCM). They investigated how the amount of EG affected the temperature distribution throughout the PV module.

II.2.6 Enhancement by modifying the geometry of the heat exchanger

Shell and multi-tube LHTESS is regarded as a pragmatic method for enhancing the heat transfer efficiency of the system [178].

In their work, Punniakodi et al. [179] used three heat transfer fluid (HTF) tubes arranged in a triangle configuration to investigate the processes of melting and solidification of phase change material (PCM) in a horizontal container. The most efficient setup was the arrangement of tubes, with a single high temperature fluid (HTF) tube positioned towards the lowest section of the shell.
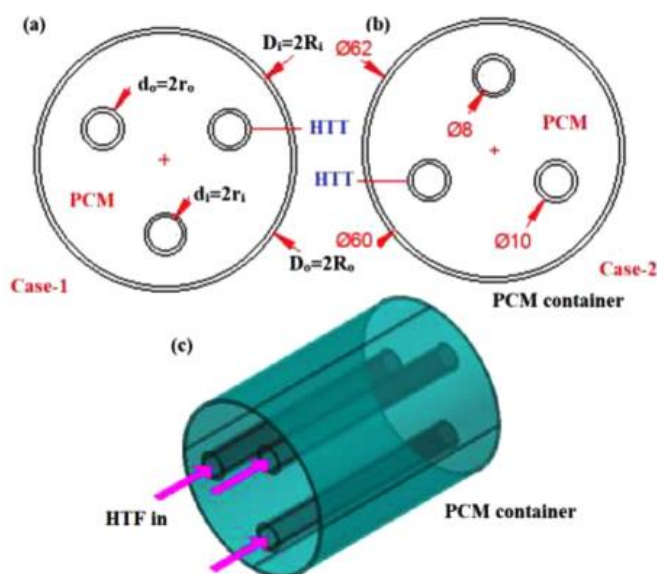
Figure II-17 PCM container and HTF tube arrangements: (a) Case-1, (b) Case-2, (c) HTF flow direction and PCM container (Dimensions are in mm).

Ma et al. [180] led sensitivity analysis and optimisation to assess the impact of various structural parameters on the charging performance of a multi-tube heat exchanger that uses PCM. These parameters included the number of tubes (factor A), eccentric distance to shell (factor B), angle ratio (factor C), and tube wall thickness (factor D). The study revealed that component A and factor B had substantial influence on the charge rate, but factor C and factor D had no discernible impact. In addition, the uneven arrangement of tube locations results in a 5.21% higher charging rate compared to the evenly distributed arrangement.
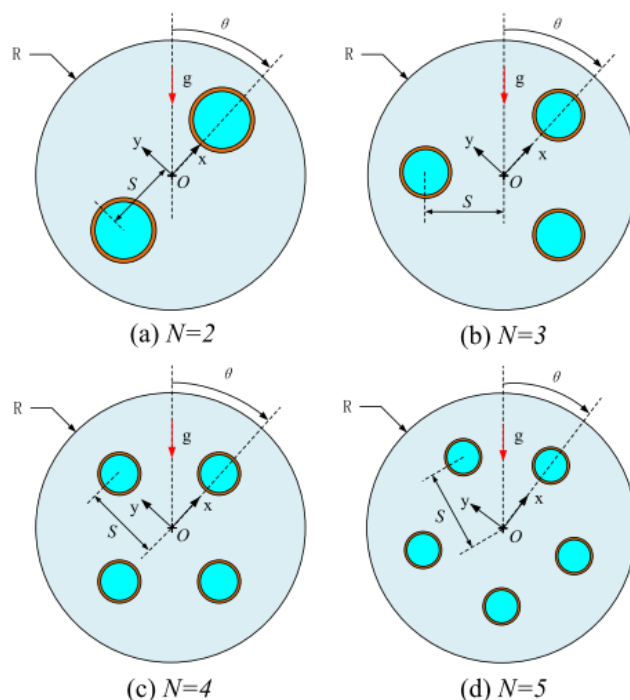
Figure II-18 Definition of structural parameters for multi-tube heat exchanger with different

Harmen et al. [181] investigated how the eccentricity of a multi-tube storage unit affects the efficiency of charging and freezing processes. The charging time of ideal eccentricities was improved by 54%, 60%, 63%, and 63% for the single tube, double tube, triple tube, and quadruple tube, respectively, as to the concentric case.
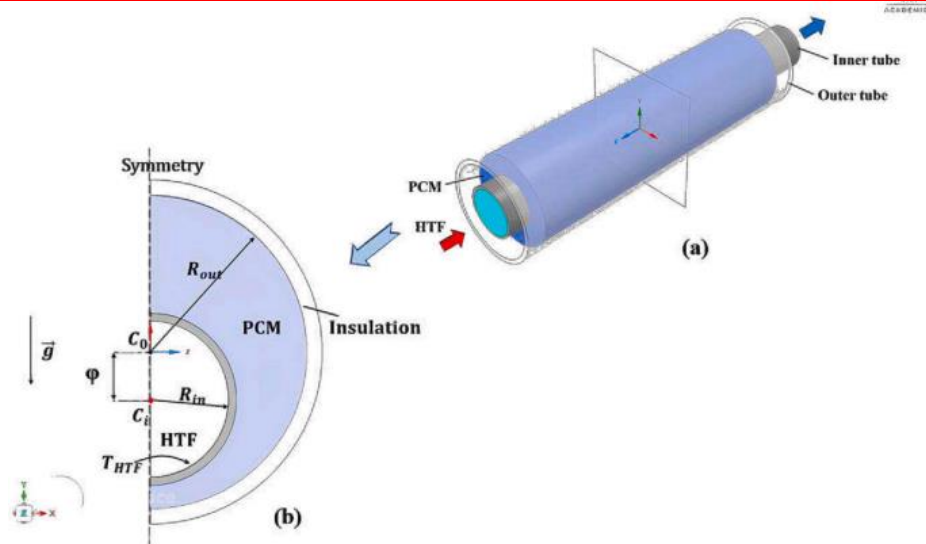
Fig. 1. Three-dimensional schematic of the physical model: horizontal single-tube LTES unit (a) and two-dimensional diagram of the computational model (b).
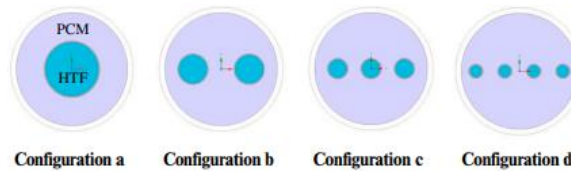
Figure II-19 Physical models: configuration a: single-tube, configuration b: two-tube, configuration c: three-tube and configuration d: four-tube

Vikas et al. [182] led a computational study to examine the melting and freezing behaviour of a shell and multi-tube latent heat thermal energy storage system (LHTESS). The purpose was to determine the most appropriate arrangement of multiple heat transfer fluid (HTF) tubes. After evaluating nine tubes arranged in eight different configurations, it was discovered that the staggered array with a high ratio of tube pitch to tube diameter worked better than the inline array.
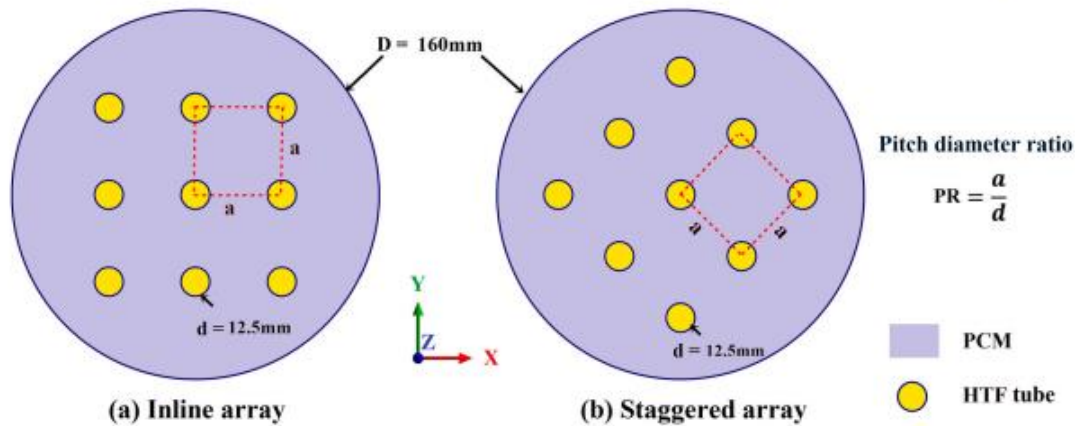
Figure II-20 The proposed MT-LHSS arrays. (a) Inline array, (b) Staggered array.

Alizadeh et al. [183] led a computational study to improve the thermal performance of a STHX by using the Koch snowflake fractal design for the inner tube. The high-temperature fluid (HTF) passes through a tube with a cross-section that follows the Koch snowflake fractal pattern. The phase change material (PCM) is located on the outside side of the tube. The Galerkin Finite Element Technique was used to model the solidification process of PCM (water). A 2D computational model was used for the study. The impact of the first three iterations (n) of the fractal pattern on the solidification process of the PCM was examined, as seen in Figure II-21. The findings demonstrated that using the Koch snowflake fractal pattern cross-section with increased iterations expedited the solidification process. This is a result of the expansion in the surface area for heat transfer and the improvement in the depth at which thermal energy may penetrate.

The colour code:
- Pipes
- HTF
- PCM
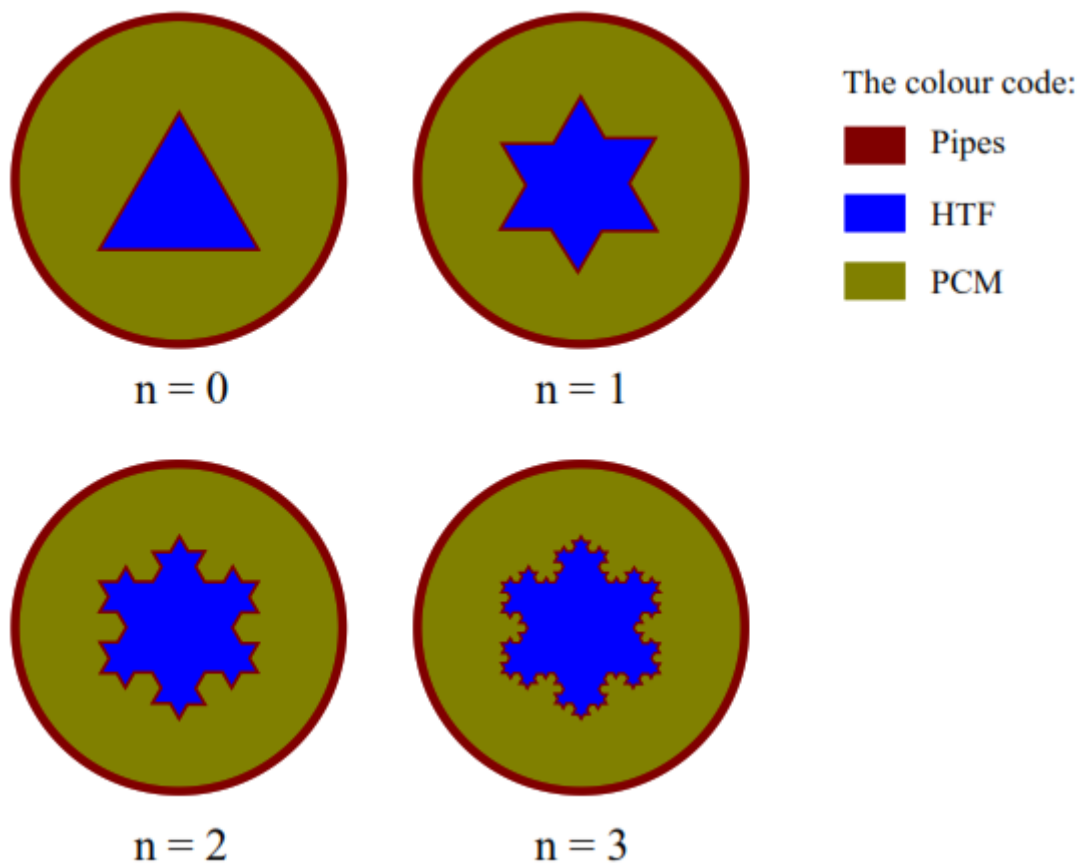
Figure II-21 The LHTES system incorporates the Koch snowflake spiral design for the inner tube of the heat transfer fluid (HTF).

.

Pourakabar and Darzi [193] conducted a computational investigation on the melting and solidification processes of phase change material (PCM) in a shell-and-tube heat exchanger (STHX). They explored different shell forms and varied the number of inner tubes to determine the optimal design (Figure II-21). A new elliptical shell form was created and compared to the traditional circular design. The phase change material (PCM) was positioned in the outer shell, while the heat transfer fluid (HTF) flowed through the inner tube/tubes. The findings indicated that the circular shell form with four inner tubes arranged in a diamond array yielded the fastest complete melting and solidification time.
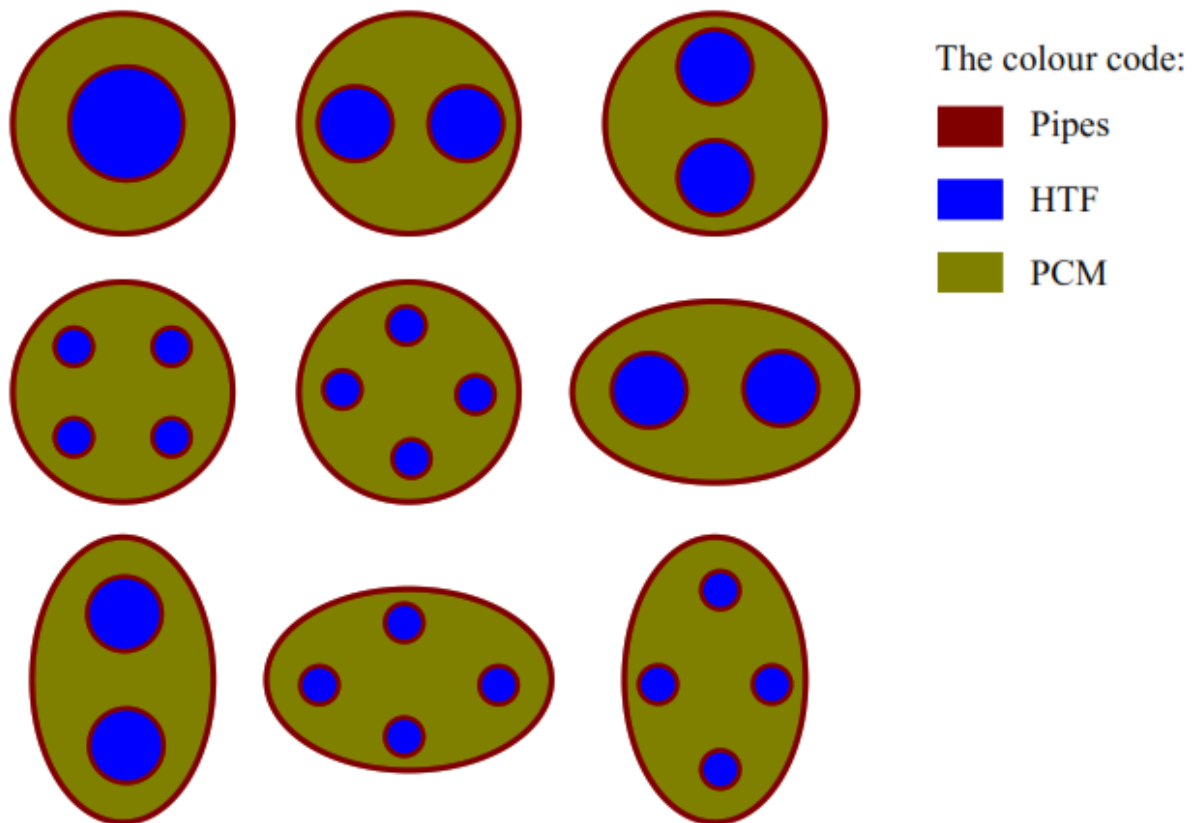
Figure II-22 Various physical configurations of a Shell-and-Tube Heat Exchanger (STHX) with varying shell forms and numbers of inner tubes.

Energy storage systems rectify the energy generation-demand imbalance and store extra or free energy that would otherwise be squandered. Energy storage might be mechanical, electronic, or thermal. The thermal energy storage technology is cheaper and denser than previous methods. Three mechanisms store thermal energy: sensible, latent, and thermochemical. Latent heat storage is chosen over sensible heat storage due to its large energy storage capacity and low temperature change. With the same volume, latent heat storage materials may store 5-14 times more energy than sensible heat storage materials. Latent heat storage materials are PCMs. A key drawback of PCMs is their low heat conductivity. Heat transfer improvement methods have been proposed to increase PCM thermal performance. Fins, porous materials, high thermal conductivity nanoparticles in the PCM, and numerous PCMs were used to improve heat transmission.

Utmost heat transmission improvement approaches of PCMs employ fins because of their simple design, cheap cost, and minimal maintenance, compared to nanoparticle dispersion and porous materials. Fins improved PCM thermal performance more than nanoparticles [15, 89]. Longitudinal, annular, plates, and pin fins were examined to increase energy storage system

thermal performance. Using longitudinal fins improved thermal performance, particularly with cylindrical PCM containers.

The inclusion of fins on the phase change material (PCM) side of the latent heat thermal energy storage (LHTES) systems does not affect the flow of the heat transfer fluid (HTF) and does not cause any drop in pressure. This characteristic gives them a distinct advantage over other systems that are not based on phase change materials (PCMs). Although there has been much research on using fins to improve the thermal efficiency of PCMs TES systems, there has been very little attention given to the geometric configuration of fins. The geometric configuration of fins significantly impacts the storage and release of energy in thermal energy storage (TES) systems that use phase change materials (PCMs) [2]. Further investigation is necessary to examine potential novel geometric configurations of the fins in order to enhance the thermal efficiency of PCMs-LHTES systems and decrease the time needed for charging and discharging.

This thesis proposes novel fin designs to enhance the thermal efficiency of thermal energy storage systems utilising phase change materials (PCMs). The recommended fin designs are then contrasted with conventional fin shapes to assess their effectiveness.

Furthermore, this literature study has demonstrated that modifying the heat exchanger design can improve the thermal efficiency of PCM TES systems.   Heat exchangers need to be built in a way that allows for a fast pace of storing and releasing thermal energy by increasing the surface area for the transmission of heat. As a result, a novel configuration for an exchange of heat

The computational techniques provide a solid foundation for resolving the phase transition issue. The intricacy of the phase shift issue has led to the majority of computational and analytical approaches for PCMs issues published so far being based on one or two-dimensional space. You may save both time and money by optimising the creation of PCM TES systems via computational modelling.

II.3 Conclusion

This chapter provides a comprehensive discussion of the definition, characteristics, and applications of phase change materials. And A synthesis of the various works relating to these subjects has been carried out to clarify and understand the characteristics of the PCM and heat transfer enhancement techniques.

Chapter: Numerical Methodology

3

CHAPTER.III   : Mathematical Methodology

T his chapter presents the equations that are involved in the heat transmission process for materials undergoing a phase shift. The defining characteristic of the charging (phase change) procedure, known as the Stefan issue, is the existence of a dynamic border between the solid and liquid phases. The calculation of heat transfer becomes more sophisticated owing to the challenge of simulating the velocity field. The numerical simulations in this study use COMSOL Multiphysics. The mathematical equations used to solve the charging procedure in COMSOL Multiphysics rely on the finite element approach and the enthalpy-permeability methodology.

III.1.1   COMSOL Multiphysics

COMSOL Multiphysics is a computational modelling software that enables the study and optimisation of designs and processes based on physics principles. This research project used COMSOL to examine the thermal impacts in a room by conducting a heat transfer analysis. COMSOL is advantageous for two primary reasons: it allows for the implementation of phase transition materials (PCM) in heat transfer analysis, and it enables the simulation of design-based parameters to a great degree.

COMSOL contains two physics modules which could be combined to form an accurate representation of an PCM container

- Heat transmission module – to study the heat transmission processes through solids and liquids on convection, conduction and radiation in detail.

- Fluid flow module – to study the laminar and/or turbulent flow of the air inside a cavity.

Initial simulations have shown that the combination of the heat transmission and liquid motion modules results in a complex and time-consuming set-up of the model. Since the scope of this project involves the simulation and evaluation of various parameters on both thermal and visual level, the studies have to become manageable with representative outcomes. Hence, only the heat transfer module is applied within a 2D simulation space to produce results regarding the temperature differences and functioning of the PCM.

Table III-1 The Properties of the PCM and the Copper

Properties material	RT-27		Copper
T_m (K)	300		
ΔH, (kJ/kg)	189		
k, (W/mK)	liquid	0.15	
	solid	0.35	401
ρ, (kg/m^3)	liquid	774	
	solid	814	8933
Source: **Durakovic and Torlak [185] and Kraiem et al. [186]**			

III.1.2   Governing equations

The governing equations containing all definitions utilised in this simulation are provided in Table 2. The equations (1–3) illustrate the Navier-Stokes equations. V represents the total flow velocity, which comprises the velocity component u in the radial direction and the velocity component v in the angular direction (θ). In addition, in order, P, ρ, μ, and, β are the pressure, density, dynamic viscosity, and thermal expansion coefficient. The last element on the right-hand side of the momentum equations (Eqs. (2) and (3)) represents the damping effect of Darcy's law. The constant A_{mush} corresponds to the mushy zone, while ε is a tiny value (0.001) in the denominator to prevent division by zero. Moreover, γ represents the proportion of liquid in a substance, which is calculated by considering changes in temperature, as shown in Equation (4). Equation (5) is the energy equation for PCM, where h denotes the sensitive enthalpy obtained using Equation (6). In Equation (6), the terms h_{ref} and C_p represent the reference enthalpy at the reference temperature and the specific heat capacity, respectively. The

calculation of the latent heat (ΔH) may be determined using the fusion latent heat (Γ), as shown in Equation (7). The thermophysical parameters of NPCM, including as dynamic viscosity, latent heat, thermal expansion coefficient, density, specific heat capacity, and thermal conductivity, may be determined using the formulae given in Table 3. The equations include three variables: np, pcm, and npcm, which represent nanoparticle, pure PCM, and NPCM, respectively. Additionally, φ denotes the volume percentage of nanoparticles.

Table III-2 The governing equations and definitions used

Equation	Expression	
Navier Stokes	$$\nabla \cdot V = 0$$	**III-1**
	$$\frac{\partial u}{\partial t} + V \cdot \nabla \cdot u = -\frac{1}{\rho_{npcm}} \nabla P + \frac{\mu_{npcm}}{\rho_{npcm}} \nabla^2 u + A_{mush} u \frac{(1-\gamma)^2}{\gamma^3 + \varepsilon}$$	**III-2**
	$$\frac{\partial v}{\partial t} + V \cdot \nabla \cdot v = -\frac{1}{\rho_{npcm}} \nabla P + \frac{\mu_{npcm}}{\rho_{npcm}} \nabla^2 v + \beta_{npcm} \vec{g}(T - T_{ref})$$ $$+ A_{mush} v \frac{(1-\gamma)^2}{\gamma^3 + \varepsilon}$$	**III-3**
Liquid fraction	$$\gamma = \begin{cases} 0 & \text{if } T < T_s \\ (T - T_s)/(T_1 - T_s) & \text{if } T_s < T < T_1 \\ 1 & \text{if } T > T_1 \end{cases}$$	**III-4**
Energy	$$\frac{\partial h}{\partial t} + \frac{\partial(\Delta H)}{\partial t} + \nabla \cdot (Vh) = \nabla \cdot \left(\frac{k_{npcm}}{(\rho C_p)_{npcm}} \nabla H \right)$$	**III-5**
Sensible Enthalpy	$$h = h_{ref} + \int_{T_{ref}}^{T} C_p dT$$	**III-6**
Latent heat	$$\Delta H = \gamma . \Gamma$$	**III-7**

Table III-3 The correlations employed in this investigation to determine the properties of NPCMs

Property	Equation		Unit	Ref.
Viscosity	$$\mu_{\text{npcm}} = 0.983 e^{(12.95\rho_p)}{}_{pcm}$$	**III-8**	N s/m2	[187]

Density	$\rho_{\text{npcm}} = \varphi_{\text{n}}\rho_{\text{np}} + (1 - \varphi)\rho_{\text{pcm}}$	**III-9**	**kg/m3**	[188]
Specific heat capacity	$\left(\rho C_{\text{p}}\right)_{\text{mpcm}} = \varphi\left(\rho C_{\text{p}}\right)_{\text{mp}} + (1 - \varphi)\left(\rho C_{\text{p}}\right)_{\text{pcm}}$	**III-10**	**J/kg K**	[188]
Latent heat thermal	$(\rho\Gamma)_{\text{mpcm}} = (1 - \varphi)(\rho\Gamma)_{pcm}$	**III-11**	**J/kg**	[187]]
Expansion coefficient	$(\rho\beta)_{\text{npcm}} = \varphi(\rho\beta)_{\text{np}} + (1 - \varphi)(\rho\beta)_{\text{pcm}}$	**III-12**	**1/ K**	[189]
Thermal conductivity	k_{npcm} $= \dfrac{k_{\text{np}} + 2k_{\text{pcm}} - 2\left(k_{\text{pcm}} - k_{\text{np}}\right)\varphi}{k_{\text{np}} + 2k_{\text{pcm}} + \left(k_{\text{pcm}} - k_{\text{np}}\right)\varphi}k_{\text{pcm}}$	**III-13**	**W/m K**	[188]

Table III-4 nanoparticle inputs in this model [196]		
Parameter	**Typical Range/Example Value**	**Units**
Nanoparticle Type	Copper (Cu)	-
Nanoparticle Size	50	Nanometers (nm)
Nanoparticle Concentration	$0 - 8$	Percentage (%)
Size Distribution	$\pm 5 - \pm 20$	Nanometers (nm)
Geometric Shape	Spherical	-

Thermal Conductivity	401	Watts/meter.Kelvin (W/m.K)
Interaction with PCM	High (depending on surface treatment)	-
Chemical Stability	Good (in inert environments)	-
Cost [79]	$50 - 500$	Dollars/kilogram (USD/kg)

The local entropy generation rate includes the thermal and frictional entropy generation rates, which are given by Eq. (13) and Eq. (14):

$$S_f'' = \frac{\mu}{T}\left\{2\left[\left(\frac{\partial v_x}{\partial x}\right)^2 + \left(\frac{\partial v_y}{\partial y}\right)^2\right] + \left(\frac{\partial v_x}{\partial y} + \frac{\partial v_y}{\partial x}\right)^2\right\} \qquad \text{III-14}$$

$$S_T'' = \frac{k}{T^2}\left[\left(\frac{\partial T}{\partial x}\right)^2 + \left(\frac{\partial T}{\partial y}\right)^2\right] \qquad \text{III-15}$$

The global entropy generation rate of the entire domain is computed as the integral of the local rates over the entire volume Eqs. (14) and (15) as

$$\dot{S}_f = \int_s S_f^{s''} ds \qquad \text{III-16}$$

$$\dot{S}_T = \int_s S_T'' ds \qquad \text{III-16}$$

Where:

$$\dot{S}_{\text{Tot}} = \dot{S}_T + \dot{S}_f \qquad \text{III-17}$$

The mean and local Nusselt numbers are of the form

$$Nu_m = \int_0^1 Nu \, dY \qquad Nu = -\frac{\partial \theta}{\partial X} \qquad \text{III-18}$$

The average Bejan number is defined as

$$Be_{\text{avg}} = \frac{S_T}{S_{\text{Tot}}}$$

III-19

III.1.3 Validation:

The existing model, represented by equations (1)– (5), has a significant degree of non-linearity. Consequently, the COMSOL programme was used to seamlessly integrate the energy and momentum equations, taking into account the specified boundary and starting conditions. This integration was done using the Galerkin weighted residual finite element technique developed by Bayat et al. [185] and Bashirpour-Bonab [190]. The present partial differential equations also use the weak form transformation. The heat and momentum equations were interconnected using Newton's constant method. The PARDISO Coupled Direct Solver was used for the computing procedure in each time step of the simulation process. The solver was run for eight iterations with a damping factor of 0.9 until the residual value of 0.001 was reached. For more details, refer to the works of Schenk and Gartner [191] and Zienkiewicz et al. [192]. The research used the Galerkin weighted residual finite element method because to its ability to decrease the complexity of the issue and provide a dependable approximation solution. The calculation cell is divided of non-uniform triangular pieces. In order to verify the accuracy of the numerical method used for converting the authorised code, the liquid fraction was compared to the findings of Darzi et al. [193].
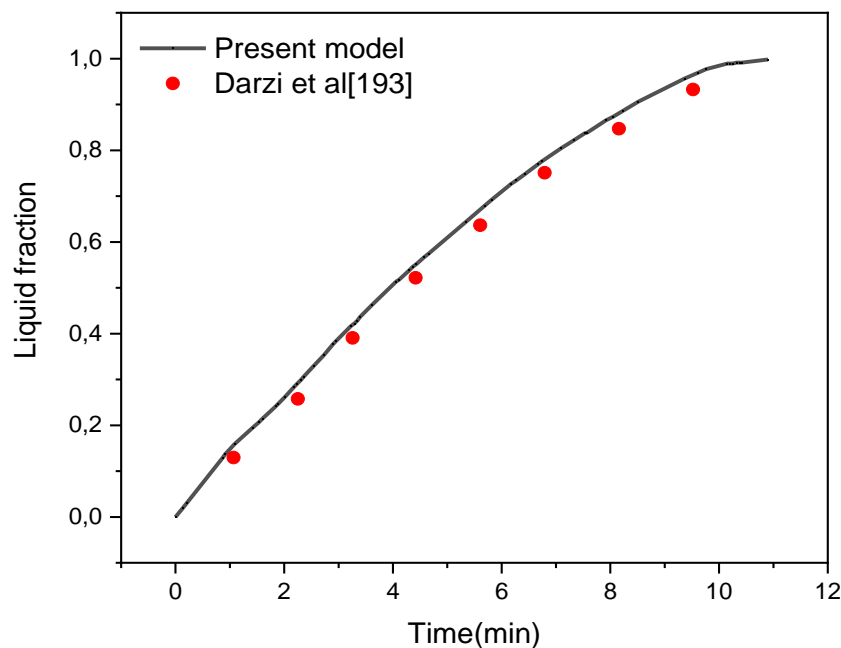
Figure III-1 Comparison of the findings presented by Darzi et al. [193] with the results of the present study

CHAPTER: First Study:

Insight into latent heat thermal energy storage: RT27 phase transition material conveying copper nanoparticles experiencing entropy generation with four distinct stepped fin surfaces

CHAPTER.IV : Insight into latent heat thermal energy storage: RT27 phase transition material conveying copper nanoparticles experiencing entropy generation with four distinct stepped fin surfaces

IV.1.1 Techniques of the investigation:

The LHTES system, consisting of two stair fins, is shown diagrammatically in Figure IV-1. Paraffin-loaded cage was supplemented with copper nanoparticles. The selected PCM has a significant latent heat capacity and demonstrates chemical durability. The dimensions of the cage, namely its width (D) and height (L), remained unchanged at 50 mm and 132 mm, respectively. The right wall was subjected to a heating power of 1000 W per square metre, while the other three walls were insulated. The nano-enhanced phase change material (PCM) was first heated to a temperature of 300 Kelvin. The stair fins were positioned in both upward and downward orientations. The geometric characteristics are fully shown in Figure 1. According to Figure 1, the stair fins had a thickness of 4 mm. Four distinct instances were simulated. In their study, Arshad et al. [194] found that the effectiveness of a phase change material (PCM) used in a heat sink is influenced by the volume of the PCM and the number of fins. They conducted an experimental examination to examine the impact of pin-fin thickness on a PCM heat sink for different input heat fluxes. The research used RT-27 and copper nanoparticles because of their special phase transition properties, which allow them to melt and solidify at precise temperatures. This makes them suitable for temperature control in a wide range of applications**.**
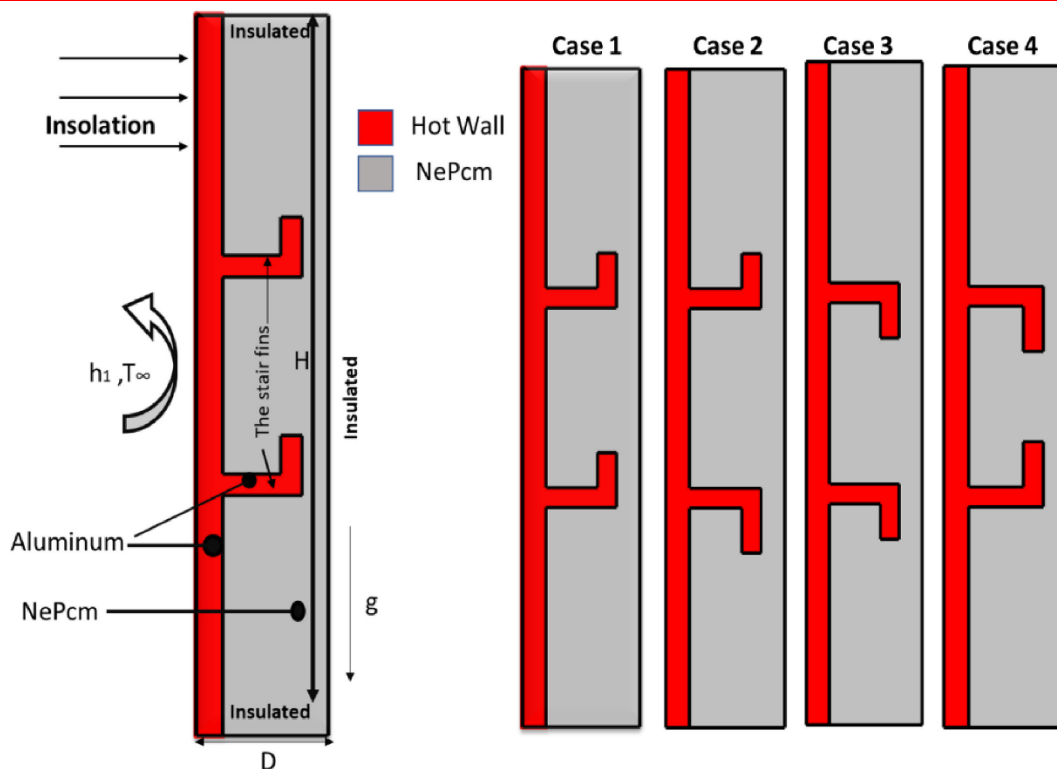
Figure IV-1 Diagram of four distinct stepped fins connected to a latent heat thermal energy storage system.

IV.1.2   Results and discussion:

The research analysed the temperature circulation, liquid percentage, thermal entropy, and frictional entropy at four different time intervals (10 minutes, 30 minutes, 60 minutes, and 90 minutes) for two fins with upward steps and two fins with downward steps, as depicted in Figure IV 2 and Figure IV 3. During the first 10 minutes, heat energy is mostly transferred to the vertical heated wall and the two upward stepped fins due to the established temperature gradient. A study conducted by Durakovic and Torlak [185] examined the usage of phase change materials (PCMs) in a temperature-responsive window system consisting of Rubitherm RT 27 and air. The study found that the heat gain into the interior can be reduced by increasing the time it takes for the PCM to melt and by adding a thicker layer of the PCM. The presence of the occurrence is also apparent, as seen in Figure IV-4 for the scenario involving fins that step upwards and downwards. After 60 minutes, the temperature differential had caused substantial heat conduction. As a result, the heat energy distribution was discovered to be highly concentrated and exceeding 334K. Heat transfer occurs as a result of the accelerated movement of atoms and molecules in a material when it is heated, and this process is dependent on time. Moreover, the larger the temperature disparity between thermal storage, the more rapidly heat energy dissipates from the hotter region. Arshad et al. [194] discovered that including paraffin

wax in the free cooling system of electronic devices using PCM reduces the base temperature of the heat sink, hence increasing the duration of operation for the electronic device. The minimal liquid percentage at the insulated walls may be readily determined during the first time period of $0 \leq t \leq 30$ minutes. After 30 minutes, it is clear that the liquid percentage around the two fins that are stepped upwards reached their maximum value. Indeed, when the duration exceeds 30 minutes, it becomes evident that the two fins, which are stepped in an upward direction, have the ability to impact the proportion of liquid present. Ma et al. [195] investigated the impact of the Reynolds number on the rate of frictional entropy formation, and observed that it is growing. It has been shown that the rate at which frictional entropy is produced in the dynamics of water carrying alumina nanoparticles increases as the Reynolds number increases.
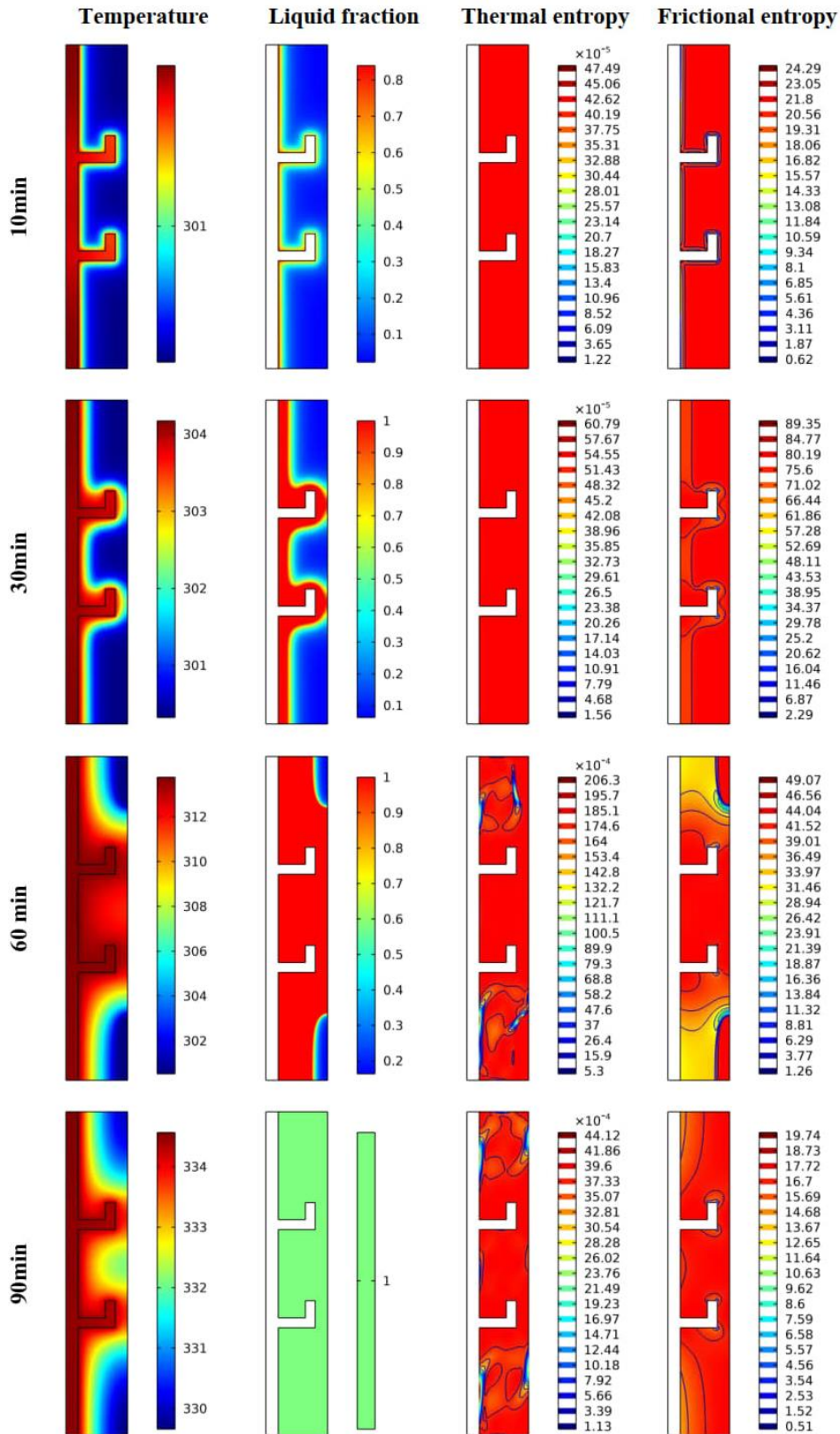
Figure IV-2 The temperature propagation, liquid percentage, thermal entropy, and frictional entropy at four specific time points are being analysed for the two-upward stepped fins.
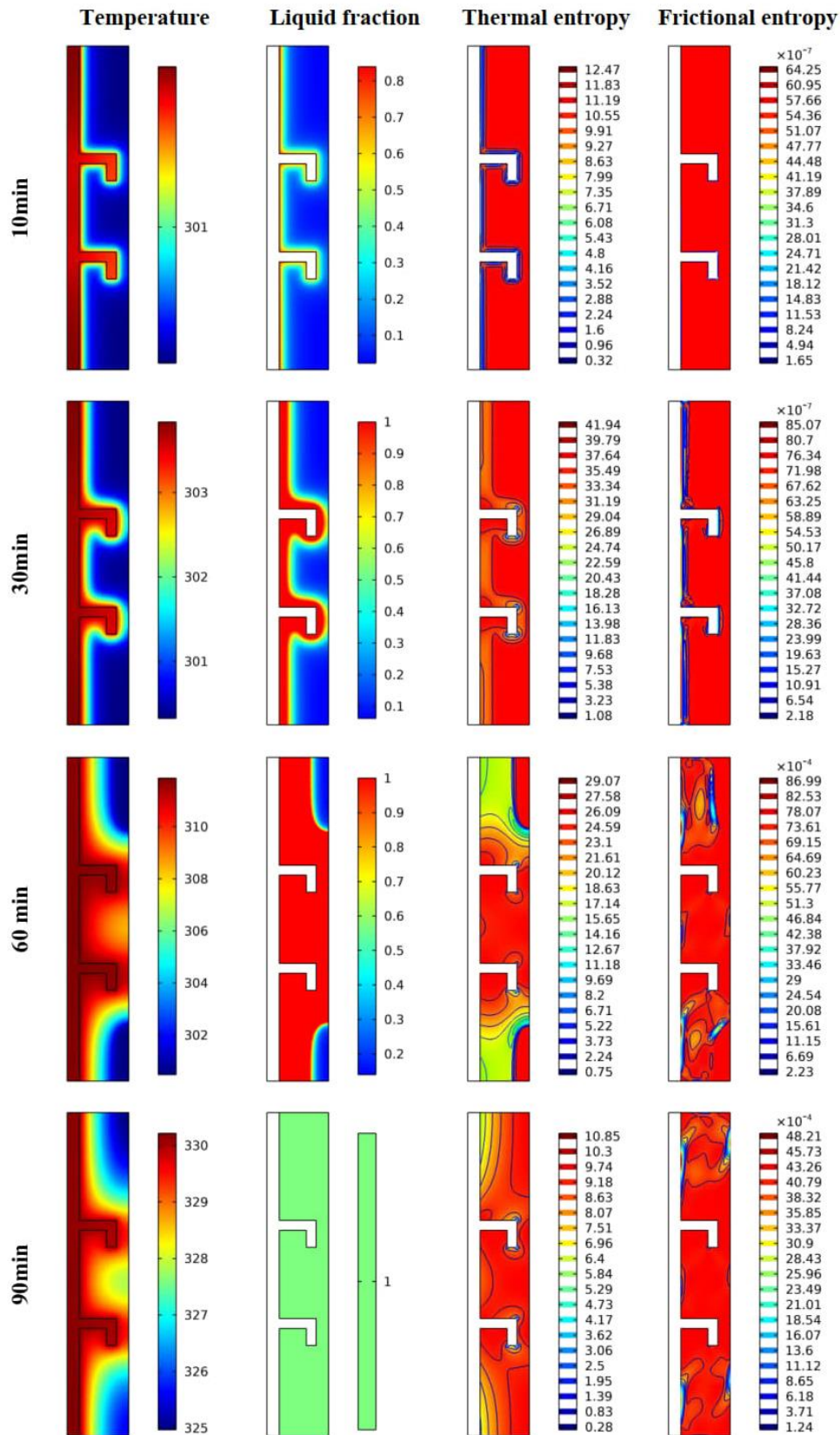
Figure IV-3 The temperature propagation, liquid percentage, thermal entropy, and frictional entropy are measured at four specific points throughout time for the two-downward stepped fins.
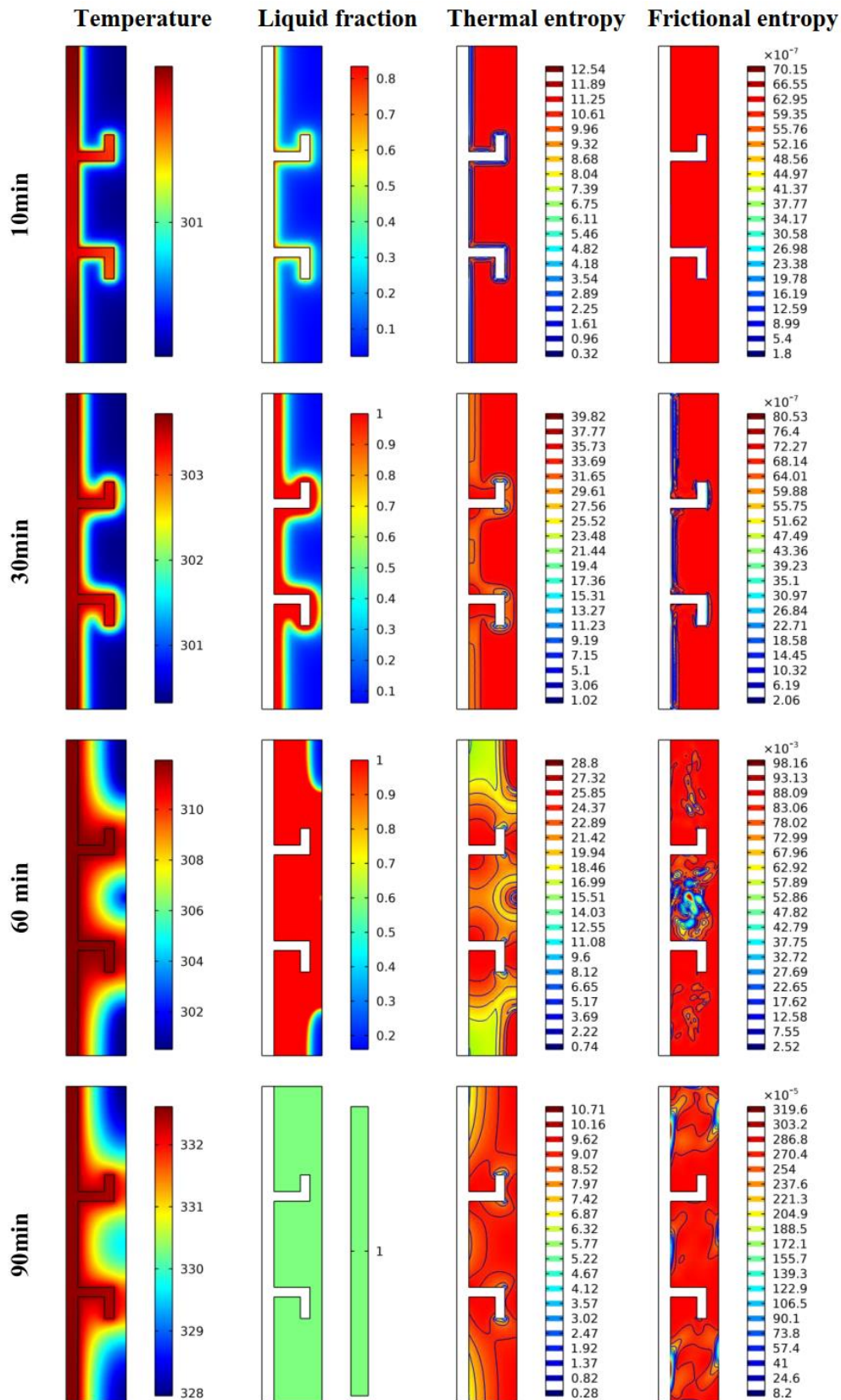
Figure IV-4 The temperature propagation, liquid percentage, thermal entropy, and frictional entropy at four specific time points are compared for both an upward and downward stepped fin.
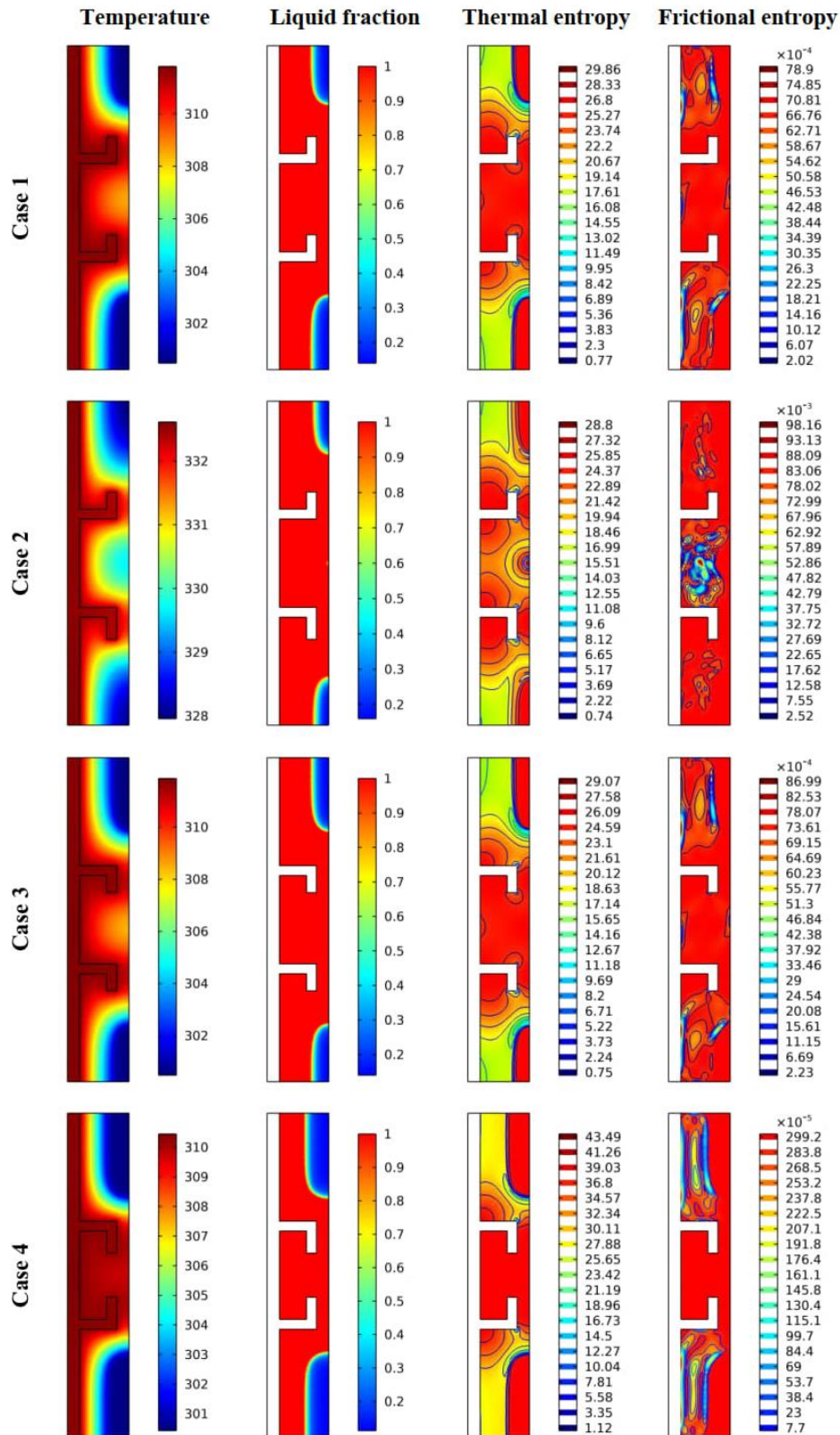
Figure IV-5 Temperature distribution, liquid fraction, thermal entropy, and frictional entropy at around 60 minutes for two-upward stepped fins, an upward and downward stepped fin, two downward stepped fins, and two-stepped fins facing one another
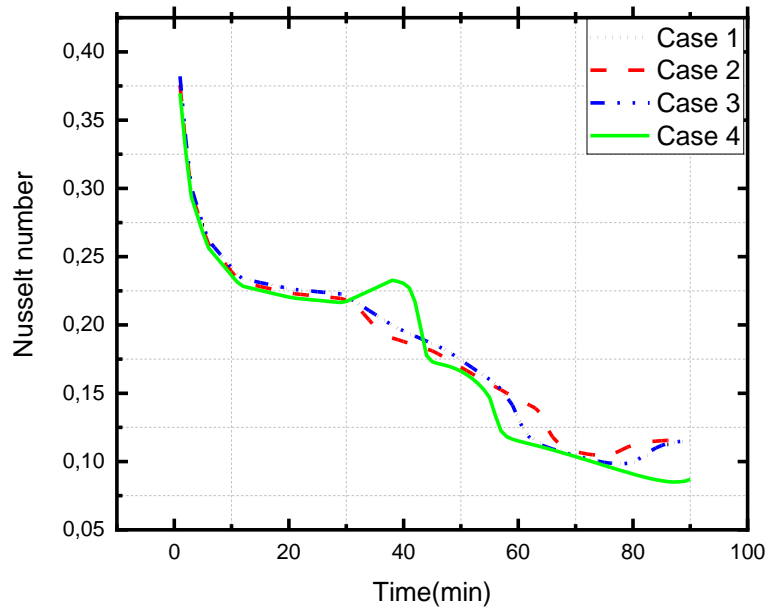
Figure IV-6 Variations in the Nusselt number over time for the four scenarios
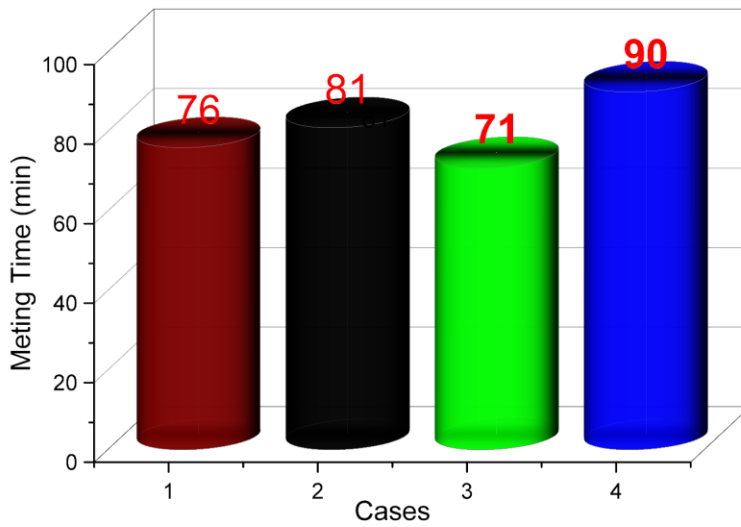
Figure IV-7 Graph illustrating the relationship between time and the number of cases for liquid fraction
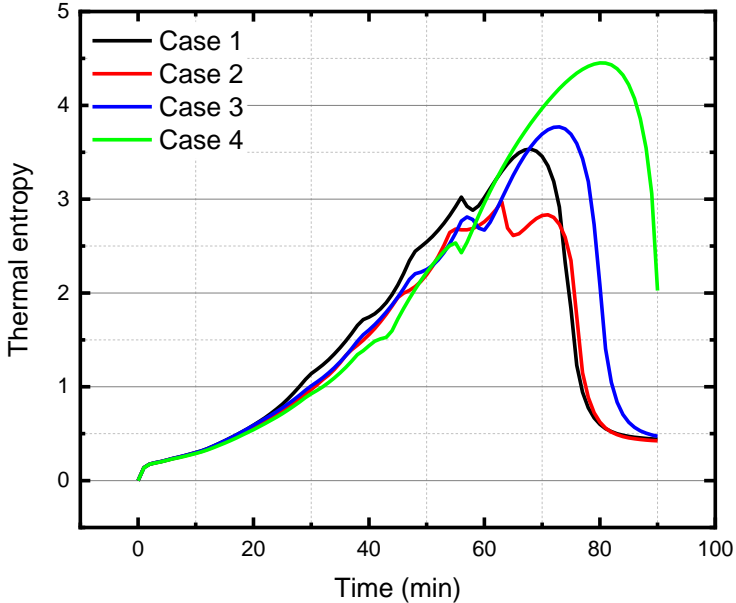
Figure IV-8 Evolution of thermal entropy over time for the four scenarios
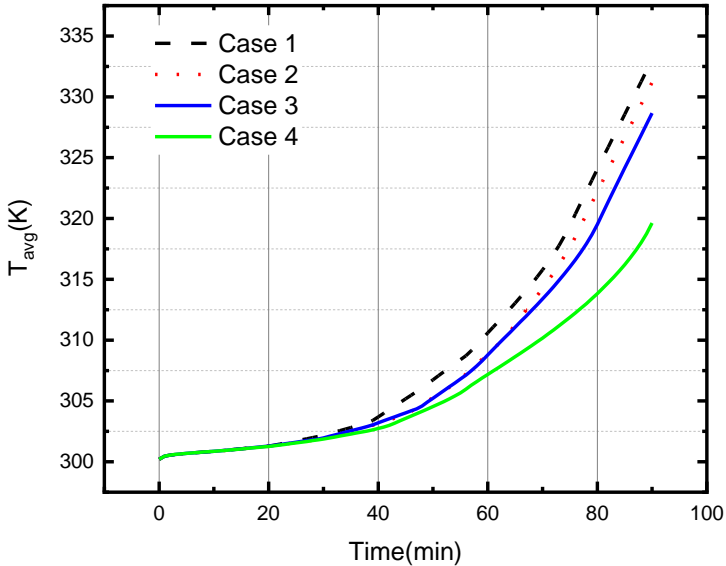
Figure IV-9 Temporal evolution of the mean temperature for the four scenarios
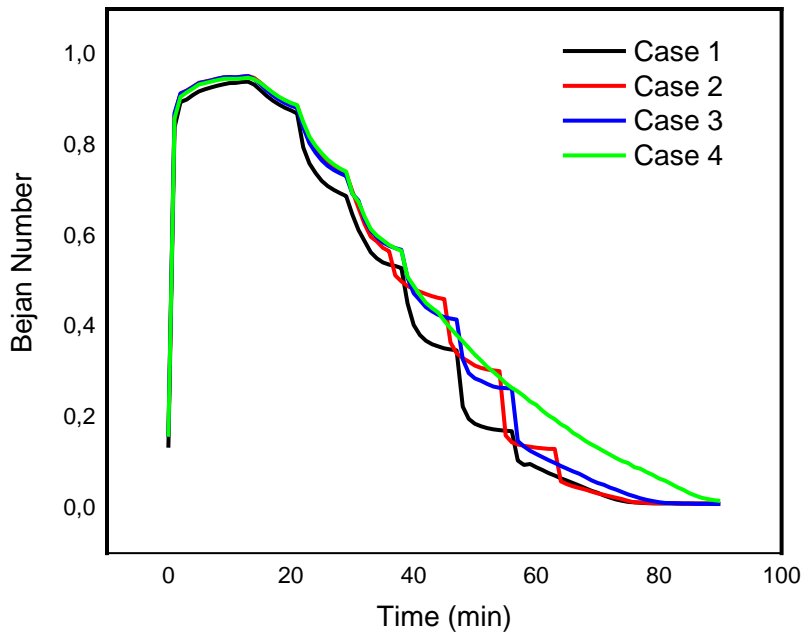
Figure IV-10 Bejan number for each of the four situations as a function of time.
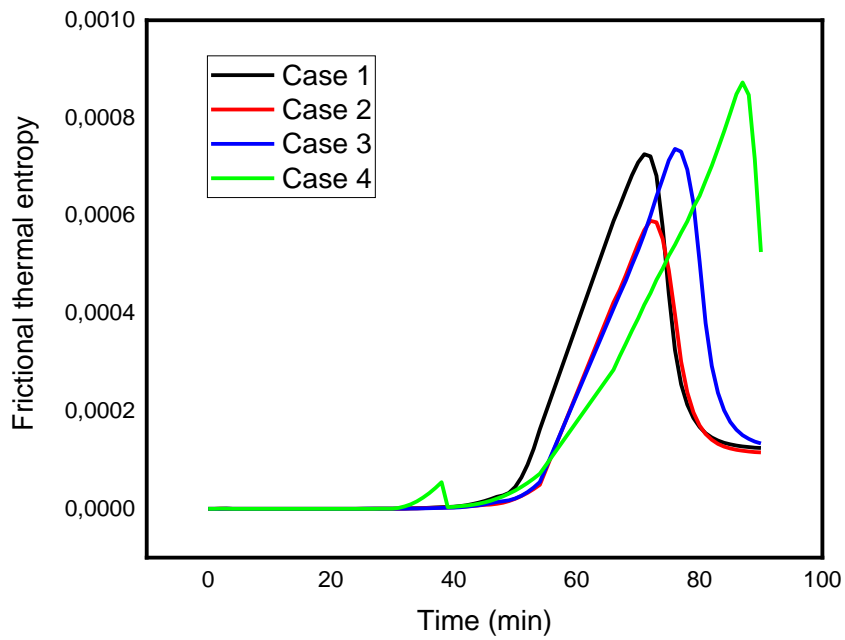
Figure IV-11 Frictional thermal entropy with time for the four cases
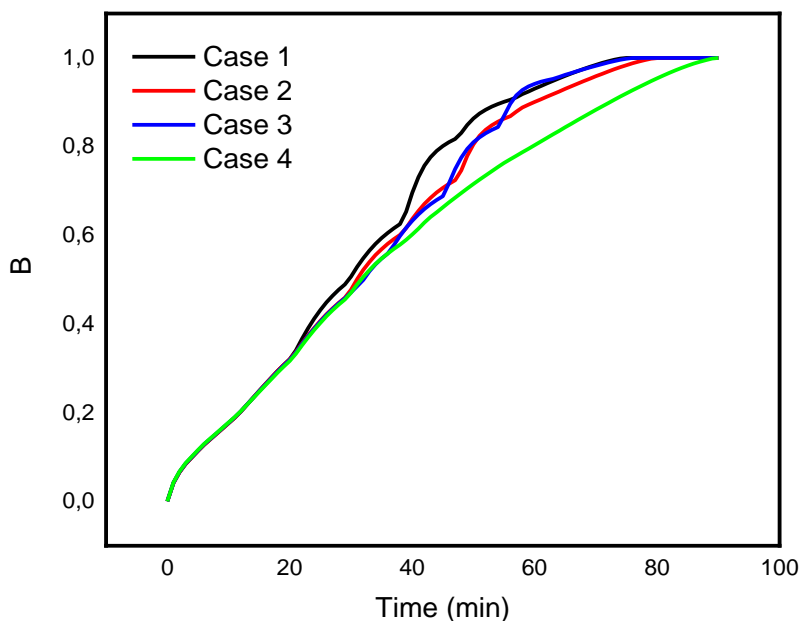
Figure IV-12 Variations in the liquid fraction over time in the four scenarios

Bashirpour-Bonab [190] observed an increase in the liquid fraction up to an ideal value over time throughout the charging process of paraffin RT82 with CuO nanoparticles. This finding suggests that the maximum liquid fraction may be achieved at a later period. This accounts for the observed fluctuation in the proportion of liquid at the 90-minute mark. Durakovic and Torlak [185] previously shown that the PCM sample has reduced temperature variation and has the ability to retain latent heat from convective and radiative sources by maintaining a lower temperature on its inner surface at the phase transition point. The thermal entropy of stored energy is a constant and increasing function of temperature that measures the amount of thermal energy that cannot be transformed into useful work. The results of this research indicate that thermal entropy increases over a longer period of time. The fractional entropy varies at different time intervals of 10 minutes, 30 minutes, 60 minutes, and 90 minutes. It is important to note that there is no substantial disparity in the temperature distribution and liquid fraction fluctuation at four specific time points for both two-upward stepped fins and two-downward stepped fins. The thermal entropy and frictional entropy of two-upward stepped fins and two-downward stepped fins exhibit different characteristics. There is a notable difference in the fractional entropy between the fins that step upward and the fins that step downward. This can be seen in instance scenario 2 of Figure IV-5. Firstly, it is quite likely that the concentration of the material between the upward and downward stepped fins is considerable. In their study, Ma et al. [195] found that a higher proportion of nanoparticle volume results in enhanced heat transmission and greater entropy generation. This occurs because an increase in concentration

leads to a corresponding increase in viscosity, which in turn enhances the development of frictional entropy and the loss of pressure.

Figure IV 6 illustrates that the Nusselt number decreases with time for all four cases: two-upward stepped fins, an upward and downward stepped fins, two-downward stepped fins, and two-stepped fins facing each other. The shortest duration for the liquid portion may be seen in the case of a fin that has both uphill and downward steps, as shown in Figure IV 7. Figure IV 8 and 9 demonstrate that thermal entropy and average temperature increase with time, but thermal entropy decreases after 60 minutes in all four scenarios. Figure IV 11 demonstrates that the Bejan number remains constant at the beginning of the time period. Over time, the Bejan number decreases for the four instances and eventually hits zero after 80 minutes. Figure IV 11 demonstrates a significant change in the thermal entropy caused by friction between 55 and 62 minutes for both an upward and a downward stepped fin. The liquid percentage increases over time in all four instances, as seen in Figure IV 12. After a duration of 40 minutes, a minimal liquid fraction is seen when two stepped fins are positioned opposite each other. However, after 80 minutes, the liquid fraction reached unity for all four instances. When two fins with a two-step design were positioned opposite each other, the proportion of liquid seemed to be much more influenced compared to the other three scenarios.

IV.2 Conclusion

This work presents an examination and discourse on a Thermal Energy Storage (TES) system that is packed with RT27 Phase Change Material (PCM) and Cu nonadditive. The emphasis is placed on four distinct instances: two fins that ascend in steps, a fin that ascends and descends in steps, two fins that descend in steps, and two fins that face each other and have steps. It is important to mention that

1. The thermal entropy and frictional entropy of two-upward stepped fins and two-downward stepped fins differ owing to the effects of gravity acceleration, the mass of RT27 phase change material, and the orientation of the inlet fins.

2. Following 30 minutes, the phenomena of heat conduction, which is the transmission of heat energy into thermal energy storage, and the liquid portion became noticeable.

3. Initially, the liquid fraction, thermal entropy, and Bejan number remain unchanged. Nevertheless, the Bejan number decreases over time, but the fluid percentage grows over time.

CHAPTER: Second Study:

Effect of Y-shaped fins on the performance of shell-and-tube thermal energy storage unit

CHAPTER.V   : Effect of Y-shaped fins on the performance of shell-and-tube thermal energy storage unit

V.1   Problem description

F igure 1 depicts a 2D presentation of the shell-and-tube latent heat thermal energy storage (LHTES) that was examined in this study. The High Temperature Fluid (HTF) is circulated via four smaller pipes with a diameter of 4 mm, while the Phase Change Material (PCM) is circulated through the larger outer shell with an inner diameter of 64 mm. Fins with a longitudinal length of 4 mm are attached to the cylindrical tubes in order to enhance heat transmission and reduce the time needed to melt the PCM. Figure 1 (a) displays the geometric measurements of STHEs, including primary tubes, tubes with two Y-shaped fins, and tubes with four Y-shaped fins. Every geometry is used with a uniform surface area to guarantee mass conservation in all configurations. The characteristics of the fin are shown in Table 1. RT27 served as the Phase Change Material (PCM), while water with input temperatures ranging from 343 K to 343 K was utilised as the Heat Transfer Fluid (HTF). In addition, copper was used for the tubes. Table 2 provides a concise overview of the characteristics of PCM. The initial temperature of the device at initial time was recorded as 366 K, and the volume was adjusted in all situations to ensure a constant amount of PCM was used.

A)   B)

C)   D)
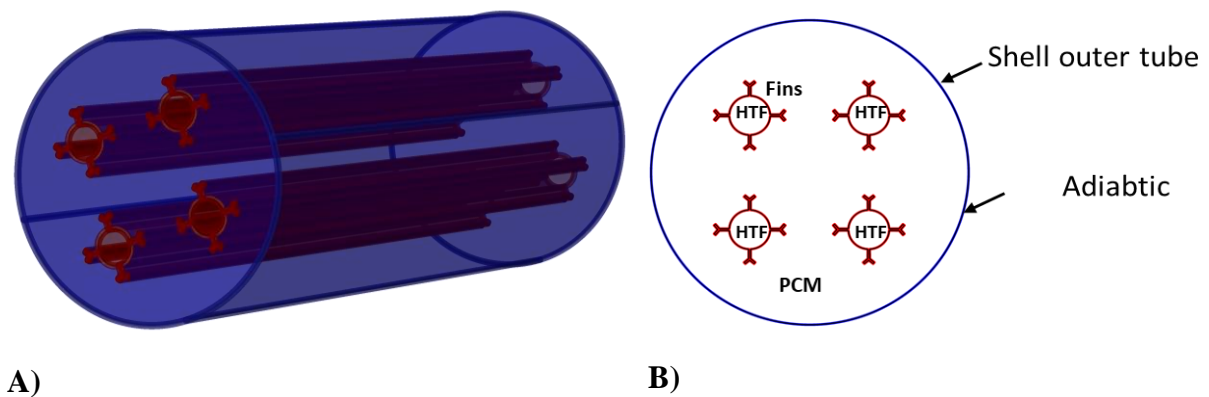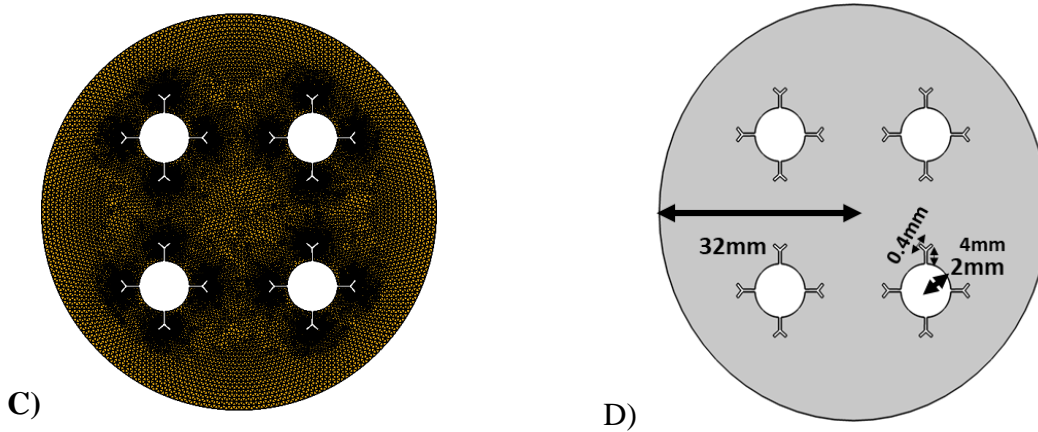
Figure V-1 *(A)* three-dimensional representation of the shell and tube with fins in a 2Y configuration. (B) A 2D depiction of the analysed model, including the imposed boundary conditions. (C) a piece of grid fabric. (D). The measurement of the fins
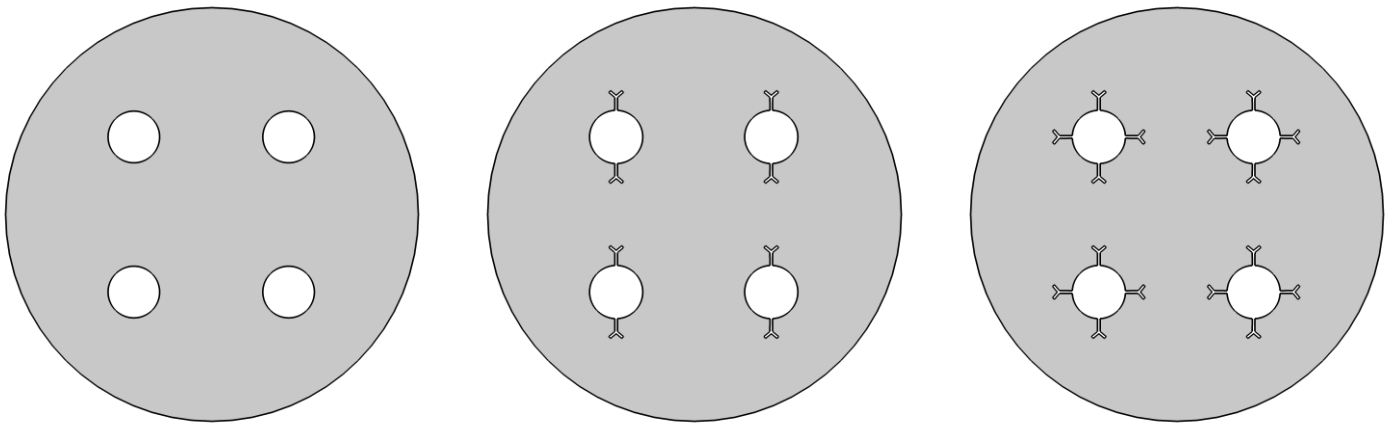
Figure V-2 various cases were considered in this study.

V.2   Results and discussion

This section discusses a thermal energy storage (TES) unit in the form of a shell-and-tube. Four tubes, both with and without fins, are used to facilitate the flow of a hot liquid. These tubes are cooled by a shell that is filled with PCM (RT27) in order to store thermal energy. Two Y-shaped fins and four Y-shaped fins are evaluated and compared in terms of heat transmission rates and the process of phase change material (PCM) melting. The melting performance of the phase change material (PCM) is further investigated by using nanoparticles (specifically copper) at various concentration ratios (0, 2, 4, 6, and 8 vol%). An investigation was conducted to examine and report on the impact of temperature, liquid fraction, and the incorporation of nanoparticles on heat transport and the melting process.

V.2.1   impact of tubes temperature:

The impact of tube temperature, as well as the occurrence of various fins, on heat transmission is shown by temperature curves in Figure V-3 (at 338 K) and Figure V-4 (at 348 K), as well as profiles in Figure 6. Figure 4 demonstrates that the inclusion of fins improves the temperature distribution from the hot tubes to the outer shell. Specifically, four Y-shaped fins outperform the scenario with just two fins. As the charging time increases, the temperature gradually rises and approaches the target temperature of 338 K. Nevertheless, a duration of 180 minutes seems to be inadequate for achieving a consistent high temperature throughout all the instances under investigation. The temperature distribution in the case of the four Y-shaped finned tubes has the greatest magnitude, indicating a significant improvement in the rate of heat transmission. The reason for this is because the inclusion of Y-shaped fins in both horizontal and vertical orientations reduces the thermal resistance of the TES unit.

Figure V-4 displays the temperature contours with a tube temperature of 348 K. The pattern shown in Fig.V-3 is replicated here, taking into account higher temperature values resulting from the hotter tubes. Increasing the temperature results in increased heat transfer rates for the same surface area. The latent heat necessary for the melting process is supplied by these, leading to a faster charging process. Therefore, increasing the heat flow at elevated temperatures accelerates the charging procedure.
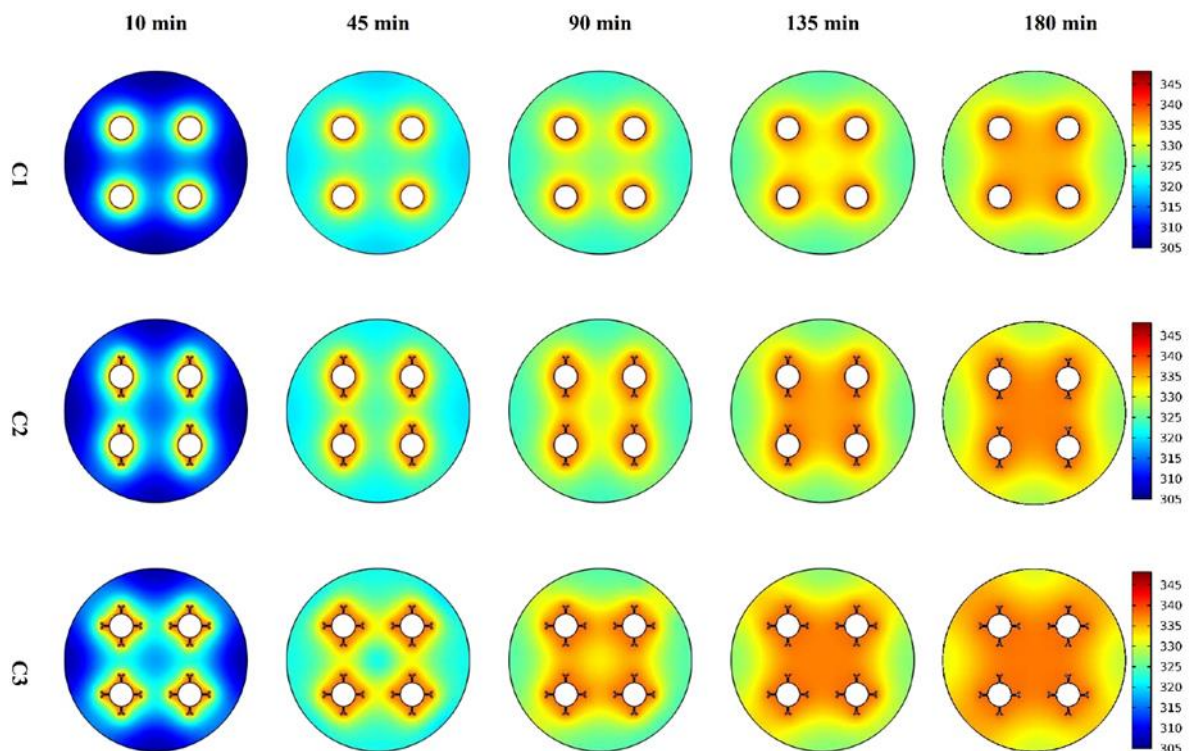
Figure V-3 The temperature profiles of the shell-and-tube thermal energy storage (TES) unit, comparing the configurations with two and four Y-shaped fins to the configuration finless. The temperature of the tube is set at 338 degrees.

Figure V-5 illustrates the variation in temperature among the three designs, with and without fins augmentation, and the two tube temperatures of 338 K and 348 K, as seen in the history profiles. It is evident that instance C3, which involves four Y-shaped finned tubes, exhibits the greatest temperature values during the whole investigation period. Conversely, the lowest temperature values are recorded in the case of naked tubes finless. The temperature values rise when the hot stream within the tube reaches a temperature of 348 K, as a result of an escalation in heating rates. The temperature rises rapidly when conduction heat transmission first occurs, then when the nano-PCM begins to melt, free convection heat transfer occurs in the liquid areas near the tubes, resulting in a noticeable but slower increase in temperature. After all phase change material (PCM) has melted, the temperature stabilises at its highest point. The highest temperature recorded for case C3 at T_{tubes} = 338 K is approximately 337.8 K at time = 226 min (Fig.V- 5(a)). Conversely, when Ttubes = 348 K, the shell temperature reaches 347.5 K at Time = 166 min (Fig. V-5(b)). These findings indicate that increasing the temperature leads to improved heat transfer rates and faster melting processes. Four Y-shaped fins may minimise almost half of the melting time. Previous studies in the literature have shown that the use of Y-shaped fins may improve the melting point [51]. The increased penetration of fins into the PCM unit reduces the thermal resistance of the unit. In comparison to the uniform radial fins (which resulted in a 14% decrease in melting time [52]) and staggered longitudinal fins (which resulted in a 36% reduction in melting time [53]), the Y-shape fins demonstrate superior improvement in the charging process.
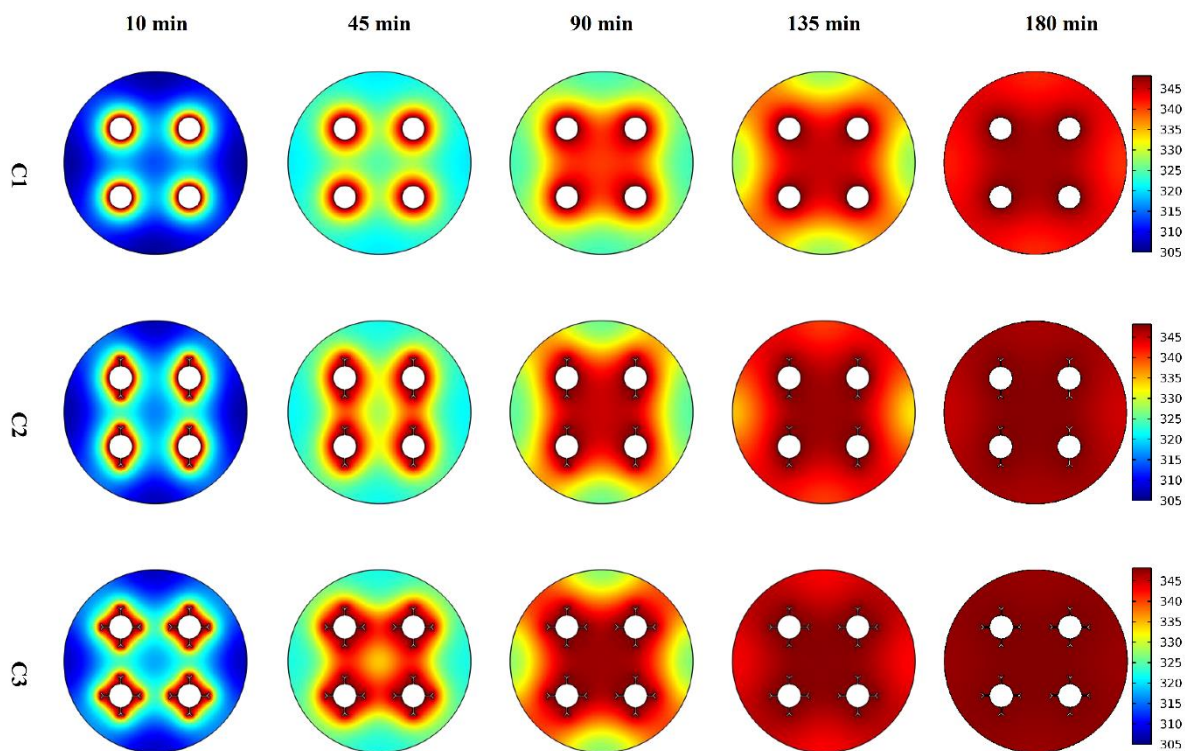
Figure V-4 The temperature distribution of the shell-and-tube thermal energy storage (TES) unit is depicted using contours. The system is shown with two and four Y-shaped structures, both with and finless. The temperature of the tube is set at 348 K.

(b)
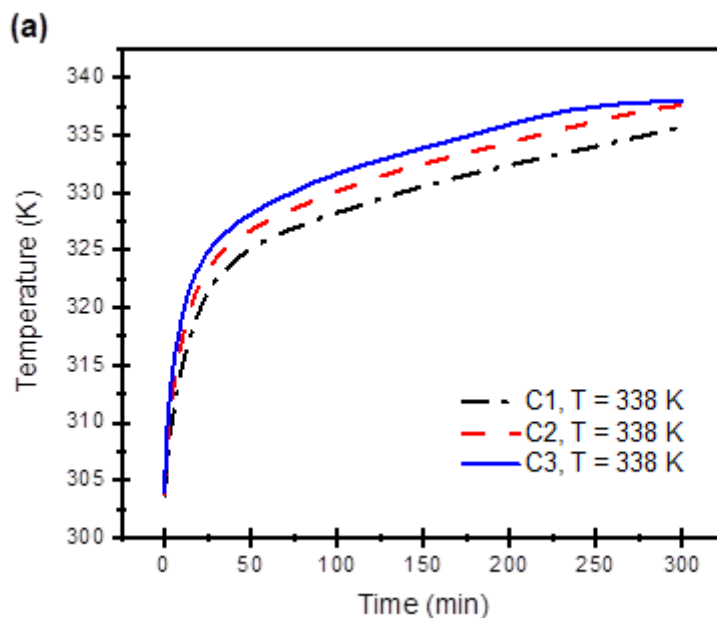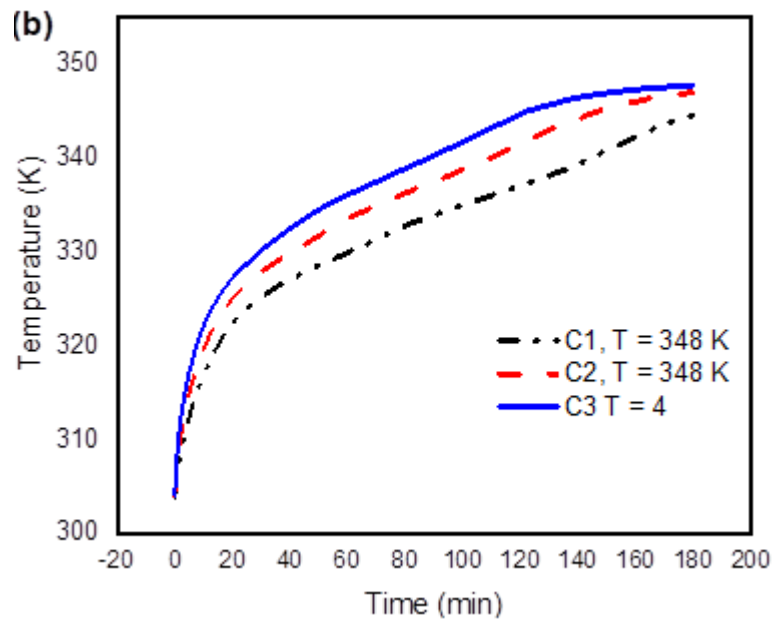
Figure V-5 The temporal temperature profiles of the shell-and-tube thermal energy storage (TES) unit are compared for three different configurations: without fins (C1), with two Y-shape fins (C2), and with four Y-shape fins (C3). The comparisons are made at two different tube temperatures: (a) 338 K and (b) 348 K.

V.2.2 Liquid portion:

The distribution and characteristics of the liquid fraction are crucial for illustrating the time process of melting. This section examines the impact of temperature and the occurrence of Y-shaped fins on the liquid fractions. Figure V-6 and Figure V-7 show the contours of the liquid fraction at temperatures of 338 K and 348 K, respectively. The rate at which melting spreads inside the shell is accelerated by increasing the applied temperature and the number of fins (specifically, four Y-shaped fins). This is because the bigger temperature differential between the tubes and the outside shell enhances the heat transfer. Additionally, the use of fins improved the overall thermal conductivity of the TES unit by dividing the huge distances between the PCM (which has poor thermal conductivity) with fins, hence decreasing the thermal resistance of the TES unit. Enhancing heat transfer rates accelerates the process of melting and reduces the duration of melting. The use of fins and higher temperatures has significant promise in increasing the energy storage capacity of PCM materials and facilitating the usage of thicker shells for enhanced energy storage.
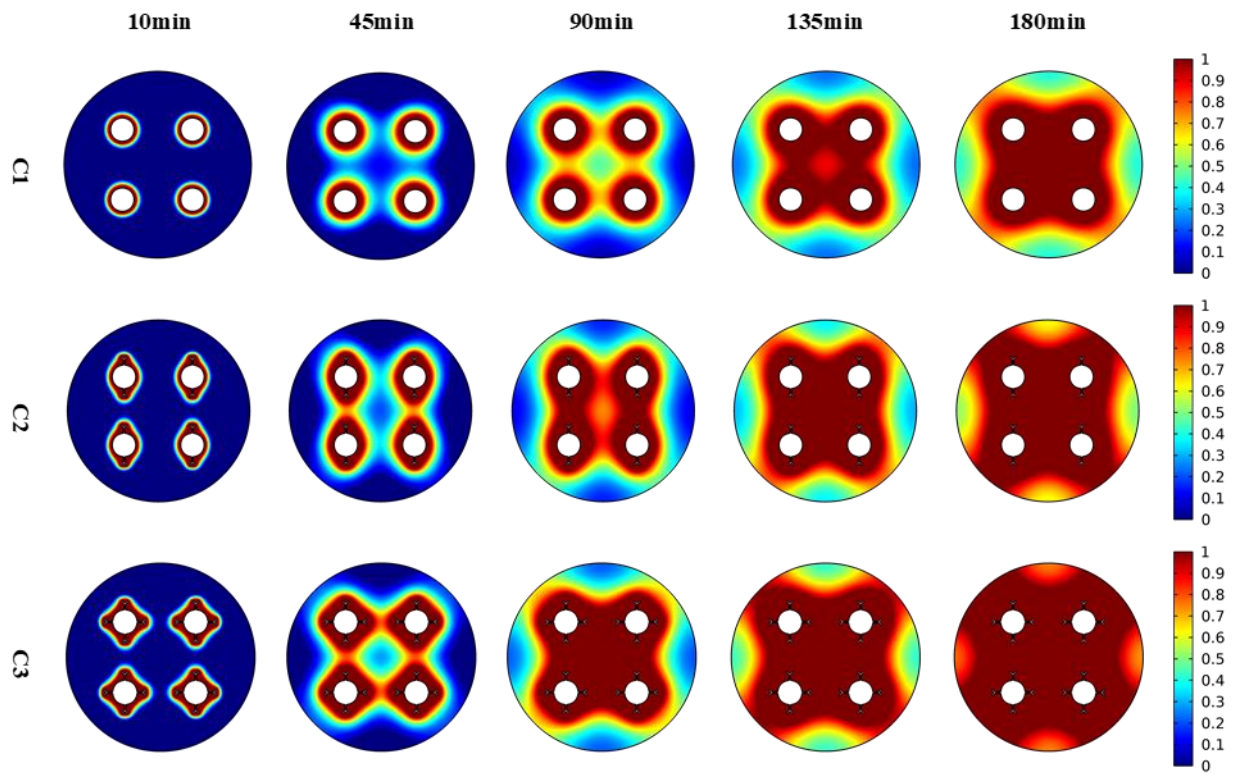
Figure V-6 The liquid portion of the profiles of the shell-and-tube thermal energy storage (TES) unit are shown for three cases: without fins (C1), with two Y-shape fins (C2), and with four Y-shape fins (C3). The temperature of the tube is set at 338 K.
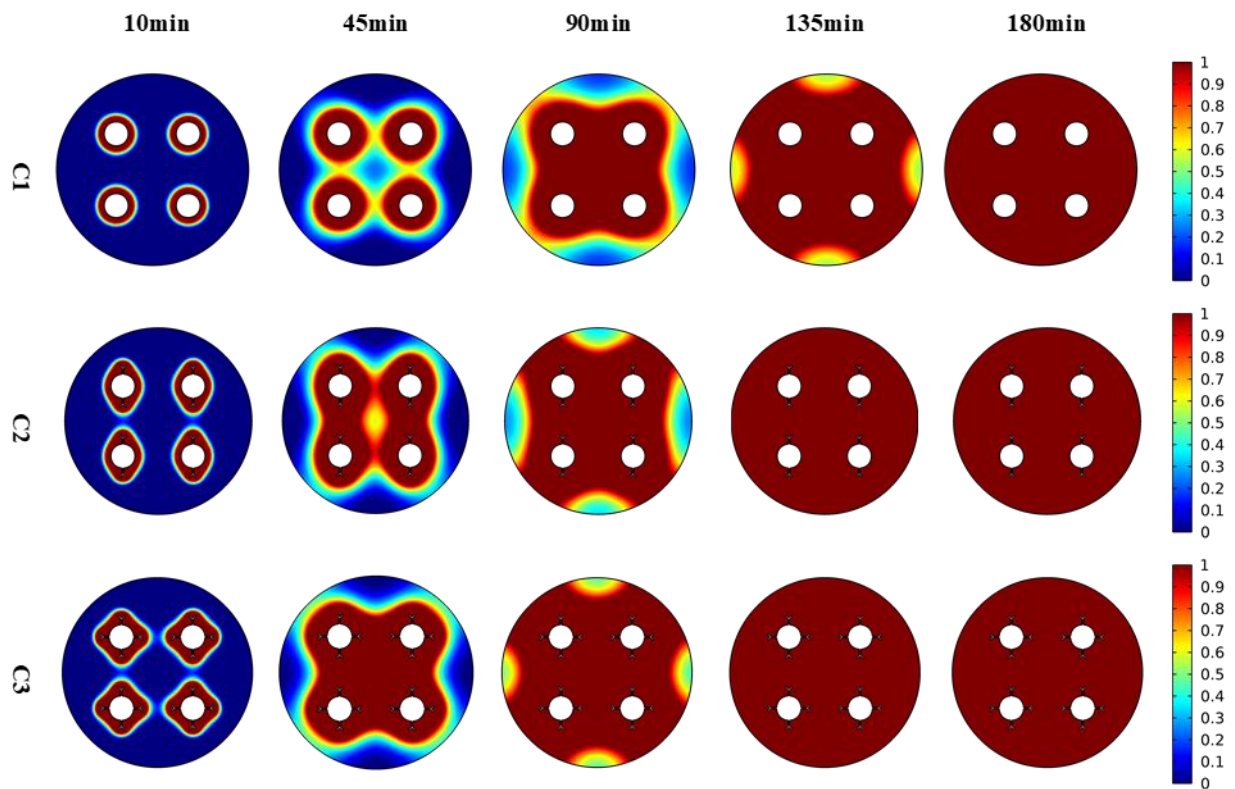
Figure V-7 Liquid fraction contours of the shell-and-tube TES unit without fins (C1) and with two (C2) and four (C3) Y-shape fins. The tube temperature implemented is 348 K

The duration necessary for complete melting of TES units is shown in Figure (a and b). The melting process takes 286 minutes for finless tubes, 243 minutes for two Y-shape finned tubes, and 193 minutes for four Y-shape finned tubes at a temperature of 338 K. Conversely, at a temperature of 338 K (as shown in Figure V-8(b)), the whole melting process takes 148 minutes for finless tubes, 126 minutes for tubes with two Y-shaped fins, and 103 minutes for tubes with four Y-shaped fins. The findings demonstrate that the use of four Y-shaped finned tubes leads to a decrease in melting time of about 48% (maximum) compared to the use of finless tubes. Furthermore, the incorporation of hotter tubes (with a temperature increase of 10 Kelvin) results in a significant decrease in melting time, namely by 87%.
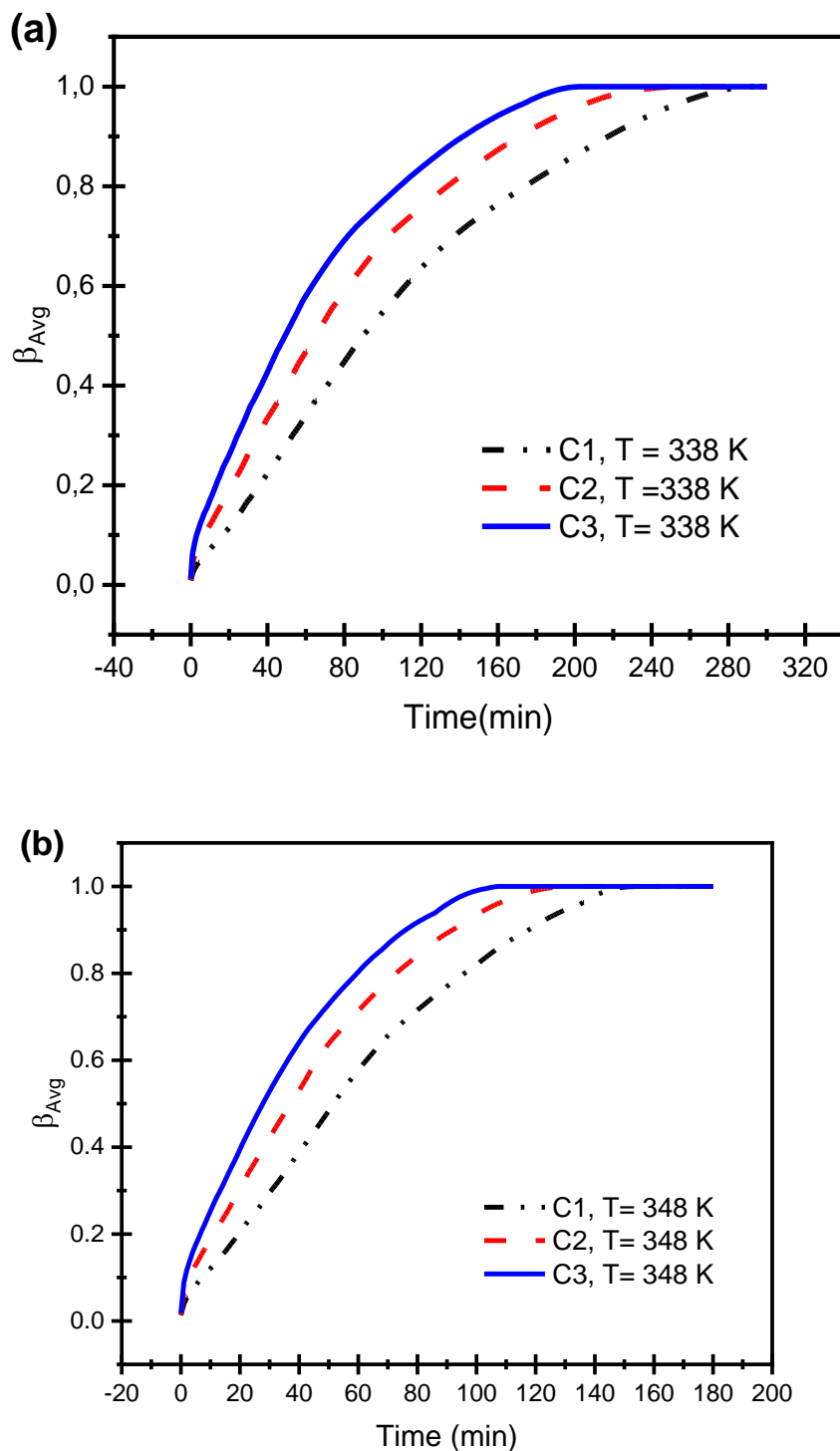
Figure V-8 The liquid portion of the profiles of the shell-and-tube thermal energy storage (TES) unit are shown for three different configurations: without fins (C1), with two Y-shape fins (C2), and with four Y-shape fins (C3). The temperature of the tube is set at 348 K.

V.2.3 Nanoparticle incorporation

The aforementioned findings demonstrate that the use of four Y-shaped finned tubes at elevated temperatures increases the rate of heat transmission and decreases the time required for melting. Modifying the nanoparticle concentration might further improve the melting rates of the TES unit. The nanoparticles exhibit greater thermal conductivity compared to the original PCM, leading to improved thermal diffusion and melting rates. This fact is shown for the examined TES unit, as seen in Figure V 9 for the TES historical average temperature (Figure V 9 (a)) and the average liquid percentage (Figure V 9 (b)). It is observed that greater temperatures and liquid fractions are achieved with larger concentrations of nanoparticles, such as eight volume percent. At a specific period of 140 minutes, the average temperature of the phase change material (PCM) is 340.6 K for the 8 vol% nano-PCM and 336.7 K for the pure PCM. There is a temperature difference of about 4 K between the two. Simultaneously, the average liquid fraction is 0.998 for a mixture containing 8 volume percent of nano-PCM and 0.899 for pure PCM. This demonstrates a 10% improvement in reducing the time it takes for the material to melt. The significance of integrating nanoparticles with PCM materials for enhanced performance is evident. The whole liquefaction process takes 179, 158, 156, and 145 minutes when using nanoparticle concentrations of 0, 2, 4, and 8 volume percent, respectively. Using a nanoparticle concentration of 4 vol% may result in a melting time reduction of around 11%, while a concentration of 8 vol% can yield a decrease of about 19%. The literature indicated that incorporating CuO nanoparticles into PCM resulted in a 9.1% improvement in the melting process [54], representing a recent advancement. Therefore, it is advisable to use four Y-shaped fins, employ elevated temperatures, and integrate larger concentrations of nanoparticles in order to achieve optimal performance for TES units.

V.3 Second conclusion:

An analysis is conducted on a thermal energy storage unit that consists of a shell and tube configuration. The study examines the performance of the unit with and without fins, while varying the temperature of the tubes. The shell contains varying amounts of copper nanoparticles mixed with PCM (RT27). The study focuses on investigating and comparing the heat transfer increase of two and four Y-shaped fins. Based on the circumstances that were applied, the following observations may be concluded:

1. With the implementation of two and four Y-formed finned tubes, there is a significant improvement in heat transmission rates and a decrease in melting time by

approximately 32% and 48% respectively, when when compared with finless tubes. That is a result of the decreases in unit thermal resistance.

2. Using a hotter tube (e.g., 348 K instead of 338 K) can result to speeding the charging process by 87%. For instance, the highest temperatures within the storage unit, which are 337.8 K and 347.5 K, are achieved after 226 and 166 minutes when the tube temperatures are set at 338 K and 348 K, correspondingly.

3. Furthermore, the integration of nano additives with phase change material (PCM) might enhance the overall thermal conductivity when the PCM undergoes the melting process. Utilising a nanoparticle concentration of 4 vol% may provide a decrease in melting time of about 11%, while a concentration of 8 vol% can yield a reduction of approximately 19%.

Therefore, considering the issues discussed above, it is advisable to equip the shell-and-tube thermal energy storage unit with four Y-shaped fins, operate it at elevated temperatures, and use nano-PCM (with a concentration of 8 vol%) in its place of pure PCM.

(b)
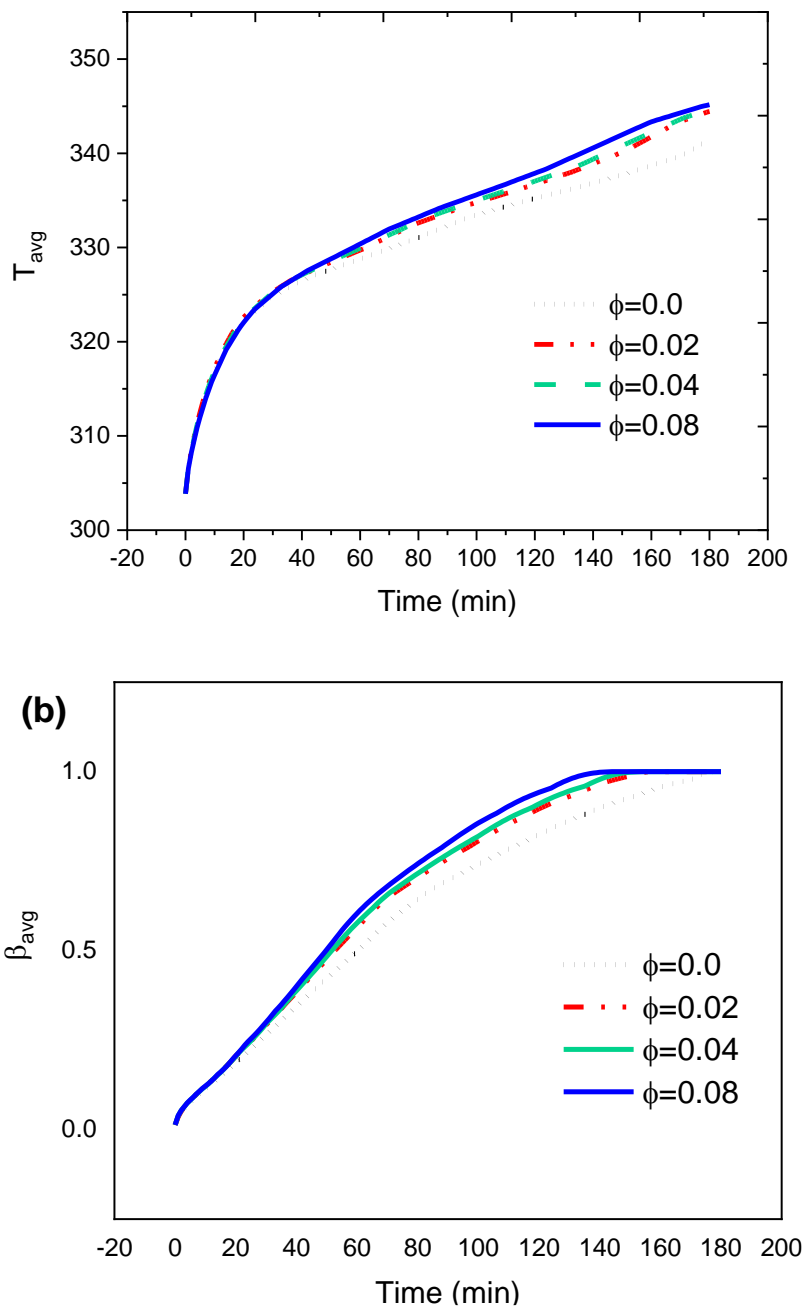
Figure V-9 impact of nano additives on the TES unit (a) mean temperature and (b) average liquid fraction for tube temperature of 338 K

Heat transmission improvement for latent heat thermal energy storage systems, founded on PCM by using wing nano additive material.

First work presents an examination and discourse on a Thermal Energy Storage (TES) system that is packed with RT27 Phase Change Material (PCM) and Cu nonadditive. The emphasis is placed on four distinct instances: two fins that ascend in steps, a fin that ascends and descends in steps, two fins that descend in steps, and two fins that face each other and have steps. It is important to mention that:

- Owing to the impact of acceleration due to gravity, the mass of RT27 phase change material, and the orientation of the intake fins, the thermal and functional entropies for two-upward stepped fins and two-downward stepped fins were unique in nature. The two-downward stepped fins enclosure yields a minimum melting time of 71 minutes.

Second Work An analysis is conducted on a thermal energy storage unit that consists of a shell and tube configuration. The study examines the performance of the unit with and without fins, while varying the temperature of the tubes. The shell contains varying amounts of copper nanoparticles mixed with PCM (RT27). The study focuses on investigating and comparing the heat transfer increase of two and four Y-shaped fins. Based on the circumstances that were applied, the following observations may be concluded:

- The findings revealed that using nanoparticles with 8 vol% enhanced the thermal conductivity during melting by 19%. The melting process was accelerated by 87% when the HTF temperature was higher (348 K). Finally, TESS with four Y-shaped fins was found to be the most effective as it achieved a 48% melting time reduction compared to the base case (case 1).
- Based on the aforementioned concerns, it is recommended to enhance the shell-and-tube thermal energy storage unit by including four Y-shaped fins, operating it at higher temperatures, and substituting pure PCM with nano-PCM at a concentration of 8 vol%.

CHAPTER.VII FUTURE SCOPE OF THE WORK

PCM is a highly promising technology for thermal management and energy storage, and it may be used in a variety of applications, including solar water desalination, solar greenhouses, solar dryers, solar stills, and other applications. The influence of fin and nanoparticale on PCM domains is the primary focus of the current research that we are doing. We are going to investigate the impact on photovoltaic panels in the future and observe how it influences the thermal and electrical efficiency of the panels.

CHAPTER.VIII   References

[1] "How solar energy could be the largest source of electricity by mid-century - News - IEA." https://www.iea.org/news/how-solar-energy-could-be-the-largest-source-of-electricity-by-mid-century (accessed Apr. 06, 2024).

[2] A. M. Abdulateef, S. Mat, J. Abdulateef, K. Sopian, and A. A. Al-Abidi, "Geometric and design parameters of fins employed for enhancing thermal energy storage systems: a review," Renewable and Sustainable Energy Reviews, vol. 82, pp. 1620–1635, Feb. 2018, doi: 10.1016/j.rser.2017.07.009.

[3] "] I. Dincer and M. Rosen, Thermal energy storage:... - Google Scholar." https://scholar.google.com/scholar?hl=fr&as_sdt=0%2C5&q=%5D+I.+Dincer+and+M.+Rosen%2C+Thermal+energy+storage%3A+systems++and++applications.+John+Wiley+%26+Sons%2C+2002.&btnG= (accessed Apr. 06, 2024).

[4] X. Cheng, X. Zhai, and R. Wang, "Thermal performance analysis of a packed bed cold storage unit using composite PCM capsules for high temperature solar cooling application," Appl Therm Eng, vol. 100, pp. 247–255, May 2016, doi: 10.1016/j.applthermaleng.2016.02.036.

[5] B. M. Diaconu, S. Varga, and A. C. Oliveira, "Numerical simulation of a solar-assisted ejector air conditioning system with cold storage," Energy, vol. 36, no. 2, pp. 1280–1291, Feb. 2011, doi: 10.1016/j.energy.2010.11.015.

[6] A. A. Al-Abidi, S. Bin Mat, K. Sopian, M. Y. Sulaiman, C. H. Lim, and A. Th, "Review of thermal energy storage for air conditioning systems," Renewable and Sustainable Energy Reviews, vol. 16, no. 8, pp. 5802–5819, Oct. 2012, doi: 10.1016/j.rser.2012.05.030.

[7] D. Zhou, C. Y. Zhao, and Y. Tian, "Review on thermal energy storage with phase change materials (PCMs) in building applications," Appl Energy, vol. 92, pp. 593–605, Apr. 2012, doi: 10.1016/j.apenergy.2011.08.025.

[8] A. Mishra, A. Shukla, and A. Sharma, "Latent heat storage through phase change materials," Resonance, vol. 20, no. 6, pp. 532–541, Jun. 2015, doi: 10.1007/s12045-015-0212-5.

[9] Z. A. Qureshi, H. M. Ali, and S. Khushnood, "Recent advances on thermal conductivity enhancement of phase change materials for energy storage system: A review," Int J Heat

Mass Transf, vol. 127, pp. 838–856, Dec. 2018, doi: 10.1016/j.ijheatmasstransfer.2018.08.049.

[10]   A. A. Al-abidi, S. Bin Mat, K. Sopian, M. Y. Sulaiman, and A. Th. Mohammed, "CFD applications for latent heat thermal energy storage: a review," Renewable and Sustainable Energy Reviews, vol. 20, pp. 353–363, Apr. 2013, doi: 10.1016/j.rser.2012.11.079.

[11]   H. IBRAHIM, A. ILINCA, and J. PERRON, "Energy storage systems—Characteristics and comparisons," Renewable and Sustainable Energy Reviews, vol. 12, no. 5, pp. 1221–1250, Jun. 2008, doi: 10.1016/j.rser.2007.01.023.

[12]   I. Sarbu and A. Dorca, "Review on heat transfer analysis in thermal energy storage using latent heat storage systems and phase change materials," Int J Energy Res, vol. 43, no. 1, pp. 29–64, Jan. 2019, doi: 10.1002/er.4196.

[13]   "Y. Tian, Heat transfer enhancement in phase change... - Google Scholar." https://scholar.google.com/scholar?hl=fr&as_sdt=0%2C5&q=Y.+Tian%2C++Heat++transfer+enhancement+in++phase++change++materials+%28PCMs%29+by+metal+foams+and+cascaded+thermal+energy+storage.++PhD+thesis%2C+University+of+Warwick%2C+2012.&btnG= (accessed Apr. 06, 2024).

[14]   A. Sharma, V. V. Tyagi, C. R. Chen, and D. Buddhi, "Review on thermal energy storage with phase change materials and applications," Renewable and Sustainable Energy Reviews, vol. 13, no. 2, pp. 318–345, Feb. 2009, doi: 10.1016/j.rser.2007.10.005.

[15]   J. M. Mahdi and E. C. Nsofor, "Solidification enhancement of PCM in a triplex-tube thermal energy storage system with nanoparticles and fins," Appl Energy, vol. 211, pp. 975–986, Feb. 2018, doi: 10.1016/j.apenergy.2017.11.082.

[16]   D. Fernandes, F. Pitié, G. Cáceres, and J. Baeyens, "Thermal energy storage: 'How previous findings determine current research priorities,'" Energy, vol. 39, no. 1, pp. 246–257, Mar. 2012, doi: 10.1016/j.energy.2012.01.024.

[17]   N. I. Ibrahim, F. A. Al-Sulaiman, S. Rahman, B. S. Yilbas, and A. Z. Sahin, "Heat transfer enhancement of phase change materials for thermal energy storage applications: A critical review," Renewable and Sustainable Energy Reviews, vol. 74, pp. 26–50, Jul. 2017, doi: 10.1016/j.rser.2017.01.169.

[18]   A. Abhat, "Low temperature latent heat thermal energy storage: Heat storage materials," Solar Energy, vol. 30, no. 4, pp. 313–332, 1983, doi: 10.1016/0038-092X(83)90186-X.

[19]   L. F. Cabeza, A. Castell, C. Barreneche, A. de Gracia, and A. I. Fernández, "Materials used as PCM in thermal energy storage in buildings: A review," Renewable and Sustainable Energy Reviews, vol. 15, no. 3, pp. 1675–1695, Apr. 2011, doi: 10.1016/j.rser.2010.11.018.

[20]   B. Lamrani, F. Kuznik, and A. Draoui, "Thermal performance of a coupled solar parabolic trough collector latent heat storage unit for solar water heating in large buildings," Renew Energy, vol. 162, pp. 411–426, Dec. 2020, doi: 10.1016/j.renene.2020.08.038.

[21]   C. A. Ikutegbe and M. M. Farid, "Application of phase change material foam composites in the built environment: A critical review," Renewable and Sustainable Energy Reviews, vol. 131, p. 110008, Oct. 2020, doi: 10.1016/j.rser.2020.110008.

[22]   Y. Su, Y. Fan, Y. Ma, Y. Wang, and G. Liu, "Flame-retardant phase change material (PCM) for thermal protective application in firefighting protective clothing," International Journal of Thermal Sciences, vol. 185, p. 108075, Mar. 2023, doi: 10.1016/j.ijthermalsci.2022.108075.

[23]   "A. Konstantinidou, V. Christina, W. Lang, Novoselac,,... - Google Scholar." https://scholar.google.com/scholar?hl=fr&as_sdt=0%2C5&q=A.+Konstantinidou%2C+V.+Christina%2C+W.+Lang%2C+Novoselac%2C%2C+Integration+of+thermal+energy+storage+in+buildings%2C+University+of+Austin%2C+Texas%2C+2010%2C+Master+Thesis&btnG= (accessed Apr. 03, 2024).

[24]   A. Sarı and K. Kaygusuz, "Some fatty acids used for latent heat storage: thermal stability and corrosion of metals with respect to thermal cycling," Renew Energy, vol. 28, no. 6, pp. 939–948, May 2003, doi: 10.1016/S0960-1481(02)00110-6.

[25]   A. M. Khudhair and M. M. Farid, "A review on energy conservation in building applications with thermal storage by latent heat using phase change materials," Energy Convers Manag, vol. 45, no. 2, pp. 263–275, Jan. 2004, doi: 10.1016/S0196-8904(03)00131-6.

[26]   S. M. Hasnain, "Review on sustainable thermal energy storage technologies, Part I: heat storage materials and techniques," Energy Convers Manag, vol. 39, no. 11, pp. 1127–1138, Aug. 1998, doi: 10.1016/S0196-8904(98)00025-9.

[27]   F. Souayfane, F. Fardoun, and P.-H. Biwole, "Phase change materials (PCM) for cooling applications in buildings: A review," Energy Build, vol. 129, pp. 396–431, Oct. 2016, doi: 10.1016/j.enbuild.2016.04.006.

[28]   D. M. Reddy Prasad, R. Senthilkumar, G. Lakshmanarao, S. Krishnan, and B. S. Naveen Prasad, "A critical review on thermal energy storage materials and systems for solar applications," AIMS Energy, vol. 7, no. 4, pp. 507–526, 2019, doi: 10.3934/energy.2019.4.507.

[29]   "Konstantinidou: Novoselac,"Integration of thermal... - Google Scholar." https://scholar.google.com/scholar_lookup?title=Integration%20of%20Thermal%20Energy%20Storage%20in%20Buildings&author=C.J.D.o.A.%20Konstantinidou&publication_year=2010 (accessed Apr. 05, 2024).

[30]   S. Ben Romdhane, A. Amamou, R. Ben Khalifa, N. M. Saïd, Z. Younsi, and A. Jemni, "A review on thermal energy storage using phase change materials in passive building applications," Journal of Building Engineering, vol. 32, p. 101563, Nov. 2020, doi: 10.1016/j.jobe.2020.101563.

[31]   R. Wen, M. Wu, B. Chen, and W. Chen, "Non-isothermal crystallization behavior of Ag nanoparticles modified expanded graphite/paraffin composite phase change material," J Energy Storage, vol. 58, p. 106371, Feb. 2023, doi: 10.1016/j.est.2022.106371.

[32]   C. Wang, L. Gao, M. Liu, S. Xia, and Y. Han, "Self-crystallization behavior of paraffin and the mechanism study of SiO_2 nanoparticles affecting paraffin crystallization," Chemical Engineering Journal, vol. 452, p. 139287, Jan. 2023, doi: 10.1016/j.cej.2022.139287.

[33]   F. Kuznik, J. Virgone, and K. Johannes, "In-situ study of thermal comfort enhancement in a renovated building equipped with phase change material wallboard," Renew Energy, vol. 36, no. 5, pp. 1458–1462, May 2011, doi: 10.1016/j.renene.2010.11.008.

[34]   J. Liu, J. Xu, Z. Su, Y. Zhang, and T. Jiang, "Preparation and characterization of $NaNO_3$ shape-stabilized phase change materials (SS-PCMs) based on anorthite ceramic

and cordierite ceramic for solar energy storage," Solar Energy Materials and Solar Cells, vol. 251, p. 112114, Mar. 2023, doi: 10.1016/j.solmat.2022.112114.

[35]   Z. Khan, Z. Khan, and A. Ghafoor, "A review of performance enhancement of PCM based latent heat storage system within the context of materials, thermal stability and compatibility," Energy Convers Manag, vol. 115, pp. 132–158, May 2016, doi: 10.1016/j.enconman.2016.02.045.

[36]   T. Hu, Z. Wu, Y. Fang, J. Niu, W. Yuan, and L. Li, "A novel metal-organic framework aerogel based hydrated salt composite phase change material for enhanced solar thermal utilization," J Energy Storage, vol. 58, p. 106354, Feb. 2023, doi: 10.1016/j.est.2022.106354.

[37]   M. Noro, R. M. Lazzarin, and F. Busato, "Solar cooling and heating plants: An energy and economic analysis of liquid sensible vs phase change material (PCM) heat storage," International Journal of Refrigeration, vol. 39, pp. 104–116, Mar. 2014, doi: 10.1016/j.ijrefrig.2013.07.022.

[38]   B. Lamrani, K. Johannes, and F. Kuznik, "Phase change materials integrated into building walls: An updated review," Renewable and Sustainable Energy Reviews, vol. 140, p. 110751, Apr. 2021, doi: 10.1016/j.rser.2021.110751.

[39]   P. Singh, R. K. Sharma, A. K. Ansu, R. Goyal, A. Sarı, and V. V. Tyagi, "A comprehensive review on development of eutectic organic phase change materials and their composites for low and medium range thermal energy storage applications," Solar Energy Materials and Solar Cells, vol. 223, p. 110955, May 2021, doi: 10.1016/j.solmat.2020.110955.

[40]   H. Akeiber, P. Nejat, M. Z. Abd. Majid, M. A. Wahid, F. Jomehzadeh, I. Zeynali Famileh, J. K. Calautit, B. R. Hughes, and S. A. Zaki, "A review on phase change material (PCM) for sustainable passive cooling in building envelopes," Renewable and Sustainable Energy Reviews, vol. 60, pp. 1470–1497, Jul. 2016, doi: 10.1016/j.rser.2016.03.036.

[41]   M. Thambidurai, K. Panchabikesan, K. M. N, and V. Ramalingam, "Review on phase change material based free cooling of buildings—The way toward sustainability," J Energy Storage, vol. 4, pp. 74–88, Dec. 2015, doi: 10.1016/j.est.2015.09.003.

[42]   J. H. C. Hendricks and W. G. J. H. M. van Sark, "Annual performance enhancement of building integrated photovoltaic modules by applying phase change

materials," Progress in Photovoltaics: Research and Applications, vol. 21, no. 4, pp. 620–630, Jun. 2013, doi: 10.1002/pip.1240.

[43]   B. Nie, A. Palacios, B. Zou, J. Liu, T. Zhang, and Y. Li, "Review on phase change materials for cold thermal energy storage applications," Renewable and Sustainable Energy Reviews, vol. 134, p. 110340, Dec. 2020, doi: 10.1016/j.rser.2020.110340.

[44]   M. A. Abdelkareem, H. M. Maghrabie, A. G. Abo-Khalil, O. H. K. Adhari, E. T. Sayed, A. Radwan, K. Elsaid, T. Wilberforce, and A. G. Olabi, "Battery thermal management systems based on nanofluids for electric vehicles," J Energy Storage, vol. 50, p. 104385, Jun. 2022, doi: 10.1016/j.est.2022.104385.

[45]   M. J. Huang, P. C. Eames, and B. Norton, "Thermal regulation of building-integrated photovoltaics using phase change materials," Int J Heat Mass Transf, vol. 47, no. 12–13, pp. 2715–2733, Jun. 2004, doi: 10.1016/j.ijheatmasstransfer.2003.11.015.

[46]   S. Khanna, K. S. Reddy, and T. K. Mallick, "Optimization of solar photovoltaic system integrated with phase change material," Solar Energy, vol. 163, pp. 591–599, Mar. 2018, doi: 10.1016/j.solener.2018.01.002.

[47]   J. Sarwar, M. R. Shad, A. Hasnain, F. Ali, K. E. Kakosimos, and A. Ghosh, "Performance Analysis and Comparison of a Concentrated Photovoltaic System with Different Phase Change Materials," Energies (Basel), vol. 14, no. 10, p. 2911, May 2021, doi: 10.3390/en14102911.

[48]   M. Emam, S. Ookawara, and M. Ahmed, "Performance study and analysis of an inclined concentrated photovoltaic-phase change material system," Solar Energy, vol. 150, pp. 229–245, Jul. 2017, doi: 10.1016/j.solener.2017.04.050.

[49]   S. Ali and M. Mustafa, "Barriers facing Micro-encapsulated Phase Change Materials Slurry (MPCMS) in Photovoltaic Thermal (PV/T) application," Energy Reports, vol. 6, pp. 565–570, Nov. 2020, doi: 10.1016/j.egyr.2020.11.012.

[50]   K. Ghasemi, S. Mahmud, and S. Tasnim, "Optimization of microencapsulated phase change material slurry-based porous heat exchanger," J Energy Storage, vol. 55, p. 105797, Nov. 2022, doi: 10.1016/j.est.2022.105797.

[51]   Z. Fu, Y. Li, X. Liang, S. Lou, Z. Qiu, Z. Cheng, and Q. Zhu, "Experimental investigation on the enhanced performance of a solar PVT system using micro-encapsulated PCMs," Energy, vol. 228, p. 120509, Aug. 2021, doi: 10.1016/j.energy.2021.120509.

[52]   H. M. Maghrabie, A. S. A. Mohamed, A. M. Fahmy, and A. A. Abdel Samee, "Performance enhancement of PV panels using phase change material (PCM): An experimental implementation," Case Studies in Thermal Engineering, vol. 42, p. 102741, Feb. 2023, doi: 10.1016/j.csite.2023.102741.

[53]   K. B. Prakash, M. K. Pasupathi, S. Chinnasamy, S. Saravanakumar, M. Palaniappan, A. Alasiri, and M. Chandrasekaran, "Energy and Exergy Enhancement Study on PV Systems with Phase Change Material," Sustainability, vol. 15, no. 4, p. 3627, Feb. 2023, doi: 10.3390/su15043627.

[54]   M. A. Sheik, M. K. Aravindan, N. Beemkumar, P. K. Chaurasiya, R. Jilte, S. Shaik, and A. Afzal, "Investigation on the thermal management of solar photo voltaic cells cooled by phase change material," J Energy Storage, vol. 52, p. 104914, Aug. 2022, doi: 10.1016/j.est.2022.104914.

[55]   Z. Arifin, B. A. Tribhuwana, B. Kristiawan, D. D. D. P. Tjahjana, S. Hadi, R. A. Rachmanto, S. D. Prasetyo, and M. Hijriawan, "The Effect of Soybean Wax as a Phase Change Material on the Cooling Performance of Photovoltaic Solar Panel," International Journal of Heat and Technology, vol. 40, no. 1, pp. 326–332, Feb. 2022, doi: 10.18280/ijht.400139.

[56]   M. Firoozzadeh, A. H. Shiravi, and M. Shafiee, "Thermodynamics assessment on cooling photovoltaic modules by phase change materials (PCMs) in critical operating temperature," J Therm Anal Calorim, vol. 144, no. 4, pp. 1239–1251, May 2021, doi: 10.1007/s10973-020-09565-3.

[57]   A. Hassan, A. Wahab, M. A. Qasim, M. M. Janjua, M. A. Ali, H. M. Ali, T. R. Jadoon, E. Ali, A. Raza, and N. Javaid, "Thermal management and uniform temperature regulation of photovoltaic modules using hybrid phase change materials-nanofluids system," Renew Energy, vol. 145, pp. 282–293, Jan. 2020, doi: 10.1016/j.renene.2019.05.130.

[58]   R. Elavarasan, K. Velmurugan, U. Subramaniam, A. Kumar, and D. Almakhles, "Experimental Investigations Conducted for the Characteristic Study of OM29 Phase Change Material and Its Incorporation in Photovoltaic Panel," Energies (Basel), vol. 13, no. 4, p. 897, Feb. 2020, doi: 10.3390/en13040897.

[59]   M. Rezvanpour, D. Borooghani, F. Torabi, and M. Pazoki, "Using CaCl2·6H2O as a phase change material for thermo-regulation and enhancing photovoltaic panels'

conversion efficiency: Experimental study and TRNSYS validation," Renew Energy, vol. 146, pp. 1907–1921, Feb. 2020, doi: 10.1016/j.renene.2019.07.075.

[60]   G. Hekimoğlu and A. Sarı, "Fly Ash/Octadecane Shape-Stabilized Composite PCMs Doped with Carbon-Based Nanoadditives for Thermal Regulation Applications," Energy & Fuels, vol. 35, no. 2, pp. 1786–1795, Jan. 2021, doi: 10.1021/acs.energyfuels.0c03369.

[61]   T. Xu, F. Wu, T. Zou, J. Li, J. Yang, X. Zhou, D. Liu, and Y. Bie, "Development of diatomite-based shape-stabilized composite phase change material for use in floor radiant heating," J Mol Liq, vol. 348, p. 118372, Feb. 2022, doi: 10.1016/j.molliq.2021.118372.

[62]   D. Zhang, C. Li, N. Lin, B. Xie, and J. Chen, "Enhanced properties of mica-based composite phase change materials for thermal energy storage," J Energy Storage, vol. 42, p. 103106, Oct. 2021, doi: 10.1016/j.est.2021.103106.

[63]   J. Huang, B. Wu, S. Lyu, T. Li, H. Han, D. Li, J.-K. Wang, J. Zhang, X. Lu, and D. Sun, "Improving the thermal energy storage capability of diatom-based biomass/polyethylene glycol composites phase change materials by artificial culture methods," Solar Energy Materials and Solar Cells, vol. 219, p. 110797, Jan. 2021, doi: 10.1016/j.solmat.2020.110797.

[64]   Q. Al-Yasiri and M. Szabó, "Building envelope-combined phase change material and thermal insulation for energy-effective buildings during harsh summer: Simulation-based analysis," Energy for Sustainable Development, vol. 72, pp. 326–339, Feb. 2023, doi: 10.1016/j.esd.2023.01.003.

[65]   P. J. Ong, Y. Y. Lum, X. Y. D. Soo, S. Wang, P. Wang, D. Chi, H. Liu, D. Kai, C.-L. K. Lee, Q. Yan, J. Xu, X. J. Loh, and Q. Zhu, "Integration of phase change material and thermal insulation material as a passive strategy for building cooling in the tropics," Constr Build Mater, vol. 386, p. 131583, Jul. 2023, doi: 10.1016/j.conbuildmat.2023.131583.

[66]   S. Wi, S. Yang, B. Yeol Yun, and S. Kim, "Exterior insulation finishing system using cementitious plaster/microencapsulated phase change material for improving the building thermal storage performance," Constr Build Mater, vol. 299, p. 123932, Sep. 2021, doi: 10.1016/j.conbuildmat.2021.123932.

[67]   Y. Liao, J. Li, S. Li, and X. Yang, "Super-elastic and shape-stable solid-solid phase change materials for thermal management of electronics," J Energy Storage, vol. 52, p. 104751, Aug. 2022, doi: 10.1016/j.est.2022.104751.

[68]   Y. Zhang, P. Wu, Y. Meng, R. Lu, S. Zhang, and B. Tang, "Flexible phase change films with enhanced thermal conductivity and low electrical conductivity for thermal management," Chemical Engineering Journal, vol. 464, p. 142650, May 2023, doi: 10.1016/j.cej.2023.142650.

[69]   K. Yang, Z. Ling, X. Fang, and Z. Zhang, "Introducing a flexible insulation network to the expanded graphite-based composite phase change material to enhance dielectric and mechanical properties for battery thermal management," J Energy Storage, vol. 66, p. 107486, Aug. 2023, doi: 10.1016/j.est.2023.107486.

[70]   S. Wu, T. Li, M. Wu, J. Xu, Y. Hu, J. Chao, T. Yan, and R. Wang, "Highly thermally conductive and flexible phase change composites enabled by polymer/graphite nanoplatelet-based dual networks for efficient thermal management," J Mater Chem A Mater, vol. 8, no. 38, pp. 20011–20020, 2020, doi: 10.1039/D0TA05904H.

[71]   X. Ge, G. Tay, Y. Hou, Y. Zhao, P. J. Sugumaran, B. Q. Thai, C. K. Ang, W. Zhai, and Y. Yang, "Flexible and leakage-proof phase change composite for microwave attenuation and thermal management," Carbon N Y, vol. 210, p. 118084, Jun. 2023, doi: 10.1016/j.carbon.2023.118084.

[72]   H. Baniasadi, M. Madani, J. Seppälä, J. B. Zimmerman, and M. R. Yazdani, "Form-stable phase change electrospun nanofibers mat with thermal regulation and biomedical multi-functionalities," J Energy Storage, vol. 68, p. 107660, Sep. 2023, doi: 10.1016/j.est.2023.107660.

[73]   X. Chen, H. Gao, G. Hai, D. Jia, L. Xing, S. Chen, P. Cheng, M. Han, W. Dong, and G. Wang, "Carbon nanotube bundles assembled flexible hierarchical framework based phase change material composites for thermal energy harvesting and thermotherapy," Energy Storage Mater, vol. 26, pp. 129–137, Apr. 2020, doi: 10.1016/j.ensm.2019.12.029.

[74]   Y.-C. Zhou, J. Yang, W.-D. Li, P. Yu, Z.-M. Zhang, L. Bai, R.-Y. Bao, and W. Yang, "Highly stretchable phase change composites for simultaneous health monitoring and thermotherapy," Chemical Engineering Journal, vol. 470, p. 144175, Aug. 2023, doi: 10.1016/j.cej.2023.144175.

[75]   L. Yu, X. Qin, G. Ke, J. Tang, and Y. Wang, "Fabrication of cotton/polyethylene glycol/stainless steel wire friction spun composite yarn and its application in electrothermal phase change textile," Composites Communications, vol. 32, p. 101152, Jun. 2022, doi: 10.1016/j.coco.2022.101152.

[76]   J. W. Ong, H. A. Abid, T. Minifie, E. S. Lin, Z. Song, M. Katariya, O. W. Liew, and T. W. Ng, "Unmanned aerial vehicle transport of frozen blood samples using phase change materials," Biosyst Eng, vol. 221, pp. 30–42, Sep. 2022, doi: 10.1016/j.biosystemseng.2022.06.008.

[77]   Z. Qin, Z. H. Low, C. Ji, and F. Duan, "Efficacy of angled metallic fins for enhancing phase change material melting," International Communications in Heat and Mass Transfer, vol. 132, p. 105921, Mar. 2022, doi: 10.1016/j.icheatmasstransfer.2022.105921.

[78]   S. A. B. Al-Omari, Z. A. Qureshi, E. Elnajjar, and F. Mahmoud, "A heat sink integrating fins within high thermal conductivity phase change material to cool high heat-flux heat sources," International Journal of Thermal Sciences, vol. 172, p. 107190, Feb. 2022, doi: 10.1016/j.ijthermalsci.2021.107190.

[79]   A. M. Saeed, A. Abderrahmane, N. A. A. Qasem, A. Mourad, M. Alhazmi, S. E. Ahmed, and K. Guedri, "A numerical investigation of a heat transfer augmentation finned pear-shaped thermal energy storage system with nano-enhanced phase change materials," J Energy Storage, vol. 53, p. 105172, Sep. 2022, doi: 10.1016/j.est.2022.105172.

[80]   A. Laouer, K. Al-Farhany, M. F. Al-Dawody, and A. L. Hashem, "A numerical study of phase change material melting enhancement in a horizontal rectangular enclosure with vertical triple fins," International Communications in Heat and Mass Transfer, vol. 137, p. 106223, Oct. 2022, doi: 10.1016/j.icheatmasstransfer.2022.106223.

[81]   B. İzgi, "Effect of fins on melting of phase change material in a closed vertical cylinder under microgravity," Appl Therm Eng, vol. 220, p. 119703, Feb. 2023, doi: 10.1016/j.applthermaleng.2022.119703.

[82]   S. Tiari, A. Hockins, and K. Shank, "Experimental study of a latent heat thermal energy storage system assisted by varying annular fins," J Energy Storage, vol. 55, p. 105603, Nov. 2022, doi: 10.1016/j.est.2022.105603.

[83]   F. He, R. Bo, C. Hu, X. Meng, and W. Gao, "Employing spiral fins to improve the thermal performance of phase-change materials in shell-tube latent heat storage units," Renew Energy, vol. 203, pp. 518–528, Feb. 2023, doi: 10.1016/j.renene.2022.12.091.

[84]   Z.-R. Li, G.-T. Fu, and L.-W. Fan, "Synergistic effects of nano-enhanced phase change material (NePCM) and fin shape on heat storage performance of a finned shell-and-tube unit: An experimental study," J Energy Storage, vol. 45, p. 103772, Jan. 2022, doi: 10.1016/j.est.2021.103772.

[85]   Z. Qin, Z. H. Low, C. Ji, and F. Duan, "Efficacy of angled metallic fins for enhancing phase change material melting," International Communications in Heat and Mass Transfer, vol. 132, p. 105921, Mar. 2022, doi: 10.1016/j.icheatmasstransfer.2022.105921.

[86]   C. Zhang, N. Wang, H. Xu, Y. Fang, Q. Yang, and F. K. Talkhoncheh, "Thermal management optimization of the photovoltaic cell by the phase change material combined with metal fins," Energy, vol. 263, p. 125669, Jan. 2023, doi: 10.1016/j.energy.2022.125669.

[87]   C. Zhang, N. Wang, H. Xu, Y. Fang, Q. Yang, and F. K. Talkhoncheh, "Thermal management optimization of the photovoltaic cell by the phase change material combined with metal fins," Energy, vol. 263, p. 125669, Jan. 2023, doi: 10.1016/j.energy.2022.125669.

[88]   M. Sanchouli, S. Payan, A. Payan, and S. A. Nada, "Investigation of the enhancing thermal performance of phase change material in a double-tube heat exchanger using grid annular fins," Case Studies in Thermal Engineering, vol. 34, p. 101986, Jun. 2022, doi: 10.1016/j.csite.2022.101986.

[89]   A. Shahsavar, A. Goodarzi, H. I. Mohammed, A. Shirneshan, and P. Talebizadehsardari, "Thermal performance evaluation of non-uniform fin array in a finned double-pipe latent heat storage system," Energy, vol. 193, p. 116800, Feb. 2020, doi: 10.1016/j.energy.2019.116800.

[90]   F. He, R. Bo, C. Hu, X. Meng, and W. Gao, "Employing spiral fins to improve the thermal performance of phase-change materials in shell-tube latent heat storage units," Renew Energy, vol. 203, pp. 518–528, Feb. 2023, doi: 10.1016/j.renene.2022.12.091.

[91]   M. Fallah Najafabadi, H. Talebi Rostami, and D. D. Ganji, "Thermal and geometrical investigation of an original double-pipe helical coil heat storage system with

kock snowflake cross-section containing phase-change material," Appl Therm Eng, vol. 226, p. 120244, May 2023, doi: 10.1016/j.applthermaleng.2023.120244.

[92]   V. G. Choudhari, A. S. Dhoble, and S. Panchal, "Numerical analysis of different fin structures in phase change material module for battery thermal management system and its optimization," Int J Heat Mass Transf, vol. 163, p. 120434, Dec. 2020, doi: 10.1016/j.ijheatmasstransfer.2020.120434.

[93]   P. Yan, W. Fan, Y. Yang, H. Ding, A. Arshad, and C. Wen, "Performance enhancement of phase change materials in triplex-tube latent heat energy storage system using novel fin configurations," Appl Energy, vol. 327, p. 120064, Dec. 2022, doi: 10.1016/j.apenergy.2022.120064.

[94]   H. Najafi Khaboshan, F. Jaliliantabar, A. Adam Abdullah, and S. Panchal, "Improving the cooling performance of cylindrical lithium-ion battery using three passive methods in a battery thermal management system," Appl Therm Eng, vol. 227, p. 120320, Jun. 2023, doi: 10.1016/j.applthermaleng.2023.120320.

[95]   F. Ren, J. Du, Y. Cai, J. Guo, Y. Liu, D. Zhang, and M. Li, "Study on thermal performance of a new optimized snowflake longitudinal fin in vertical latent heat storage," J Energy Storage, vol. 50, p. 104165, Jun. 2022, doi: 10.1016/j.est.2022.104165.

[96]   Y. S. Sun, Y. Han, G. D. Li, H. Y. Shen, X. M. Chi, and C. Y. Zhang, "Numerical study of high-temperature cascaded packed bed thermal energy storage system," Case Studies in Thermal Engineering, vol. 37, p. 102258, Sep. 2022, doi: 10.1016/j.csite.2022.102258.

[97]   X. Cheng and X. Zhai, "Thermal performance analysis and optimization of a cascaded packed bed cool thermal energy storage unit using multiple phase change materials," Appl Energy, vol. 215, pp. 566–576, Apr. 2018, doi: 10.1016/j.apenergy.2018.02.053.

[98]   D. Zhang, F. Zhang, S. Tang, C. Guo, and X. Qin, "Performance evaluation of cascaded storage system with multiple phase change materials," Appl Therm Eng, vol. 185, p. 116384, Feb. 2021, doi: 10.1016/j.applthermaleng.2020.116384.

[99]   W. Guo, Z. He, A. Mawire, and P. Zhang, "Parametric investigation of charging and discharging performances of a cascaded packed bed thermal energy storage system," J Energy Storage, vol. 57, p. 106229, Jan. 2023, doi: 10.1016/j.est.2022.106229.

[100]   R. Elbahjaoui, "Improvement of the thermal performance of a solar triple concentric-tube thermal energy storage unit using cascaded phase change materials," J Energy Storage, vol. 42, p. 103047, Oct. 2021, doi: 10.1016/j.est.2021.103047.

[101]   R. A. Kishore, C. Booten, M. V. A. Bianchi, J. Vidal, and R. Jackson, "Evaluating cascaded and tunable phase change materials for enhanced thermal energy storage utilization and effectiveness in building envelopes," Energy Build, vol. 260, p. 111937, Apr. 2022, doi: 10.1016/j.enbuild.2022.111937.

[102]   Y. S. Sun, Y. Han, G. D. Li, H. Y. Shen, X. M. Chi, and C. Y. Zhang, "Numerical study of high-temperature cascaded packed bed thermal energy storage system," Case Studies in Thermal Engineering, vol. 37, p. 102258, Sep. 2022, doi: 10.1016/j.csite.2022.102258.

[103]   J. M. Mahdi and E. C. Nsofor, "Multiple-segment metal foam application in the shell-and-tube PCM thermal energy storage system," J Energy Storage, vol. 20, pp. 529–541, Dec. 2018, doi: 10.1016/j.est.2018.09.021.

[104]   J. M. Mahdi, H. I. Mohammed, E. T. Hashim, P. Talebizadehsardari, and E. C. Nsofor, "Solidification enhancement with multiple PCMs, cascaded metal foam and nanoparticles in the shell-and-tube energy storage system," Appl Energy, vol. 257, p. 113993, Jan. 2020, doi: 10.1016/j.apenergy.2019.113993.

[105]   S. Bashiri Mousavi, M. Adib, M. Soltani, A. R. Razmi, and J. Nathwani, "Transient thermodynamic modeling and economic analysis of an adiabatic compressed air energy storage (A-CAES) based on cascade packed bed thermal energy storage with encapsulated phase change materials," Energy Convers Manag, vol. 243, p. 114379, Sep. 2021, doi: 10.1016/j.enconman.2021.114379.

[106]   S. Bashiri Mousavi, P. Ahmadi, P. Hanafizadeh, and S. Khanmohammadi, "Dynamic simulation and techno-economic analysis of liquid air energy storage with cascade phase change materials as a cold storage system," J Energy Storage, vol. 50, p. 104179, Jun. 2022, doi: 10.1016/j.est.2022.104179.

[107]   M. Y. Abdollahzadeh Jamalabadi, "Use of Nanoparticle Enhanced Phase Change Material for Cooling of Surface Acoustic Wave Sensor," Fluids, vol. 6, no. 1, p. 31, Jan. 2021, doi: 10.3390/fluids6010031.

[108]   A. M. Abdulateef, M. Jaszczur, Q. Hassan, R. Anish, H. Niyas, K. Sopian, and J. Abdulateef, "Enhancing the melting of phase change material using a fins–nanoparticle combination in a triplex tube heat exchanger," J Energy Storage, vol. 35, p. 102227, Mar. 2021, doi: 10.1016/j.est.2020.102227.

[109]   S. Algarni, S. Mellouli, T. Alqahtani, K. Almutairi, A. khan, and A. Anqi, "Experimental investigation of an evacuated tube solar collector incorporating nano-enhanced PCM as a thermal booster," Appl Therm Eng, vol. 180, p. 115831, Nov. 2020, doi: 10.1016/j.applthermaleng.2020.115831.

[110]   M. Aqib, A. Hussain, H. M. Ali, A. Naseer, and F. Jamil, "Experimental case studies of the effect of Al2O3 and MWCNTs nanoparticles on heating and cooling of PCM," Case Studies in Thermal Engineering, vol. 22, p. 100753, Dec. 2020, doi: 10.1016/j.csite.2020.100753.

[111]   A. Badakhsh, K.-H. An, C. W. Park, and B.-J. Kim, "Effects of Biceramic AlN-SiC Microparticles on the Thermal Properties of Paraffin for Thermal Energy Storage," J Nanomater, vol. 2018, pp. 1–10, Sep. 2018, doi: 10.1155/2018/8632350.

[112]   C. Barreneche, M. Martín, J. Calvo-de la Rosa, M. Majó, and A. Fernández, "Own-Synthetize Nanoparticles to Develop Nano-Enhanced Phase Change Materials (NEPCM) to Improve the Energy Efficiency in Buildings," Molecules, vol. 24, no. 7, p. 1232, Mar. 2019, doi: 10.3390/molecules24071232.

[113]   M. Bashar and K. Siddiqui, "Experimental investigation of transient melting and heat transfer behavior of nanoparticle-enriched PCM in a rectangular enclosure," J Energy Storage, vol. 18, pp. 485–497, Aug. 2018, doi: 10.1016/j.est.2018.06.006.

[114]   M. Dastmalchi and F. A. Boyaghchi, "Exergy and economic analyses of nanoparticle-enriched phase change material in an air heat exchanger for cooling of residential buildings," J Energy Storage, vol. 32, p. 101705, Dec. 2020, doi: 10.1016/j.est.2020.101705.

[115]   R. Elbahjaoui and H. El Qarnia, "Transient behavior analysis of the melting of nanoparticle-enhanced phase change material inside a rectangular latent heat storage unit," Appl Therm Eng, vol. 112, pp. 720–738, Feb. 2017, doi: 10.1016/j.applthermaleng.2016.10.115.

[116]   R. Y. Farsani, A. Raisi, A. A. Nadooshan, and S. Vanapalli, "Does nanoparticles dispersed in a phase change material improve melting characteristics?," International Communications in Heat and Mass Transfer, vol. 89, pp. 219–229, Dec. 2017, doi: 10.1016/j.icheatmasstransfer.2017.10.006.

[117]   S. Ghafari, J. Khorshidi, S. Niazi, and F. Samari, "Melting study of nano-enhanced phase change material (NePCM) inside a sphere by using of image processing and volume shrinkage methods," J Energy Storage, vol. 44, p. 103376, Dec. 2021, doi: 10.1016/j.est.2021.103376.

[118]   M. Ghalambaz, A. Doostani, A. J. Chamkha, and M. A. Ismael, "Melting of nanoparticles-enhanced phase-change materials in an enclosure: Effect of hybrid nanoparticles," Int J Mech Sci, vol. 134, pp. 85–97, Dec. 2017, doi: 10.1016/j.ijmecsci.2017.09.045.

[119]   H. Javadi, J. F. Urchueguia, S. S. Mousavi Ajarostaghi, and B. Badenes, "Numerical Study on the Thermal Performance of a Single U-Tube Borehole Heat Exchanger Using Nano-Enhanced Phase Change Materials," Energies (Basel), vol. 13, no. 19, p. 5156, Oct. 2020, doi: 10.3390/en13195156.

[120]   M. Khatibi, R. Nemati-Farouji, A. Taheri, A. Kazemian, T. Ma, and H. Niazmand, "Optimization and performance investigation of the solidification behavior of nano-enhanced phase change materials in triplex-tube and shell-and-tube energy storage units," J Energy Storage, vol. 33, p. 102055, Jan. 2021, doi: 10.1016/j.est.2020.102055.

[121]   L. Liang and X. Chen, "Preparation and Thermal Properties of Eutectic Hydrate Salt Phase Change Thermal Energy Storage Material," International Journal of Photoenergy, vol. 2018, pp. 1–9, 2018, doi: 10.1155/2018/6432047.

[122]   H. Maher, K. A. Rocky, R. Bassiouny, and B. B. Saha, "Synthesis and thermal characterization of paraffin-based nanocomposites for thermal energy storage applications," Thermal Science and Engineering Progress, vol. 22, p. 100797, May 2021, doi: 10.1016/j.tsep.2020.100797.

[123]   M. A. Marcos, D. Cabaleiro, S. Hamze, L. Fedele, S. Bobbo, P. Estellé, and L. Lugo, "NePCM Based on Silver Dispersions in Poly(Ethylene Glycol) as a Stable Solution for Thermal Storage," Nanomaterials, vol. 10, no. 1, p. 19, Dec. 2019, doi: 10.3390/nano10010019.

[124]   M. P, G. K. P, K. V, M. M, M. M. K, and V. R, "Thermal energy storage behaviour of nanoparticle enhanced PCM during freezing and melting," Phase Transitions, vol. 91, no. 3, pp. 254–270, Mar. 2018, doi: 10.1080/01411594.2017.1372760.

[125]   M. ÖZel, "DETERMINATION OF INDOOR DESIGN TEMPERATURE, THERMAL CHARACTERISTICS AND INSULATION THICKNESS UNDER HOT CLIMATE CONDITIONS," Isi Bilimi Ve Teknigi Dergisi/ Journal of Thermal Science and Technology, vol. 42, no. 1, pp. 49–62, 2022, doi: 10.47480/ISIBTED.1107440.

[126]   C. Nie, J. Liu, and S. Deng, "Effect of geometric parameter and nanoparticles on PCM melting in a vertical shell-tube system," Appl Therm Eng, vol. 184, p. 116290, Feb. 2021, doi: 10.1016/j.applthermaleng.2020.116290.

[127]   M. T. Nitsas and I. P. Koronaki, "Thermal Analysis of Pure and Nanoparticle-Enhanced PCM—Application in Concentric Tube Heat Exchanger," Energies (Basel), vol. 13, no. 15, p. 3841, Jul. 2020, doi: 10.3390/en13153841.

[128]   M. K. Pasupathi, K. Alagar, M. J. S. P, M. M.M, and G. Aritra, "Characterization of Hybrid-nano/Paraffin Organic Phase Change Material for Thermal Energy Storage Applications in Solar Thermal Systems," Energies (Basel), vol. 13, no. 19, p. 5079, Sep. 2020, doi: 10.3390/en13195079.

[129]   R. Prabakaran, S. Sidney, D. M. Lal, C. Selvam, and S. Harish, "Solidification of Graphene-Assisted Phase Change Nanocomposites inside a Sphere for Cold Storage Applications," Energies (Basel), vol. 12, no. 18, p. 3473, Sep. 2019, doi: 10.3390/en12183473.

[130]   S. Santhosh, M. Satish, A. Yadav, and A. Anish Madhavan, "Thermal analysis of Fe2O3 - myristic acid nanocomposite for latent heat storage," Mater Today Proc, vol. 43, pp. 3795–3798, 2021, doi: 10.1016/j.matpr.2020.11.412.

[131]   M. M. Thalib, A. M. Manokar, F. A. Essa, N. Vasimalai, R. Sathyamurthy, and F. P. Garcia Marquez, "Comparative Study of Tubular Solar Stills with Phase Change Material and Nano-Enhanced Phase Change Material," Energies (Basel), vol. 13, no. 15, p. 3989, Aug. 2020, doi: 10.3390/en13153989.

[132]   M. Zaidan, M. A.-Int. J. Mech. Mechatron. Eng, and undefined 2018, "Improvement in heat transfer inside a phase change energy systemQ2International Journal of Mechanical and Materials Engineering; H-Index: 28 SJR: Q2 CORE: NA ABDC: NA

FT50: NA," researchgate.netMJ Zaidan, MH AlhamdoInt. J. Mech. Mechatron. Eng, 2018•researchgate.net, vol. 18, no. 05, pp. 180505–3737, 2018, Accessed: Apr. 05, 2024. [Online]. Available: https://www.researchgate.net/profile/Ghassan-Smaisim/post/Simulation_of_Paraffin_Wax_in_Ansys_Fluent/attachment/5bdaa927cfe4a 76455fecd2c/AS%3A688056273227777%401541056807500/download/Improvement+in +Heat+Transfer+Inside+a+phase+change+energy+system.pdf

[133]   Y. Zhou, Y. Jiang, F. Liu, Q. L.-J. of O. Research, and undefined 2016, "Thermal conductivity and thermal mechanism of aluminum nanoparticles/octadecane composite phase change materials from molecular dynamics simulations Q3Journal of Ovonic Research; H-Index: 14 SJR: Q3 CORE: NA ABDC: NA FT50: NA," chalcogen.roY Zhou, Y Jiang, F Liu, Q LiJournal of Ovonic Research, 2016•chalcogen.ro, vol. 12, no. 2, pp. 49–58, Accessed: Apr. 05, 2024. [Online]. Available: https://chalcogen.ro/49_ZhouY.pdf

[134]   Y. Zhuang, Z. Liu, and W. Xu, "Experimental investigation on the non-Newtonian to Newtonian rheology transition of nanoparticles enhanced phase change material during melting," Colloids Surf A Physicochem Eng Asp, vol. 629, p. 127432, Nov. 2021, doi: 10.1016/j.colsurfa.2021.127432.

[135]   N. Aslfattahi, S. Rahman, M. F. Mohd Sabri, and A. Arifutzzaman, "Experimental Investigation of Thermal Stability and Enthalpy of Eutectic Alkali Metal Solar Salt Dispersed with MgO Nanoparticles," International Journal of Technology, vol. 10, no. 6, p. 1112, Nov. 2019, doi: 10.14716/ijtech.v10i6.3568.

[136]   M. Chieruzzi, G. F. Cerritelli, A. Miliozzi, J. M. Kenny, and L. Torre, "Heat capacity of nanofluids for solar energy storage produced by dispersing oxide nanoparticles in nitrate salt mixture directly at high temperature," Solar Energy Materials and Solar Cells, vol. 167, pp. 60–69, Aug. 2017, doi: 10.1016/j.solmat.2017.04.011.

[137]   V. Mayilvelnathan and A. Valan Arasu, "Experimental investigation on thermal behavior of graphene dispersed erythritol PCM in a shell and helical tube latent energy storage system," International Journal of Thermal Sciences, vol. 155, p. 106446, Sep. 2020, doi: 10.1016/j.ijthermalsci.2020.106446.

[138]   R. Manickam, P. Kalidoss, … S. S.-… R. J. of, and undefined 2019, "Erythritol based nano-PCM for solar thermal energy storageQ2Journal of Solar Energy Engineering; H-Index: 87 SJR: Q2 CORE: NA ABDC: NA FT50: NA 1Journal of Solar Energy Engineering; H-Index: 87 VHB: NA FNEGE: NA CoNRS: NA HCERE: NA CCF: NA

BFI: 1 AJG: NA +," academia.eduR Manickam, P Kalidoss, S Suresh, S VenkatachalapathyInternational Research Journal of Engineering and Technology (IRJET), 2019•academia.edu, p. 1631, 2008, Accessed: Apr. 05, 2024. [Online]. Available: https://www.academia.edu/download/59813911/IRJET-V6I434720190620-73547-qppowj.pdf

[139] M. K. Saranprabhu and K. S. Rajan, "Magnesium oxide nanoparticles dispersed solar salt with improved solid phase thermal conductivity and specific heat for latent heat thermal energy storage," Renew Energy, vol. 141, pp. 451–459, Oct. 2019, doi: 10.1016/j.renene.2019.04.027.

[140] R. P. Singh, J. Y. Sze, S. C. Kaushik, D. Rakshit, and A. Romagnoli, "Thermal performance enhancement of eutectic PCM laden with functionalised graphene nanoplatelets for an efficient solar absorption cooling storage system," J Energy Storage, vol. 33, p. 102092, Jan. 2021, doi: 10.1016/j.est.2020.102092.

[141] K. u Mekrisuh, S. Giri, Udayraj, D. Singh, and D. Rakshit, "Optimal design of the phase change material based thermal energy storage systems: Efficacy of fins and/or nanoparticles for performance enhancement," J Energy Storage, vol. 33, p. 102126, Jan. 2021, doi: 10.1016/j.est.2020.102126.

[142] M. Vivekananthan and V. A. Amirtham, "Characterisation and thermophysical properties of graphene nanoparticles dispersed erythritol PCM for medium temperature thermal energy storage applications," Thermochim Acta, vol. 676, pp. 94–103, Jun. 2019, doi: 10.1016/j.tca.2019.03.037.

[143] D. Han, B. Guene Lougou, Y. Xu, Y. Shuai, and X. Huang, "Thermal properties characterization of chloride salts/nanoparticles composite phase change material for high-temperature thermal energy storage," Appl Energy, vol. 264, p. 114674, Apr. 2020, doi: 10.1016/j.apenergy.2020.114674.

[144] Y. Xiong, Z. Wang, Y. Wu, P. Xu, Y. Ding, C. Chang, and C. Ma, "Performance enhancement of bromide salt by nano-particle dispersion for high-temperature heat pipes in concentrated solar power plants," Appl Energy, vol. 237, pp. 171–179, Mar. 2019, doi: 10.1016/j.apenergy.2019.01.026.

[145] P. D. Myers, T. E. Alam, R. Kamal, D. Y. Goswami, and E. Stefanakos, "Nitrate salts doped with CuO nanoparticles for thermal energy storage with improved heat

transfer," Appl Energy, vol. 165, pp. 225–233, Mar. 2016, doi: 10.1016/j.apenergy.2015.11.045.

[146] N. S. Bondareva, N. S. Gibanov, and M. A. Sheremet, "Computational Study of Heat Transfer inside Different PCMs Enhanced by Al2O3 Nanoparticles in a Copper Heat Sink at High Heat Loads," Nanomaterials, vol. 10, no. 2, p. 284, Feb. 2020, doi: 10.3390/nano10020284.

[147] M. R. Hajizadeh, A. N. Keshteli, and Q.-V. Bach, "Solidification of PCM within a tank with longitudinal-Y shape fins and CuO nanoparticle," J Mol Liq, vol. 317, p. 114188, Nov. 2020, doi: 10.1016/j.molliq.2020.114188.

[148] Kh. Hosseinzadeh, M. A. Erfani Moghaddam, A. Asadi, A. R. Mogharrebi, B. Jafari, M. R. Hasani, and D. D. Ganji, "Effect of two different fins (longitudinal-tree like) and hybrid nano-particles (MoS_2-TiO_2) on solidification process in triplex latent heat thermal energy storage system," Alexandria Engineering Journal, vol. 60, no. 1, pp. 1967–1979, Feb. 2021, doi: 10.1016/j.aej.2020.12.001.

[149] F. Li, A. Almarashi, M. Jafaryar, M. R. Hajizadeh, and Y.-M. Chu, "Melting process of nanoparticle enhanced PCM through storage cylinder incorporating fins," Powder Technol, vol. 381, pp. 551–560, Mar. 2021, doi: 10.1016/j.powtec.2020.12.026.

[150] J. M. Mahdi, S. Lohrasbi, D. D. Ganji, and E. C. Nsofor, "Simultaneous energy storage and recovery in the triplex-tube heat exchanger with PCM, copper fins and Al2O3 nanoparticles," Energy Convers Manag, vol. 180, pp. 949–961, Jan. 2019, doi: 10.1016/j.enconman.2018.11.038.

[151] M. E. Nakhchi, M. Hatami, and M. Rahmati, "A numerical study on the effects of nanoparticles and stair fins on performance improvement of phase change thermal energy storages," Energy, vol. 215, p. 119112, Jan. 2021, doi: 10.1016/j.energy.2020.119112.

[152] Q. Ren, F. Meng, and P. Guo, "A comparative study of PCM melting process in a heat pipe-assisted LHTES unit enhanced with nanoparticles and metal foams by immersed boundary-lattice Boltzmann method at pore-scale," Int J Heat Mass Transf, vol. 121, pp. 1214–1228, Jun. 2018, doi: 10.1016/j.ijheatmasstransfer.2018.01.046.

[153]   S. Bilal, N. Z. Khan, I. A. Shah, J. Awrejcewicz, A. Akgül, and M. B. Riaz, "Heat and Flow Control in Cavity with Cold Circular Cylinder Placed in Non-Newtonian Fluid by Performing Finite Element Simulations," Coatings, vol. 12, no. 1, p. 16, Dec. 2021, doi: 10.3390/coatings12010016.

[154]   M. K. Koukou, G. Dogkas, M. Gr. Vrachopoulos, J. Konstantaras, C. Pagkalos, K. Lymperis, V. Stathopoulos, G. Evangelakis, C. Prouskas, L. Coelho, and A. Rebola, "Performance Evaluation of a Small-Scale Latent Heat Thermal Energy Storage Unit for Heating Applications Based on a Nanocomposite Organic PCM," ChemEngineering, vol. 3, no. 4, p. 88, Nov. 2019, doi: 10.3390/chemengineering3040088.

[155]   M. Mahdavi, S. Tiari, and V. Pawar, "A numerical study on the combined effect of dispersed nanoparticles and embedded heat pipes on melting and solidification of a shell and tube latent heat thermal energy storage system," J Energy Storage, vol. 27, p. 101086, Feb. 2020, doi: 10.1016/j.est.2019.101086.

[156]   I. A. Shah, S. Bilal, A. Akgül, M. Omri, J. Bouslimi, and N. Z. Khan, "Significance of cold cylinder in heat control in power law fluid enclosed in isosceles triangular cavity generated by natural convection: A computational approach," Alexandria Engineering Journal, vol. 61, no. 9, pp. 7277–7290, Sep. 2022, doi: 10.1016/j.aej.2021.12.071.

[157]   Q. Ren, F. Meng, and P. Guo, "A comparative study of PCM melting process in a heat pipe-assisted LHTES unit enhanced with nanoparticles and metal foams by immersed boundary-lattice Boltzmann method at pore-scale," Int J Heat Mass Transf, vol. 121, pp. 1214–1228, Jun. 2018, doi: 10.1016/j.ijheatmasstransfer.2018.01.046.

[158]   S. Tiari, M. Mahdavi, V. Thakore, and S. Joseph, "Thermal Analysis of a High-Temperature Heat Pipe-Assisted Thermal Energy Storage System With Nano-Enhanced Phase Change Material," Nov. 2018. doi: 10.1115/IMECE2018-86481.

[159]   S. Tiari, O. L. Rose, and M. Mahdavi, "DISCHARGING PROCESS OF A HIGH-TEMPERATURE HEAT PIPE-ASSISTED THERMAL ENERGY STORAGE SYSTEM WITH NANO-ENAHNCED PHASE CHANGE MATERIAL," in Proceeding of 4th Thermal and Fluids Engineering Conference, 2019, pp. 1763–1772. doi: 10.1615/TFEC2019.tes.028083.

[160]   H. Kim, Y.-S. Kim, L. Kwac, H. Shin, S. Lee, U. Lee, and H. Shin, "Latent Heat Storage and Thermal Efficacy of Carboxymethyl Cellulose Carbon Foams Containing Ag,

Al, Carbon Nanotubes, and Graphene in a Phase Change Material," Nanomaterials, vol. 9, no. 2, p. 158, Jan. 2019, doi: 10.3390/nano9020158.

[161]   A. Shahzad, M. Imran, M. Tahir, S. Ali Khan, A. Akgül, S. Abdullaev, C. Park, H. Y. Zahran, and I. S. Yahia, "Brownian motion and thermophoretic diffusion impact on Darcy-Forchheimer flow of bioconvective micropolar nanofluid between double disks with Cattaneo-Christov heat flux," Alexandria Engineering Journal, vol. 62, pp. 1–15, Jan. 2023, doi: 10.1016/j.aej.2022.07.023.

[162]   Q. Yu, C. Zhang, Y. Lu, Q. Kong, H. Wei, Y. Yang, Q. Gao, Y. Wu, and A. Sciacovelli, "Comprehensive performance of composite phase change materials based on eutectic chloride with SiO2 nanoparticles and expanded graphite for thermal energy storage system," Renew Energy, vol. 172, pp. 1120–1132, Jul. 2021, doi: 10.1016/j.renene.2021.03.061.

[163]   J. M. Mahdi, H. I. Mohammed, E. T. Hashim, P. Talebizadehsardari, and E. C. Nsofor, "Solidification enhancement with multiple PCMs, cascaded metal foam and nanoparticles in the shell-and-tube energy storage system," Appl Energy, vol. 257, p. 113993, Jan. 2020, doi: 10.1016/j.apenergy.2019.113993.

[164]   M. A. E. Moghaddam and D. D. Ganji, "A comprehensive evaluation of the vertical triplex-tube heat exchanger with PCM, concentrating on flow direction, nanoparticles and multiple PCM implementation," Thermal Science and Engineering Progress, vol. 26, p. 101124, Dec. 2021, doi: 10.1016/j.tsep.2021.101124.

[165]   P. T. Sardari, H. I. Mohammed, D. Giddings, G. S. walker, M. Gillott, and D. Grant, "Numerical study of a multiple-segment metal foam-PCM latent heat storage unit: Effect of porosity, pore density and location of heat source," Energy, vol. 189, p. 116108, Dec. 2019, doi: 10.1016/j.energy.2019.116108.

[166]   Z.-Q. Zhu, Y.-K. Huang, N. Hu, Y. Zeng, and L.-W. Fan, "Transient performance of a PCM-based heat sink with a partially filled metal foam: Effects of the filling height ratio," Appl Therm Eng, vol. 128, pp. 966–972, Jan. 2018, doi: 10.1016/j.applthermaleng.2017.09.047.

[167]   J. M. Mahdi, H. I. Mohammed, E. T. Hashim, P. Talebizadehsardari, and E. C. Nsofor, "Solidification enhancement with multiple PCMs, cascaded metal foam and nanoparticles in the shell-and-tube energy storage system," Appl Energy, vol. 257, p. 113993, Jan. 2020, doi: 10.1016/j.apenergy.2019.113993.

[168]   M. M. Heyhat, S. Mousavi, and M. Siavashi, "Battery thermal management with thermal energy storage composites of PCM, metal foam, fin and nanoparticle," J Energy Storage, vol. 28, p. 101235, Apr. 2020, doi: 10.1016/j.est.2020.101235.

[169]   A. NematpourKeshteli, M. Iasiello, G. Langella, and N. Bianco, "Increasing melting and solidification performances of a phase change material-based flat plate solar collector equipped with metal foams, nanoparticles, and wavy wall-Y-shaped surface," Energy Convers Manag, vol. 291, p. 117268, Sep. 2023, doi: 10.1016/j.enconman.2023.117268.

[170]   S. M. Hashem Zadeh, S. A. M. Mehryan, M. Ghalambaz, M. Ghodrat, J. Young, and A. Chamkha, "Hybrid thermal performance enhancement of a circular latent heat storage system by utilizing partially filled copper foam and Cu/GO nano-additives," Energy, vol. 213, p. 118761, Dec. 2020, doi: 10.1016/j.energy.2020.118761.

[171]   S. Davoodabadi Farahani, A. Davoodabadi Farahani, A. Jazari mamoei, and A. H. Mosavi, "Numerical simulation of NEPCM series two-layer solidification process in a triple tube with porous fin," Case Studies in Thermal Engineering, vol. 28, p. 101407, Dec. 2021, doi: 10.1016/j.csite.2021.101407.

[172]   H. Li, C. Hu, H. Wang, Y. He, X. Hu, and D. Tang, "Thermal effect of nanoparticles on the metal foam composite phase change material: A pore-scale study," International Journal of Thermal Sciences, vol. 179, p. 107709, Sep. 2022, doi: 10.1016/j.ijthermalsci.2022.107709.

[173]   G. K. Amudhalapalli and J. K. Devanuri, "Prediction of transient melt fraction in metal foam - nanoparticle enhanced PCM hybrid shell and tube heat exchanger: A machine learning approach," Thermal Science and Engineering Progress, vol. 46, p. 102241, Dec. 2023, doi: 10.1016/j.tsep.2023.102241.

[174]   N. S. Bondareva and M. A. Sheremet, "Numerical simulation of heat transfer performance in an enclosure filled with a metal foam and nano-enhanced phase change material," Energy, vol. 296, p. 131123, Jun. 2024, doi: 10.1016/j.energy.2024.131123.

[175]   B. Lu, Y. Zhang, D. Sun, and X. Jing, "Experimental investigation on thermal properties of paraffin/expanded graphite composite material for low temperature thermal energy storage," Renew Energy, vol. 178, pp. 669–678, Nov. 2021, doi: 10.1016/j.renene.2021.06.070.

[176]   G. Jiang, J. Huang, Y. Fu, M. Cao, and M. Liu, "Thermal optimization of composite phase change material/expanded graphite for Li-ion battery thermal management," Appl Therm Eng, vol. 108, pp. 1119–1125, Sep. 2016, doi: 10.1016/j.applthermaleng.2016.07.197.

[177]   B. Karami, N. Azimi, and S. Ahmadi, "Increasing the electrical efficiency and thermal management of a photovoltaic module using expanded graphite (EG)/paraffin-beef tallow-coconut oil composite as phase change material," Renew Energy, vol. 178, pp. 25–49, Nov. 2021, doi: 10.1016/j.renene.2021.06.067.

[178]   Vikas, A. Yadav, and S. Samir, "Melting dynamics analysis of a multi-tube latent heat thermal energy storage system: Numerical study," Appl Therm Eng, vol. 214, p. 118803, Sep. 2022, doi: 10.1016/j.applthermaleng.2022.118803.

[179]   B. M. S. Punniakodi, N. Shah, V. K. Rathore, and R. Senthil, "Numerical study on melting of phase change material in a horizontal container using multi heat transfer tubes," J Taiwan Inst Chem Eng, vol. 131, p. 104214, Feb. 2022, doi: 10.1016/j.jtice.2022.104214.

[180]   X. Ma, Q. Zhang, J. Wang, and C. Yue, "Sensitivity analysis and optimization of structural parameters of a phase change material based multi-tube heat exchanger under charging condition," J Energy Storage, vol. 56, p. 105940, Dec. 2022, doi: 10.1016/j.est.2022.105940.

[181]   Y. Harmen, Y. Chhiti, M. El Fiti, M. Salihi, and C. Jama, "Eccentricity analysis of annular multi-tube storage unit with phase change material," J Energy Storage, vol. 64, p. 107211, Aug. 2023, doi: 10.1016/j.est.2023.107211.

[182]   Vikas, A. Yadav, S. Samir, and M. Arıcı, "Performance assessment of multi-tube inline and staggered array based latent heat storage system," J Energy Storage, vol. 68, p. 107770, Sep. 2023, doi: 10.1016/j.est.2023.107770.

[183]   M. Alizadeh, Kh. Hosseinzadeh, H. Mehrzadi, and D. D. Ganji, "Investigation of LHTESS filled by Hybrid nano-enhanced PCM with Koch snowflake fractal cross section in the presence of thermal radiation," J Mol Liq, vol. 273, pp. 414–424, Jan. 2019, doi: 10.1016/j.molliq.2018.10.049.

[184]   A. Pourakabar and A. A. Rabienataj Darzi, "Enhancement of phase change rate of PCM in cylindrical thermal energy storage," Appl Therm Eng, vol. 150, pp. 132–142, Mar. 2019, doi: 10.1016/j.applthermaleng.2019.01.009.

[185]   B. Durakovic and M. Torlak, "Experimental and numerical study of a PCM window model as a thermal energy storage unit," International Journal of Low-Carbon Technologies, Oct. 2016, doi: 10.1093/ijlct/ctw024.

[186]   M. Kraiem, M. Karkri, S. Ben Nasrallah, patrick sobolciak, M. Fois, and N. A. Alnuaimi, "Thermophysical Characterization and Numerical Investigation of Three Paraffin Waxes as Latent Heat Storage Materials," Mar. 2019, doi: 10.20944/PREPRINTS201903. 0034.V1.

[187]   R. P. Singh, S. C. Kaushik, and D. Rakshit, "Melting phenomenon in a finned thermal storage system with graphene nano-plates for medium temperature applications," Energy Convers Manag, vol. 163, pp. 86–99, May 2018, doi: 10.1016/j.enconman.2018.02.053.

[188]   M. Parsazadeh and X. Duan, "Numerical study on the effects of fins and nanoparticles in a shell and tube phase change thermal energy storage unit," Appl Energy, vol. 216, pp. 142–156, Apr. 2018, doi: 10.1016/j.apenergy.2018.02.052.

[189]   M. Gorzin, M. J. Hosseini, M. Rahimi, and R. Bahrampoury, "Nano-enhancement of phase change material in a shell and multi-PCM-tube heat exchanger," J Energy Storage, vol. 22, pp. 88–97, Apr. 2019, doi: 10.1016/j.est.2018.12.023.

[190]   H. Bashirpour-Bonab, "Investigation and optimization of PCM melting with nanoparticle in a multi-tube thermal energy storage system," Case Studies in Thermal Engineering, vol. 28, p. 101643, Dec. 2021, doi: 10.1016/j.csite.2021.101643.

[191]   O. Schenk and K. Gärtner, "Solving unsymmetric sparse systems of linear equations with PARDISO," Future Generation Computer Systems, vol. 20, no. 3, pp. 475–487, Apr. 2004, doi: 10.1016/j.future.2003.07.011.

[192]   "Zienkiewicz: The finite element method for fluid... - Google Scholar." https://scholar.google.com/scholar_lookup?title=The%20Finite%20Element%20Method%20For%20Fluid%20Dynamics&author=O.C.%20Zienkiewicz&publication_year=2013 (accessed Apr. 06, 2024).

[193]   A. Rabinataj Darzi, H. Hassanzadeh Afrouzi, M. Khaki, and M. Abbasi, "Unconstrained melting and solidification inside rectangular enclosure," Journal of Fundamental and Applied Sciences, vol. 7, no. 3, p. 436, Sep. 2015, doi: 10.4314/jfas.v7i3.10.

[194]   A. Arshad, H. M. Ali, M. Ali, and S. Manzoor, "Thermal performance of phase change material (PCM) based pin-finned heat sinks for electronics devices: Effect of pin thickness and PCM volume fraction," Appl Therm Eng, vol. 112, pp. 143–155, Feb. 2017, doi: 10.1016/j.applthermaleng.2016.10.090.

[195]   H. Ma, Z. Duan, L. Su, X. Ning, J. Bai, and X. Lv, "Fluid Flow and Entropy Generation Analysis of Al2O3–Water Nanofluid in Microchannel Plate Fin Heat Sinks," Entropy, vol. 21, no. 8, p. 739, Jul. 2019, doi: 10.3390/e21080739.

[196]   Zhao, Z. B., Liu, J. D., Du, X. Y., Wang, Z. Y., Zhang, C., & Ming, S. F. (2022). Fabrication of silver nanoparticles/copper nanoparticles jointly decorated nitride flakes to improve the thermal conductivity of polymer composites. Colloids and Surfaces A: Physicochemical and Engineering Aspects, 635, 128104.